

Université de Montréal

# **Direct Regulation of HCN Ion Channels by Cannabinoids**

By Sultan Mayar

Department of Biochemistry and Molecular Medicine  
Faculty of Medicine  
Université de Montréal

Thesis presentation in looking to  
obtain Master's degree in Biochemistry

July 2021

© Sultan Mayar, 2021

Université de Montréal

# **Direct Regulation of HCN Ion Channels by Cannabinoids**

By Sultan Mayar

Thesis evaluated by Jury members:

James G. Omichinski  
President of Jury

Nazzareno D'Avanzo  
Research Director

Graciela Pineyro  
Jury Member

July 2021

© Sultan Mayar, 2021

## Résumé

Les cannabinoïdes sont une large classe de molécules qui agissent principalement sur les neurones, affectant la sensation de douleur, l'appétit, l'humeur, l'apprentissage et la mémoire. Des récepteurs cannabinoïdes spécifiques (CBR) ont été identifiés dans les neurones et d'autres types de cellules. Cependant, l'activation des CBR ne peut pas modifier directement l'excitabilité électrique des neurones, car les CBR ne génèrent pas de signaux électriques par eux-mêmes. Au lieu de cela, le potentiel membranaire et la signalisation électrique dans toutes les cellules excitables, y compris les neurones, sont générés par des canaux ioniques intégrés dans la membrane cellulaire. Récemment, il a été démontré que le cannabinoïde synthétique WIN55,212-2 affecte la mémoire en activant les récepteurs CB1, entraînant des changements de signalisation qui affectent le courant  $I_h$  généré par les canaux cycliques (HCN) activés par l'hyperpolarisation. Cependant, il a également été démontré que les cannabinoïdes régulent directement la fonction de plusieurs canaux ioniques, indépendamment de l'activation du CBR. Nous examinons ici si les cannabinoïdes, le  $\Delta^9$ -tétrahydrocannabidiol (THC) et le cannabidiol (CBD), que l'on trouve dans le cannabis sativa, peuvent réguler directement les canaux HCN1. En utilisant une pince de tension à deux électrodes (TEVC), sur des ovocytes de *Xenopus*, qui n'expriment pas de CBR, nous surveillons les changements dans la relation courant-tension, la cinétique de déclenchement et la dépendance à la tension des courants HCN1 dans des concentrations croissantes de cannabinoïdes. Nos données suggèrent que le CBD et le THC modulent directement le courant de HCN1. Étant donné que les cannabinoïdes sont des molécules thérapeutiques prometteuses pour le traitement de plusieurs troubles neurologiques, comprendre quelles cibles ils affectent, le mécanisme de leur régulation et comment ils se lient à des cibles potentielles sont des étapes essentielles de leur utilisation en tant que thérapies efficaces et du développement de cibles plus puissantes et plus efficaces médicaments spécifiques.

**Mot-cles:** Canaux HCN, courant d'hyperpolarisation ( $I_h$ ), récepteurs CB1, cannabinoïdes, relation courant-tension, cinétique de déclenchement, signalisation électrique.

## Abstract

Cannabinoids are a broad class of molecules that act primarily on neurons, affecting pain sensation, appetite, mood, learning and memory. Specific cannabinoid receptors (CBRs) have been identified in neurons, and other cell types. However, activating CBRs cannot directly alter electrical excitability in neurons, since CBRs do not generate electrical signals on their own. Instead, membrane potential and electrical signaling in all excitable cells, including neurons, are generated by ion channels embedded in the cell membrane. Recently, it has been shown that the synthetic cannabinoid WIN55,212-2 effects memory by activating CB1 receptors, leading to signaling changes that affect the  $I_h$  current generated by hyperpolarization-activated cyclic-nucleotide gated (HCN) channels. However, cannabinoids have also been shown to directly regulate the function of several ion channels, independently of CBR activation. Here we examine whether cannabinoids,  $\Delta^9$ -tetrahydrocannabinol (THC) and cannabidiol (CBD), which are found in *cannabis sativa*, can directly regulate HCN1 channels. Using two-electrode voltage clamp (TEVC), on *Xenopus* oocytes, which do not express CBRs, we monitor changes in the current-voltage relationship, gating kinetics, and voltage-dependence of HCN1 currents in increasing concentrations of cannabinoids. Our data suggests CBD and THC directly modulate HCN1 current. Since cannabinoids are promising therapeutic molecules for the treatment of several neurological disorders, understanding what targets they affect, the mechanism of their regulation, and how they bind to potential targets are critical steps in their use as effective therapies and the development of more potent and target specific drugs.

**Keywords:** HCN channel, hyperpolarization current ( $I_h$ ) CB1 receptors, cannabinoids, current-voltage relationship, gating kinetics, electrical signaling.

# Table of Contents

Résumé.....	III
Abstract.....	IV
Table of Contents .....	V
List of Figures.....	VIII
List of Tables .....	XI
Abbreviations .....	XII
Acknowledgements .....	XV
<b>1. Introduction.....</b>	<b>1</b>
<b>1.1. Hyperpolarization activated cyclic-nucleotide gated (HCN) channels .....</b>	<b>2</b>
<b>1.1.1. Discovering the Action Potential .....</b>	<b>2</b>
<b>1.1.2. Discovering the <math>I_h</math> current .....</b>	<b>5</b>
i. Preliminary studies in cardiac cells.....	5
ii. Contradictions and characterization of $I_f / I_h$ .....	6
iii. Reinterpreting $I_h$ and further characterization .....	8
<b>1.1.3. Physiological role of the <math>I_h / I_f</math> current.....</b>	<b>9</b>
i. $I_f$ in the heart .....	9
ii. $I_h$ in the brain .....	11
<b>1.1.4. Regulation of <math>I_h</math> current and uncovering HCN channels .....</b>	<b>12</b>
i. Regulation by cyclic-nucleotides.....	12
ii. Discovering the HCN channel and isoforms.....	14
iii. Regulation by lipids .....	15
iv. Regulation by auxiliary proteins .....	16
<b>1.1.5. Structural characteristics of HCN channels.....</b>	<b>16</b>
<b>1.2. Cannabinoids.....</b>	<b>20</b>
<b>1.2.1. Origins and family of cannabinoids .....</b>	<b>20</b>

i.	Exogenous cannabinoids .....	20
ii.	Endogenous cannabinoids .....	21
iii.	Synthetic cannabinoids .....	23
1.2.2.	Cannabinoid receptors .....	24
i.	Discovery of isoforms and unique characteristics.....	24
ii.	Structural characteristics .....	24
iii.	Cannabinoid receptor ligands.....	26
1.2.3.	Regulatory and signaling pathways .....	27
1.2.4.	Physiological and therapeutic properties of cannabinoids .....	30
1.2.5.	Regulation of ion channels by cannabinoids .....	32
i.	Transient receptor potential (TRP) channels.....	32
ii.	Potassium channels .....	33
iii.	Sodium channels .....	33
iv.	Calcium channels .....	34
v.	Indirect modulation of HCN channels .....	34
1.3.	Objectives & Hypothesis .....	36
2.	Materials and Methods.....	38
2.1.	Drugs and reagents .....	38
2.2.	Molecular biology and cell expression .....	38
2.3.	Electrophysiological recordings.....	39
2.4.	Data analysis and statistics.....	40
2.5.	Intracellular cGMP Assay.....	41
3.	Results .....	42
3.1.	Cannabidiol activates TRPV1 channels.....	42
3.2.	Time dependent regulation of HCN1 by cannabinoids .....	45
3.3.	Insights into the mechanism of cannabinoid regulation of HCN1 channels .....	55
3.3.1.	Role of cyclic-nucleotide binding domain (CNBD).....	55
3.3.2.	Manipulating membrane fluidity with Triton-X 100 .....	62

<b>4. Discussion .....</b>	<b>66</b>
<b>4.1. Regulation of HCN1 channels by CBD and THC .....</b>	<b>66</b>
<b>4.2. Mechanistic insights into the modulation of HCN1 by CBD and THC .....</b>	<b>69</b>
<b>4.3. Physiological and therapeutic applications .....</b>	<b>71</b>
<b>4.4. Future directions .....</b>	<b>72</b>
<b>4.4.1. Short term.....</b>	<b>72</b>
<b>i. Other cannabinoids.....</b>	<b>72</b>
<b>ii. Monitor intracellular cGMP/cAMP in Xenopus oocytes .....</b>	<b>73</b>
<b>iii. FLIPR Potassium Assay .....</b>	<b>75</b>
<b>4.4.2. Long term .....</b>	<b>76</b>
<b>i. Patch-clamp electrophysiology .....</b>	<b>76</b>
<b>ii. Structural studies .....</b>	<b>76</b>
<b>iii. Putative binding site and computational studies .....</b>	<b>77</b>
<b>Conclusion .....</b>	<b>78</b>
<b>References.....</b>	<b>79</b>

## List of Figures

<b>Figure 1: Schematic of the regulation of an action potential by ion channels (Adapted from (Campbell et al., 2008)).....</b>	<b>4</b>
<b>Figure 2: Measurement of <math>I_f</math> current in sino-atrial (SA) nodes (Adapted from (H. F. Brown et al., 1979b)). .....</b>	<b>7</b>
<b>Figure 3: Action of cardiac currents in various tissues of the heart (Adapted from (Hume &amp; Grant, 2015)) .....</b>	<b>10</b>
<b>Figure 4: Action potential in a neuronal cell's axon hillock (Adapted from (Molnar, 2019)) .....</b>	<b>11</b>
<b>Figure 5: Investigating the regulation of <math>I_h</math> by cAMP (Adapted from (D. DiFrancesco &amp; Tortora, 1991)) .....</b>	<b>13</b>
<b>Figure 6: Structure of human HCN1 channel (Adapted from (Lee &amp; Roderick, 2017)) .....</b>	<b>17</b>
<b>Figure 7: Ion channel characteristic: Domain swapping (Adapted from (Lee &amp; Roderick, 2017; Matthies et al., 2018)) .....</b>	<b>19</b>
<b>Figure 8: Examples of exogenous cannabinoids.....</b>	<b>21</b>
<b>Figure 9: Examples of endogenous cannabinoids .....</b>	<b>22</b>
<b>Figure 10: Examples of synthetic cannabinoids.....</b>	<b>23</b>
<b>Figure 11: Structure of human CB1 receptor bound to AM841 and G-protein coupled complex (Adapted from (T. Hua et al., 2020)).....</b>	<b>26</b>
<b>Figure 12: Mechanics of the endocannabinoid system (ECS) (Adapted from (Donvito et al., 2018)).....</b>	<b>29</b>
<b>Figure 13: Physiological avenues of cannabinoid modulation in various parts of the brain (Adapted from (NIDA, 2021)).....</b>	<b>31</b>

<b>Figure 14: Regulation of <math>I_h</math> by activation of CBR1 (Adapted from (Vargish &amp; McBain, 2016)).</b>	<b>35</b>
.....	
<b>Figure 15: Indirect and proposed direct regulation of CBD on HCN1 channels.....</b>	<b>37</b>
<b>Figure 16: Electrophysiological characteristics of TRPV1 ion channels.....</b>	<b>42</b>
<b>Figure 17: Regulation of TRPV1 by cannabidiol (CBD).....</b>	<b>43</b>
<b>Figure 18: Time and concentration dependent regulation of HCN1 by cannabinoids. ....</b>	<b>46</b>
<b>Figure 19: Cannabidiol's distinct regulation in HCN1 channels. ....</b>	<b>47</b>
<b>Figure 20: HCN1 stepwise protocol.....</b>	<b>48</b>
<b>Figure 21: HCN1-WT current in presence of cannabidiol (CBD). ....</b>	<b>49</b>
<b>Figure 22: Regulation of HCN1-WT by cannabidiol (CBD).....</b>	<b>50</b>
<b>Figure 23: HCN1-WT current in presence of <math>\Delta^9</math>-tetrahydrocannabidiol (THC).....</b>	<b>51</b>
<b>Figure 24: Regulation of HCN1-WT by <math>\Delta^9</math>-tetrahydrocannabidiol (THC).....</b>	<b>52</b>
<b>Figure 25: Regulation of HCN1-WT by methanol (MeOH). ....</b>	<b>53</b>
<b>Figure 26: Insights into the HCN1-<math>\Delta</math>CNBD construct. ....</b>	<b>55</b>
<b>Figure 27: HCN1-<math>\Delta</math>CNBD current in presence of cannabidiol (CBD).. ....</b>	<b>56</b>
<b>Figure 28: Regulation of HCN1-<math>\Delta</math>CNBD by cannabidiol (CBD). ....</b>	<b>57</b>
<b>Figure 29: HCN1-<math>\Delta</math>CNBD current in presence of <math>\Delta^9</math>-tetrahydrocannabidiol (THC).....</b>	<b>58</b>
<b>Figure 30: Regulation of HCN1-<math>\Delta</math>CNBD by <math>\Delta^9</math>-tetrahydrocannabidiol (THC).....</b>	<b>59</b>
<b>Figure 31: Regulation of HCN1-<math>\Delta</math>CNBD by methanol (MeOH). ....</b>	<b>60</b>
<b>Figure 32: Graphical representation of membrane fluidity. ....</b>	<b>62</b>
<b>Figure 33: HCN1-WT current in presence of Triton-X 100 (TX-100).....</b>	<b>63</b>
<b>Figure 34: Regulation of HCN1-WT by Triton-X 100 (TX-100).....</b>	<b>64</b>

**Figure 35: Intracellular cGMP concentrations in *Xenopus* oocytes in presence of cannabinoids..... 74**

**\*PROTEIN STRUCTURES WERE CREATED USING CHIMERA (Pettersen et al., 2004)**

**\*ALL FIGURES WERE CREATED OR EDITED USING BIORENDER.COM**

## **List of Tables**

**Table 1: Steady state activation data for HCN1-WT in presence of cannabinoids ..... 54**

**Table 2: Steady state activation data for HCN1- $\Delta$ CNBD in presence of cannabinoids ..... 61**

**Table 3: Steady state activation data for HCN1-WT in presence of TX-100 ..... 65**

## Abbreviations

HCN: Hyperpolarized-activated cyclic-nucleotide gated

CNG: Cyclic-nucleotide gated

$I_{K2}$ : Strong inward rectification current

$I_{Kr}$ : Delayed rectifier potassium current

$I_f$ : “funny current”

$I_h$ : Inward current activated by hyperpolarization

$V_m$ : Membrane potential

SAN: Sino-atrial nodes

AVN: Atrioventricular nodes

EPSPs: excitatory postsynaptic potentials

IPSPs: inhibitory postsynaptic potentials

M-type  $K^+$  current: Potassium invoked current in  $K_v7$  channels

cAMP: Cyclic adenosine monophosphate

cGMP: Cyclic guanine monophosphate

cCMP: Cyclic cytidine monophosphate

PKA: Protein kinase A

PIP<sub>2</sub>: Phosphatidylinositol-4,5-bisphosphate

M $\beta$ CD: Methyl- $\beta$ -cyclodextrin

$K_v$ : Voltage-gated potassium channel

KCNE2: Voltage-gated potassium channel (subfamily E regulatory subunit 2)

TRP8b: Transient receptor potential channel

PDB: Protein data bank

HCND: HCN domain

VSD: Voltage sensor domain

CNBD: Cyclic-nucleotide binding domain

PD: Pore domain

GYG: Glycine-tyrosine-glycine selectivity filter

Cryo-EM: Cryogenic Electron Microscopy

NMR: Nuclear Magnetic Resonance

eCB: Endogenous cannabinoid  
CB1: Cannabinoid receptor type 1  
CB2: Cannabinoid receptor type 2  
GPCR: G protein-coupled receptor  
CBD: Cannabidiol  
THC:  $\Delta^9$ -tetrahydrocannabidiol  
CBDV: Cannabidivarin  
THCV: Tetrahydrocannabivarin  
CBN: Cannabinol  
pCB: phytocannabinoids  
AEA: Anandamide  
2-AG: 2-Arachidonoylglycerol  
2-AGE: 2-Arachidonyl glyceryl ether  
NADA: N-Arachidonoyl dopamine  
WIN 55,212: Potent aminoalkylindole synthetic cannabinoid  
ECS: Endocannabinoid system  
CNS: Central nervous system  
PNS: Peripheral nervous system  
CRIP1a: Cannabinoid receptor interacting protein a  
CRIP1b: Cannabinoid receptor interacting protein b  
TRPV1: Transient receptor potential channel 1 (subfamily V member 1, Vanilloid receptor 1)  
ABHD6:  $\alpha/\beta$ -hydrolase domain-6  
ABHD12:  $\alpha/\beta$ -hydrolase domain-12  
DAGL- $\alpha$ : diacylglycerol lipase- $\alpha$   
FABP: fatty acid binding protein  
FAAH: fatty acid amide hydrolase  
MAGL: monoacylglycerol lipase  
NAPE: N-arachidonoyl phosphatidylethanolamine  
PPAR- $\alpha$ : peroxisome proliferator-activated receptor alpha  
BLA: basolateral amygdala  
GIRK1/4: G-protein coupled inwardly rectifying potassium channel

I<sub>Kr</sub>: delayed rectifier potassium current

hERG: human Ether-à-go-go-Related channel

Na<sub>v</sub>M: Voltage-gated sodium channels isolated from *M. marinus*

JNKs: c-Jun N-terminal kinases

NOS: nitric oxide synthase

GC: guanylyl cyclase

TX-100: Triton-X 100

CHO cells: Chinese hamster ovarian cells

HEK cells: Human embryonic kidney cells

N2a: Neuro2a cells (neuroblastoma cell line)

## Acknowledgements

There was a point in time where I thought pursuing graduate studies was improbable. And all was impossible to achieve. To say that my time at the Université de Montréal was memorable would be an understatement.

I would like to take the time to thank my supervisor Dr. Nazzareno D'Avanzo for his relentless support through times of struggle and the countless conversations about my project, life, and future studies. It will forever mold my upcoming scientific journey. And lab member, Yoann Lussier, thank you for your mentorship, answering all my pertinent questions and all the great conversations we had outside and inside the laboratory.

To my parents and sister, whom I love whole heartedly. Thank you for your endless support in this journey and for putting up with the times I came home stressed.

Finally, to my loving girlfriend. Thank you for being my partner, friend, source of motivation and the reason for my high drive for success. I do not know how I will ever repay you for relentless push to make me who I am today.

*Learning never exhausts the mind.*

--Leonardo da Vinci

# 1. Introduction

Ion channels are a family of proteins which regulate the rate of permeability of ions such as sodium, potassium, and calcium. Different classes of these transmembrane proteins serve a specific purpose in the cell's lifespan. Embedded within the plasma membrane, ion channels also regulate the passage of water and other small molecules. The open and closed gating mechanism of ion channels are regulated by different variables such as changes in membrane potential ( $V_m$ ), ligand binding and interaction with different auxiliary proteins. The regulatory mechanism underlining each ion channel leads to the opening or closing of a hydrophilic pore which allows passage of ions and molecules. The directional movement of ions is regulated by an electrochemical gradient exhibited by the cell. Additionally, ion channels and in parallel ionotropic receptors are part of the main proteins which generate membrane potential and electrical signaling in excitable cells, such as neurons and muscle cells.

Hyperpolarization activated cyclic-nucleotide gated (HCN) channels are ion channels which generate the  $I_h$  or pacemaker current. Prior to the discovery of HCN channels, the pacemaker current  $I_h$  was found to be present in the cardiac tissues of various species including human (Dario DiFrancesco, 1985).  $I_h$  was later discovered to be present in neurons of the central and peripheral nervous systems as well. Distinct from other voltage-dependent cation channels, HCN channel opening (activation) occurs when the membrane is hyperpolarized rather than depolarized. When these channels open, they permit a net influx of  $Na^+$  ions, that then depolarizes the cell membrane, which then causes the channels to close (deactivate). Therefore, this autoregulation of HCN channels provides rhythmic activity regulation, membrane potential regulation, and pace making activity to excitable cells. HCN channels have been an important component in understanding various diseases such as neurological disorders, cardiac abnormalities, mood stabilization and sleep wake cycles. There are various regulatory pathways which modulate the pacemaker current produced by HCN channels. Several studies have been conducted to investigate HCN regulation by different auxiliary proteins, small molecules, and lipids. For example, HCN channels have been shown to be regulated by cholesterol and phosphoinositide (Fürst & D'Avanzo, 2015; Pian, Bucchi, Decostanzo, Robinson, & Siegelbaum, 2007). Cannabinoids are an important class of lipids that have been shown to be linked in a potential treatment of disorders linked to altered HCN

channel function including, epilepsy, pain, anxiety, mood, and circadian cycles.

Cannabinoids are small, generally lipophilic ligands which can either be extracted from plants *cannabis sativa* (exogenous), naturally found in the human body (endogenous) or synthetically produced. But cannabinoids are not simply ligands which are sitting in the plasma membrane like a phospholipid or cholesterol, the main course of action of these molecules are through receptors. The two main targets for cannabinoid binding are cannabinoid receptors (CBR 1 & 2) and TRPV1 ion channels (Pumroy et al., 2019). Both part of the endocannabinoid system (ECS) in humans and animals, cannabinoids and cannabinoid receptors are studied for their potential therapeutic applications. In addition to acting on CBRs, cannabinoids have been shown to regulate various channels independently of CBRs, including TRP, sodium, potassium, and calcium ion channels (Ahrens et al., 2009; Chemin et al., 2001; Starkus et al., 2019; Pumroy et al., 2019).

Cannabinoids appear to be effective therapeutics for several neurological disorders (Cooray et al., 2020; Iannotti et al., 2014) in which HCN channels have been suggested as potential therapeutic targets, including epilepsy, pain, major mood disorders, etc. (Ku & Han, 2017; Peng et al., 2010; Ramírez et al., 2018). Various studies have shown that cannabinoids which act as ligands can modulate different ion channels. Knowing this, we hypothesize that HCN channels could be directly modulated by cannabinoids. Using electrophysiological measurements, we want to unravel the molecular mechanism by which cannabinoids regulate HCN channels. Our data indicates cannabidiol (CBD) and  $\Delta^9$ -tetrahydrocannabidiol (THC) modulate the overall hyperpolarization current in HCN1 channels. We also attempt to determine the mechanism of action, including whether CBD and THC alter HCN1 currents through changes in membrane fluidity.

## **1.1. Hyperpolarization activated cyclic-nucleotide gated (HCN) channels**

### **1.1.1. Discovering the Action Potential**

Electrical excitability in neuronal and cardiac cells have been studied since the start of the 19<sup>th</sup> century. A preliminary model of the now named action potential, which represents electrical excitability in cells, was created in 1952 by Hodgkin and Huxley. The first action potentials were

recorded using the giant squid axon as a mammalian model for a subsequent replacement for small nerve fibers (Hodgkin & Huxley, 1939). Voltage-clamp techniques revealed several changes in membrane potential when the sample was placed in varying ionic solutions at different concentrations. First, the resting membrane potential, a fixed voltage of a cell would correspond to an equal quantity of potassium and sodium influx and efflux (Hodgkin & Huxley, 1952). Changes in the inward current corresponded to sodium ions propagating and an increased shift (depolarization) of the membrane potential (Hodgkin & Huxley, 1952). Changes in outward current corresponded to potassium ions propagating and a decreasing shift (repolarization) of the membrane potential (Hodgkin & Huxley, 1952). At the time, repolarization, and the reestablishment of the resting membrane potential ( $V_m$ ), was speculated to end with a spike in voltage towards more negative potentials.

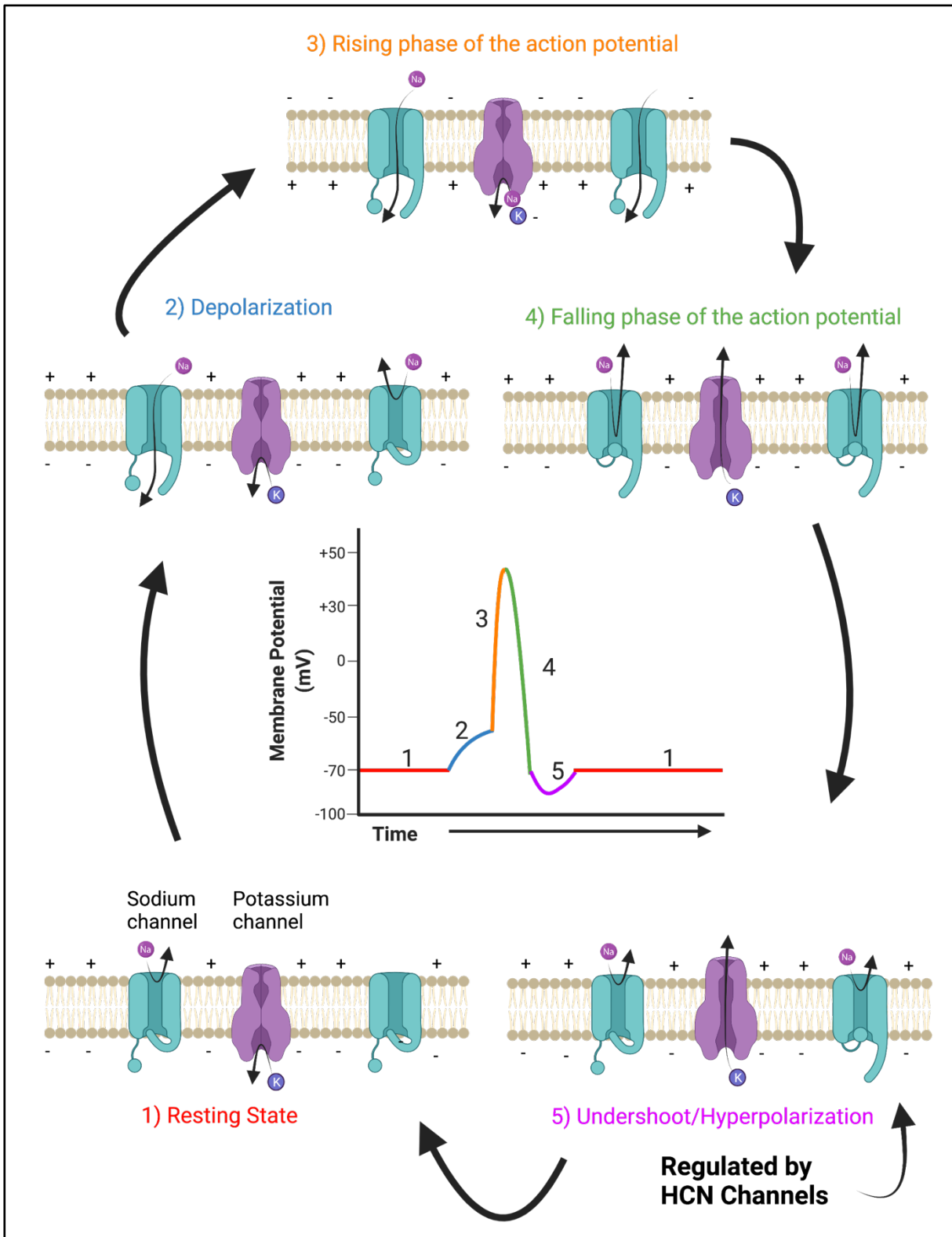


**Figure 1: Schematic of the regulation of an action potential by ion channels (Adapted from (Campbell et al., 2008))**

Changes in electrical excitability and ionic concentrations are not coordinated arbitrarily by the membrane. The physiological process is mechanistically coordinated by various ion channels. The voltage sensitivity and gating properties of ion channels such as potassium, sodium, calcium channels make up the ebbs and flows of an action potential process (Fig. 1). The figure above illustrates each step in which ion channels mechanistically coordinate the action potential. The center of the image represents an action potential profile. At each time point in the profile, a different ion channel is activated, deactivated or in a resting state. The membrane starts by exhibiting a resting state in which an equilibrium is reached between both sodium and potassium ion channels. Upon the rapid spontaneous opening of sodium channels a depolarization occurs and the membrane potential increases to positive potentials. Once the peak of the action potential is reached, sodium channels are maximally activated allowing for a rapid influx of sodium ions through the membrane. Further, upon the falling phase of the action potential, sodium channels rapidly close and deactivate all while potassium channels are in their activation phase. This process called repolarization, allows the cell to return to its resting membrane potential. The final phase in the action potential profile is called hyperpolarization or an undershoot which deals with a sudden decrease in the membrane potential, past the resting state potential. This segment was later identified as the  $I_h$  current.

### **1.1.2. Discovering the $I_h$ current**

#### **i. Preliminary studies in cardiac cells**

Several studies led to the discovery of the hyperpolarization current,  $I_h$ . The first intracellular electrode recordings studying the cardiac component in an action potential used mammalian cardiac tissue isolated from dog heart (Draper & Weidmann, 1951). It was hypothesized that by modifying the extracellular concentration of sodium ions around the tissue that there would be a change in the diastolic depolarization of the cells. Therefore, in the event of a sudden increase in net inward sodium, diastolic current would fall and play a role in auto-rhythmicity in cardiac cells (Draper & Weidmann, 1951). Probing the underlying mechanism further, in 1968 Noble and Tsien spearheaded the characterization of the “pacemaker current” (Noble & Tsien, 1968). Kinetics and rectification properties of the supposed pure potassium ionic nature of the current were studied.

Electrophysiological recordings in cardiac Purkinje fibers, revealed a slow outward and deactivating potassium current upon applying hyperpolarization voltages, which again had a role in pacemaker activity. Due to its potassium ionic nature and time-dependent decay under hyperpolarized conditions, the current was identified as “ $I_{K2}$ ” (Noble & Tsien, 1968).

## **ii. Contradictions and characterization of $I_f / I_h$**

Inconsistencies between the various studies on  $I_h$  tarnished the understanding of the kinetics and ionic nature of this elusive current. The current’s characteristics had discrepancies such as not behaving ideally upon deactivation and it being abolished when studies were conducted in a sodium-free environment (Dario DiFrancesco, 1985). Additionally, the preliminary studies of the pacemaker were shown to be inconclusive as they failed to include the use of the two-microelectrode voltage-clamp technique. The method was discovered in 1976 by Noma and Irisawa and was used to demonstrate that the current was voltage dependent (Noma & Irisawa, 1976). Whether or not the current was inward or outward and activated by depolarization or hyperpolarization was still eluding electrophysiologists at the time. To study the inward potassium current component, it had to be separated from its impeding and overlaying outward potassium current component. Purkinje cells exhibit this overlaying phenomenon hence, the study was moved to sino-atrial (SA) nodes in mammalian cells (H. a. D. D. a. N. S. Brown, 1979; Dario DiFrancesco, 1985). Sino-atrial (SAN) and atrioventricular (AVN) myocytes or nodes were cardiac muscle cells which were the focus of many studies involving the pacemaker current. Using this mammalian model in addition to the two-microelectrode electrophysiological technique, the hyperpolarization current was seen in a new light.

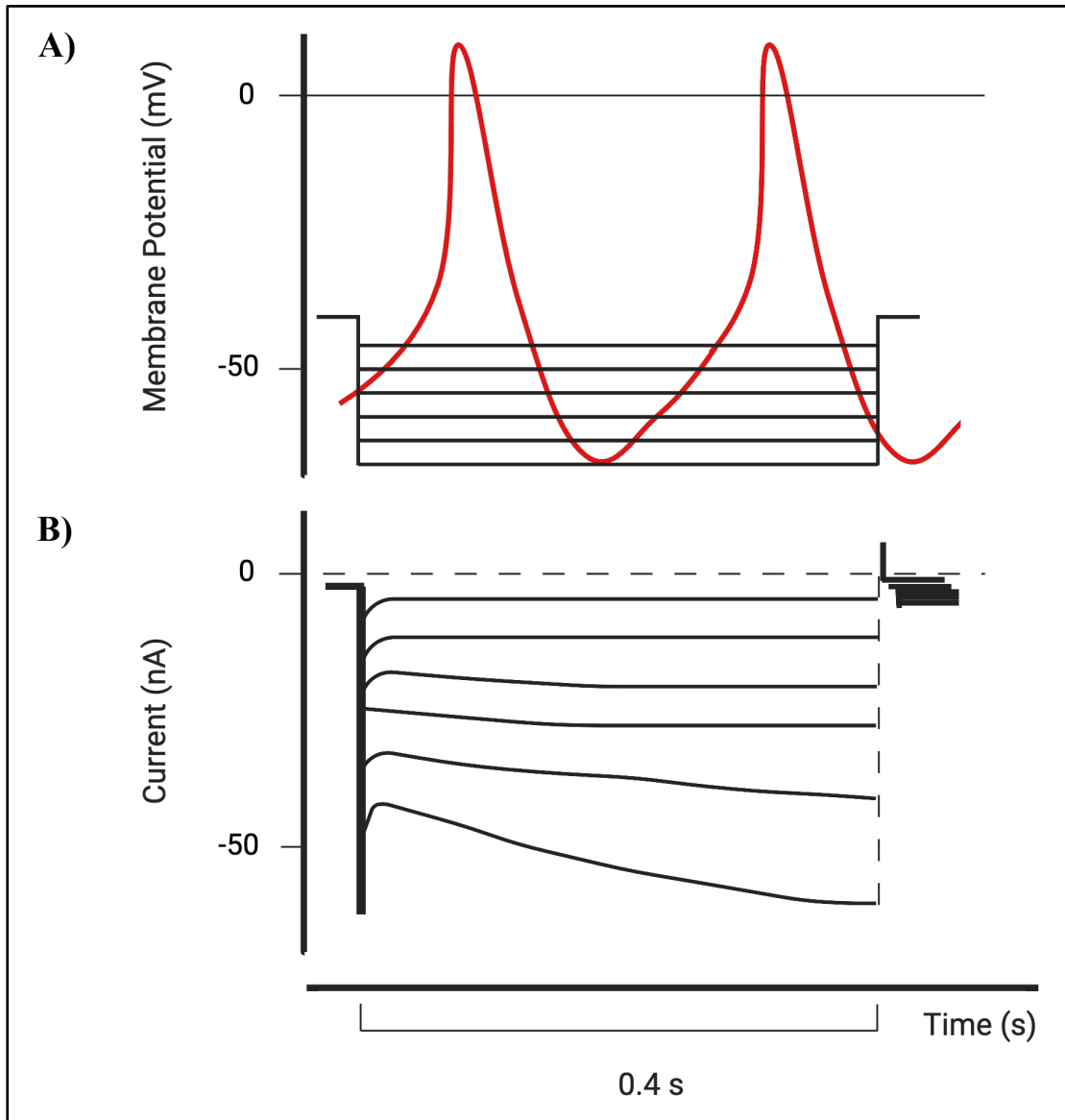


**Figure 2: Measurement of  $I_f$  current in sino-atrial (SA) nodes** (Adapted from (H. F. Brown et al., 1979b)).

The funny current ( $I_f$ ) was the nomenclature used to describe a current which exhibited distinct characteristics.  $I_f$  was activated in a negative voltage range, therefore the current was studied by hyperpolarizing the cell membrane (H. Brown et al., 1979a). A stepwise protocol (holding at -42 mV) was applied, which consisted of hyperpolarized pulses (Fig. 2A). The idea was to focus on the pacemaker current. The voltage protocol was applied over the course of 0.4 seconds, and it was clear at a given voltage a corresponding hyperpolarized current would ensue (Fig. 2B). This also

meant that there were changes in the  $I_f$  as it had a time dependency in correlation to the increasing hyperpolarized voltages (Fig. 2A & B). The exploratory study in SA nodes also revealed adrenaline dependent activation of the  $I_f$  current (H. F. Brown et al., 1979b). Changes in potassium ion concentration surrounding the cells demonstrated a steady increase in current conductance (H. a. D. D. a. N. S. Brown, 1979). Later, the current which activated upon hyperpolarization, was named the hyperpolarization current  $I_h$  (Yanagihara & Irisawa, 1980).

### **iii. Reinterpreting $I_h$ and further characterization**

Electrophysiological studies in cardiac cells revealed key kinetic properties of the  $I_f / I_h$  current. However, the results obtained by Noble and Tsien in Purkinje cells needed to be reinterpreted due to discrepancies with other studies. The determination of the differences and similarities of the  $I_h$  current in the different types of cardiac cells (SA nodes, AV nodes and Purkinje) were at a standstill up until previous studies using cesium were reanalyzed. It was previously shown that cesium can block the  $I_{K2}$  current in Purkinje cells (Isenberg, 1976). However, cesium was only shown to block the inward portion of the current. Therefore, there was a need to differentiate the inward and outward currents to determine whether the pacemaker current in Purkinje cells was similar to the current studied in SA nodes. The effects of compounds such as cesium, potassium and rubidium on the current were studied in calf Purkinje cells (D. DiFrancesco, 1982). Cesium was shown to deplete and inhibit  $I_f$  rapidly and rubidium also inhibits  $I_f$ , however, to a lesser extent (D. DiFrancesco, 1982).  $I_f$  can was activated by an increase in extracellular potassium concentration. Interestingly, in the presence of 5 mM of barium, the current was activated to more negative potentials (D. DiFrancesco, 1981). These studies revealed the true ionic, mechanistic, and kinetic nature of the hyperpolarized activated currents. However, several minor details remained ambiguous about the properties of the pacemaker current. It was later confirmed that both potassium and sodium ions affected the currents activation (Dario DiFrancesco, 1985). Electrophysiological studies in single isolated cardiac Purkinje cells, confirmed the ambiguities left to determine about the current. For instance, the isolation of thick fibers derived from Purkinje cells showed that the inward current, which is regulated by sodium and potassium ions, was in fact the pacemaker current (Callewaert, 1984). In addition, there was confirmation on the activation of the current during hyperpolarization (Callewaert, 1984). The mechanics, kinetics, and regulatory

aspects of the current do not properly portray the pacemaker current. It due to its ionic nature that it was speculated to be modulated by cation channels. Therefore, several physiologists were keen on discovering the current's role in physiology and the in human body.

### **1.1.3. Physiological role of the $I_h$ / $I_f$ current**

#### **i. $I_f$ in the heart**

The role of the pacemaker current differs between cell types, specifically between cardiac cells and non-cardiac cells. However, the basic properties of the current remained similar between cell type. Using experiments previously conducted with adrenaline as a reference, the physiological function of the current was examined. The diastolic “slow phase” is the depolarization step in an action potential. Cardiac cells tend to relax and prepare for the eventual initiation of a new action potential (D. DiFrancesco, 1993). It was discovered that the range of hyperpolarized voltages in which the  $I_h$  current is activated, falls within the same range in which these diastolic events occurs (Dario DiFrancesco, 1985). Therefore, it was hypothesized that the pacemaker current contributes to the spontaneous portion of the action potential in cardiac cells, modulating the resting membrane potential and rhythmicity. It was imperative that the cell line used in voltage-clamp experiments be tested at the voltage range indicative of hyperpolarization events to be classified as a cell which expresses the pacemaker current.

Several moving parts make up a single heartbeat. AV nodes, SA nodes, Purkinje fibers are the predominant cardiac tissues which are involved in spontaneous pacemaker activity in the heart (Fig. 3). The organ undergoes two forms of cardiac activity; a non-nodal form derived from the network of Purkinje fibers embedded in the surrounding tissue of the heart and a nodal form derived from AV and SA nodes. Regular sinus rhythm starts at the SA node. Its slow diastolic potassium driven inward current is a major contributor to the speed of the depolarization in an action potential (D. DiFrancesco et al., 1979). Like SA nodes, AV nodes are once again involved in spontaneous depolarization, heartbeat automaticity and underlie a predominantly slow potassium current in a later phase of the action potential. It was also speculated and later confirmed that the nodal form of cardiac activity was modulated by slow L-type calcium channels (Zipes & Fischer, 1974). The second mode in a cardiac current event (non-nodal) stems from Purkinje fibers

which were one of the first cardiac tissues studied in electrophysiology. These fibers are responsible for quick action potentials and exhibit a rapid depolarizing sodium current modulated by voltage-gated sodium ion channels. Rapidity in the current often leads to an overshoot. Calcium channels modulate the slow repolarization phase. Which leads to a faster potassium channel modulation of the repolarization back to the resting membrane potential. To drive a regular sinus rhythm every aspect of nodal and non-nodal cardiac pace making must be sustained to avoid irregularities such as atrial fibrillation (quicker than regular heartbeat) and bradycardia (slower than regular heartbeat).

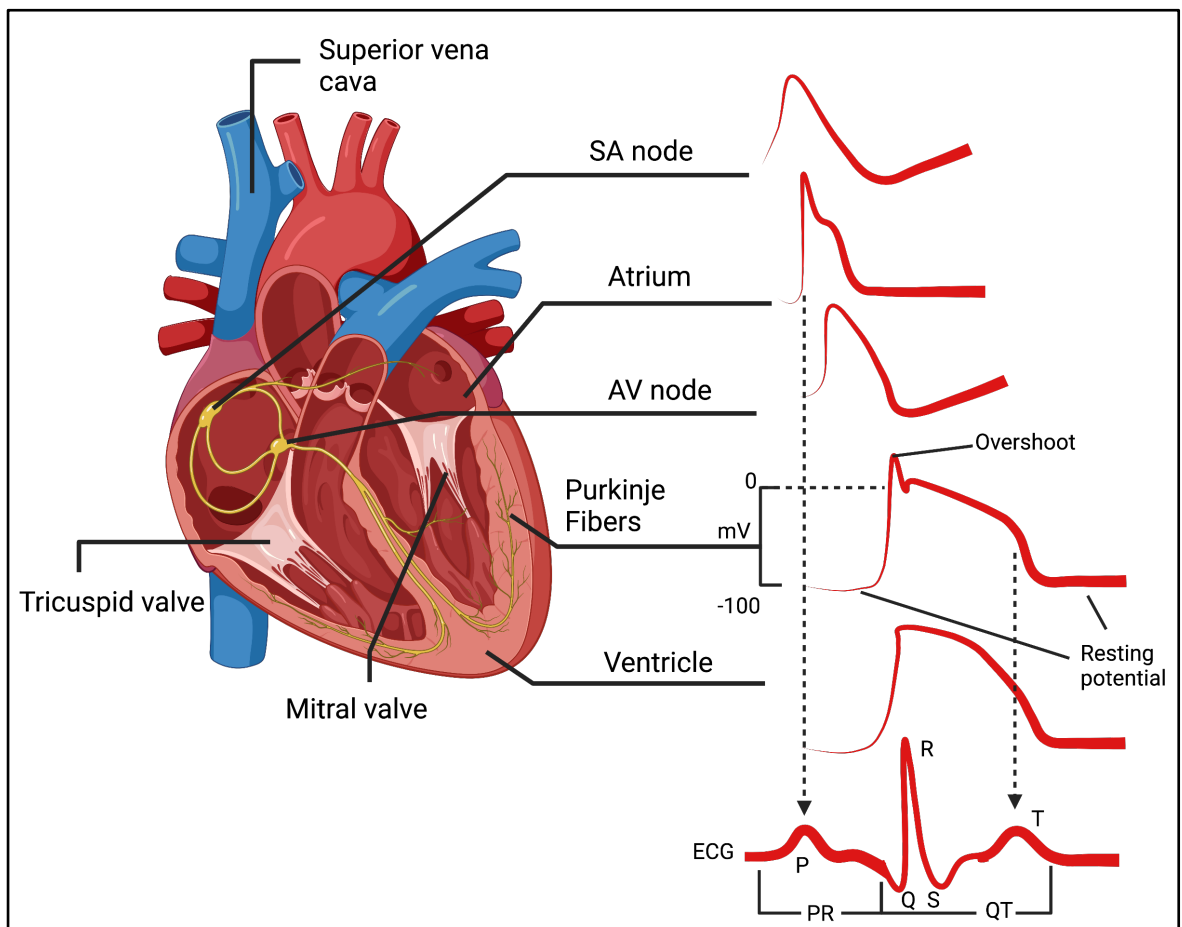


**Figure 3: Action of cardiac currents in various tissues of the heart** (Adapted from (Hume & Grant, 2015))

## ii. $I_h$ in the brain

In addition to its imperative role in cardiac physiology, the pacemaker current has also been known to regulate various functions in neuronal cells such as, synaptic plasticity and neuronal excitability (Baruscotti, 2005). Specifically in neurons, during the creation of rhythmic activity due to  $I_h$ , there is a resulting pacemaker depolarization (Pape, 1996). One of the first studies looking into the modulation of  $I_h$  in neurons, used isolated vertebrate rods from salamander retina (Bader et al., 1982). The single-pipette voltage-clamp technique provided insights in the inward rectifying current. In addition to being activated upon hyperpolarization, the current was blocked after adding extracellular cesium and activated (~50%) after an increase in extracellular potassium ion concentration.

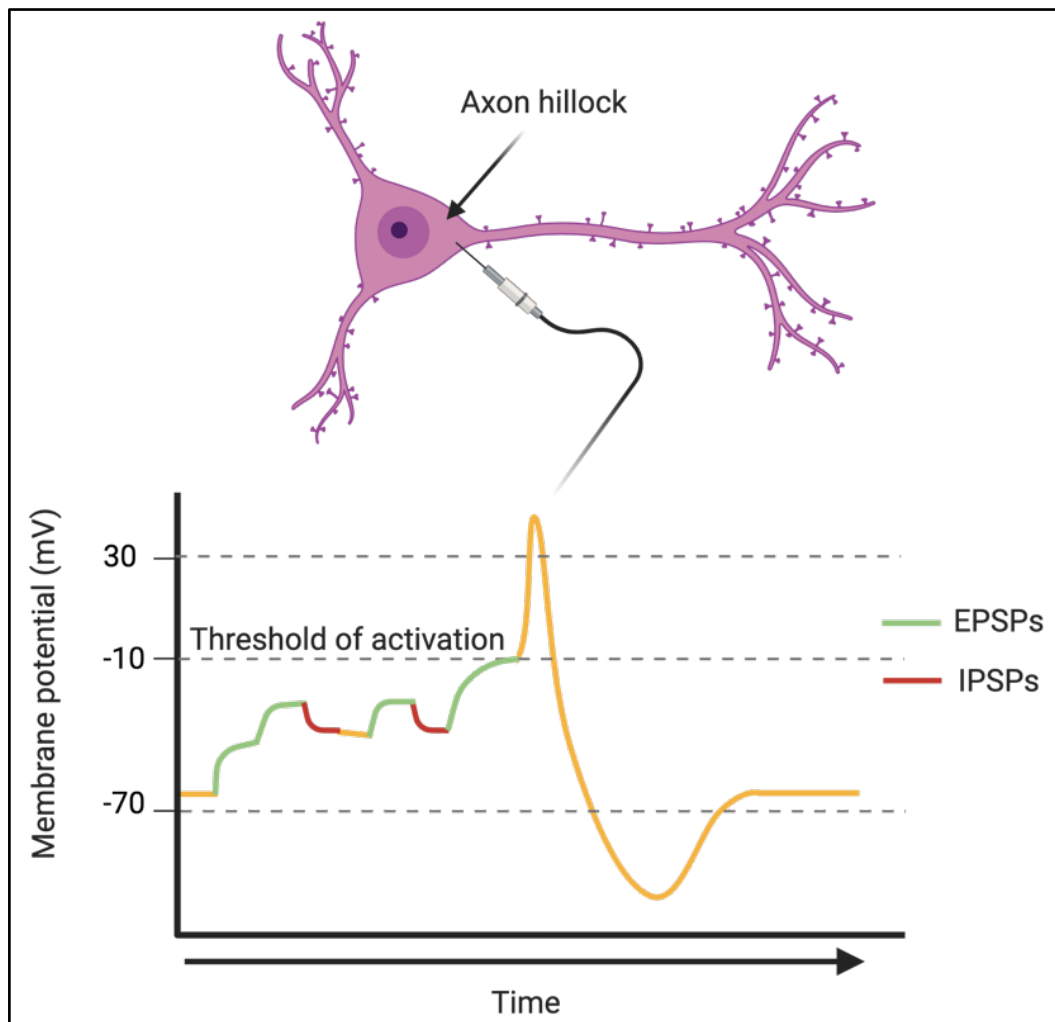


Figure 4: Action potential in a neuronal cell's axon hillock (Adapted from (Molnar, 2019))

Today, slice electrophysiology with a whole cell approach is used to study the role of the hyperpolarized current neurons. The axon hillock (Fig. 4) is the segment in a neuron where an electrical impulse is generated and reveals several important characteristics of an action potential in the brain. Excitatory postsynaptic potential (EPSPs) and inhibitory postsynaptic potentials (IPSPs) demonstrate the ebbs and flows (summation) of membrane potentials, which determines if an action potential reaches its threshold of activation (Fig 4). EPSPs are characterized as a sudden depolarization, due to the rapid opening of sodium channels. IPSPs are seen as an action potential inhibitor, regulated by an influx of chloride ions which hyperpolarize the cell membrane (more negative  $V_m$ ). The role  $I_h$  plays in the temporal summation of EPSPs and IPSPs is intricate.  $I_h$  is shown to significantly reduce the overall temporal summation in a neuronal action potential, therefore promoting the excitatory action potential. Additionally,  $I_h$  is responsible, in a time-dependent manner for rebound firing in onset neurons and for an after-hyperpolarization event (Koch & Grothe, 2003). More recently, it was determined that through the interactions with a M-type potassium current,  $I_h$  is responsible for EPSP inhibition, which means the threshold of activation is not reached (George et al., 2009). The role the  $I_h$  current plays in neurons is intriguing, but it remains understudied. Concomitantly, the kinetics and physiological nature of the  $I_h$  current differs between each region of a neuron or origin of the neuronal cell.

#### **1.1.4. Regulation of $I_h$ current and uncovering HCN channels**

##### **i. Regulation by cyclic-nucleotides**

As previously mentioned,  $I_h$  was identified and characterized through a series of voltage-electrode experiments. Kinetic and physiological properties of the  $I_h$  current pushed electrophysiologists to provide insights as to how the current is regulated. Different modulators of  $I_h$  would give an idea as to how the current is activated, inactivated, or inhibited. Adrenaline is a molecular hormone which was proven to activate the pacemaker current (H. F. Brown et al., 1979b). Eventually, the pacemaker current was speculated to be modulated through a second messenger ligand in cyclic adenosine monophosphate (cAMP) (Fig. 5A). This mode of regulation in turn effects neuronal and cardiac physiology. The secondary messenger ligand has also been

linked to the regulation of several other ion channels. However, the link between the pacemaker current  $I_h$  and cAMP remained unclear.

Given the current exhibited mechanistic changes with manipulations in sodium, potassium, and calcium extracellular ion concentrations, in addition to the blocking by cesium, a link between an ion channel and the  $I_h$  current was hypothesized. In 1991, changes in intracellular cAMP was shown to directly activate the ion channel associated to the pacemaker current (D. DiFrancesco & Tortora, 1991). Using cell-attached electrophysiology in SA node myocytes, cardiac pacemaker channels with their associated ( $I_f$ ) current were monitored and studied. The direct activation by cAMP was studied with parallel experiments. A constant repetitive pulse voltage of -105 mV was applied to the cell in conjunction with the absence (1) wash in (2) and wash out (3) of 100  $\mu\text{M}$  cAMP (Fig. 5B & C). A time course (60 seconds) revealed a 10 pA increase in current (Fig. 5B).

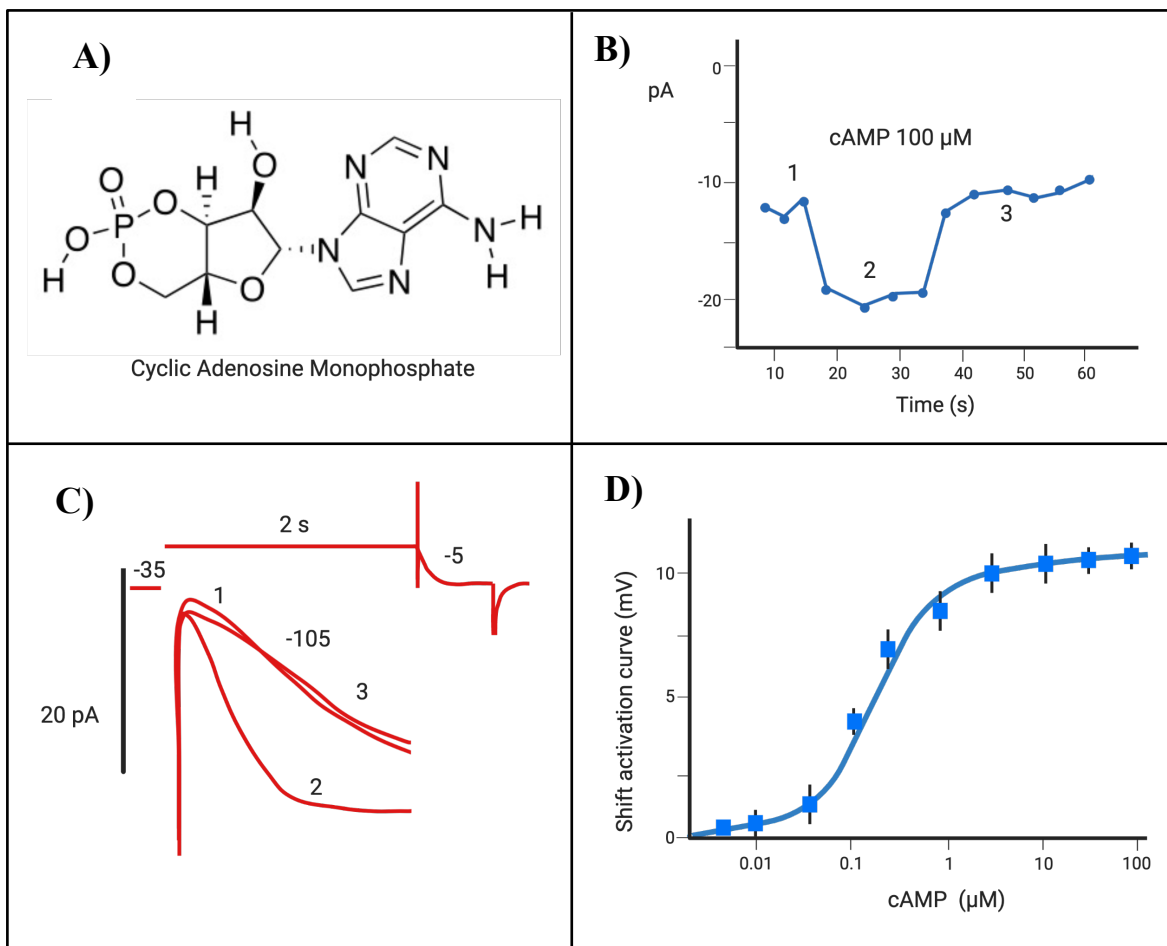


**Figure 5: Investigating the regulation of  $I_h$  by cAMP** (Adapted from (D. DiFrancesco & Tortora, 1991))

In addition to its rapid reversibility, cAMP was shown to act as an independent current activator. In the absence of extracellular adenosine triphosphate (ATP) which activates endogenous kinases such as catalytic subunit protein kinase A (PKA), the current was still activated by cAMP (Fig. 5C). The addition of various concentrations of cAMP (0.01-100  $\mu$ M), revealed a +10 mV depolarizing shift in voltage-dependent activation of the pacemaker current (Fig. 5D). The effect of other secondary messenger ligands such as cyclic guanine monophosphate (cGMP) and cyclic cytidine monophosphate (cCMP) were also studied.  $I_f$  was shown to be activated by cGMP and cCMP. However, the activation occurred through weaker specificity (D. DiFrancesco & Tortora, 1991). The ionic nature, voltage dependency, and cyclic-nucleotide regulation of the current are characteristics which are commonly found in ion channels.

## ii. Discovering the HCN channel and isoforms

Various families of ion channels which are embedded in the membrane are regulated by ligands and changes in the lipid bilayer. The ion channel responsible for the native pacemaker current was originally hypothesized to be part of the cyclic-nucleotide-gated (CNG) channel family because of its modulation by cAMP and part of the voltage-gated potassium channel family due to its voltage dependency (B. Santoro et al., 1997). The first hyperpolarization activated cyclic-nucleotide (HCN) channel was unexpectedly identified in 1997. A novel ion channel called, *mBCNG-1*, was identified, sequenced, and shown to interact (through yeast two-hybrid) with the domain of the N-src SH3 bait protein, which is highly expressed in neurons. *mBCNG-1* was shown to have distinct characteristics, like those in the voltage-gated potassium channel family. However, the newly discovered protein also exhibited non-selective ion behavior and contained a cyclic-nucleotide binding domain (CNBD) situated at its C-terminus (Bina Santoro et al., 1998). The channel was shown to be more selective for potassium than sodium ions (4:1). This selectivity ratio, when compared to the ones found in traditional potassium channels are quite different as they exhibit a hundred-fold (100:1) selectivity for potassium. The novel and newly characterized channel had similarities to various well-known families of ion channels, however, determining there was a need to establish a link between the channel and the pacemaker current.

The isoforms of *mBCNG-1*, *mBCNG-2,3,4* (mHCN1,2,3,4), were isolated from *Mus musculus* (mouse) (Bina Santoro et al., 1998). The isoforms also had a highly conserved 80 to 91% sequence

homology (Monteggia et al., 2000). Additionally, they were proven to have similar and conservative structures, like in the family of voltage gated potassium channels. More importantly, confirmation of the link between the pacemaker current and the original HCN isoforms was found. RNA encoding for *mBCNG-1* channels were expressed in *Xenopus* oocytes to characterize the kinetics of  $I_h$  currents. Then the channels were activated (direct modulation) with increasing concentrations of intracellular cAMP and the channels were blocked upon the addition of cesium (Bina Santoro et al., 1998). Hence, the identity of the channel behind the pacemaker current was determined. The four isoforms of HCN have been isolated in both brain and heart cells of various species. However, each isoform is expressed in varying amounts depending on the origin of the tissue used for analysis. For example, HCN1 and HCN2 are predominantly expressed in neuronal cells while HCN4 and HCN2 are predominant in cardiac cells (Calejo et al., 2014). Each isoform is quite different in their role and mode in which they are regulated. As previously mentioned, cAMP and cGMP regulate the voltage-dependence of HCN channels. Although not all HCN isoforms conform to the same level of activation in the presence of a cyclic-nucleotide. Upon cAMP binding, HCN2 and HCN4 isoforms are known to exhibit large activation while HCN1 and HCN3 undergo a weaker activation (He, 2014). Further studies revealed, channel kinetics were dissimilar between isoforms. HCN1 has the quickest activation kinetics upon hyperpolarization while HCN4 exhibits the slowest activation kinetics (He, 2014).

### **iii. Regulation by lipids**

In addition to cyclic-nucleotides, lipids such as, phosphatidylinositol-4,5-bisphosphate (PIP<sub>2</sub>) (Zolles, 2006) and cholesterol (Fürst & D'Avanzo, 2015) are also known to allosterically regulate HCN channels. Like cAMP and through varying degrees of activation, each isoform is distinct in sensitivity to the natural level of PIP<sub>2</sub> or cholesterol in the cell membrane. However, it is important to note, activation of cAMP is independent of the activation by lipids. PIP<sub>2</sub> prompts channel opening and slows down channel kinetics (slower closure) by activating the voltage dependency of HCN channels to more depolarized potentials by +20 mV (Pian et al., 2006; Zolles, 2006). Electrostatic interactions between the negatively charged head groups of the lipid and residues in the HCN channel causes dilation of the pore (Zolles, 2006). Therefore, these electrostatic interactions modulate channel gating by lipids. Using methyl- $\beta$ -cyclodextrin (M $\beta$ CD) a

macrocyclic compound which can be used to sequester cholesterol out of the membrane, human isoforms HCN1, 2 and 4 were also shown to be modulated by changes in cholesterol content. Enriching or depleting cholesterol in the lipid composition of CHO-K1 cells expressing the isoforms lead to different levels of modulation. It was determined that HCN1, 2 and 4 exhibited a decrease in current density upon cholesterol depletion and HCN4 underwent a +10 mV depolarizing shift in steady-state activation (Fürst & D'Avanzo, 2015).

#### **iv. Regulation by auxiliary proteins**

HCN channels have been known to establish protein-protein interactions with protein kinases. Protein kinases are known to be regulators of various ion channels and modulate the expression level of HCN proteins (He, 2014). Controlling the expression level of HCN channels has an adverse effect on the total basal pacemaker current generated by the cell upon hyperpolarization. In 1997, Wu and Cohen identified that tyrosine kinase phosphorylation was a  $I_h$  current inhibitor (Wu, 1997). Hinting at a possible protein-protein interaction, HCN channels are also known to be indirectly regulated by several auxiliary proteins (He, 2014). KCNE2, for example, is a single-helix membrane spanning protein that regulates several potassium channels (Abbott, 2015). When expressed simultaneously with HCN4, KCNE2 has been shown to increase the activation kinetics of the pacemaker current (Decher, 2003; Lussier et al., 2019). TRIP8b, another auxiliary protein, has also been shown to modulate HCN channels (Bina Santoro et al., 2011b). TRIP8b interact with the HCN1 protein at two positions, near the cyclic-nucleotide binding domain (CNBD) and with a triple amino acid moiety (Ser-Asn-Leu) (Bina Santoro et al., 2011b). These interactions were revealed to inhibit HCN1 channel opening and modulate trafficking (Bina Santoro et al., 2011b). The cellular signaling of HCN proteins is highly regulated and has several modulators. Therefore, prior to the discovery of new modulatory avenues on HCN channels, several well characterized modulators must be considered.

#### **1.1.5. Structural characteristics of HCN channels**

HCN channels form tetramers (four subsequent subunits) and they are comprised of six characteristic transmembrane domains, which are all common characteristics in  $K_v$  and CNG

channels (Craven & Zagotta, 2006). The four subunits of the channel surround and make up the pore domain in a symmetrical fashion (Zagotta et al., 2003). Out of the channel's six helical domains (S1-S6), S1 through S4 are the domains responsible for sensing voltage changes throughout the membrane. This cluster of S1-S4 is named the voltage sensor domain (VSD) (Fig. 6). The novel HCN domain (HCND) which is in direct contact with S4, was also identified (Lee & Roderick, 2017). When the channel is in a tetrameric form, it is hypothesized that the HCND acts as an anchor, which is part of the C-linker. The S5-S6 domains line the pore and regulate ion permeation (pore domain (PD)). The C-linker domain connects the S6 with the cyclic-nucleotide binding domain (CNBD) (Fig. 6). As the name suggests, the CNBD is regulated by cyclic-nucleotides such as cAMP and cGMP. This modulation activates the channel by relieving the inhibition by the CNBD and shifts the voltage-dependency to more positive voltages, hence increasing the probability that the channel is open at a given voltage.

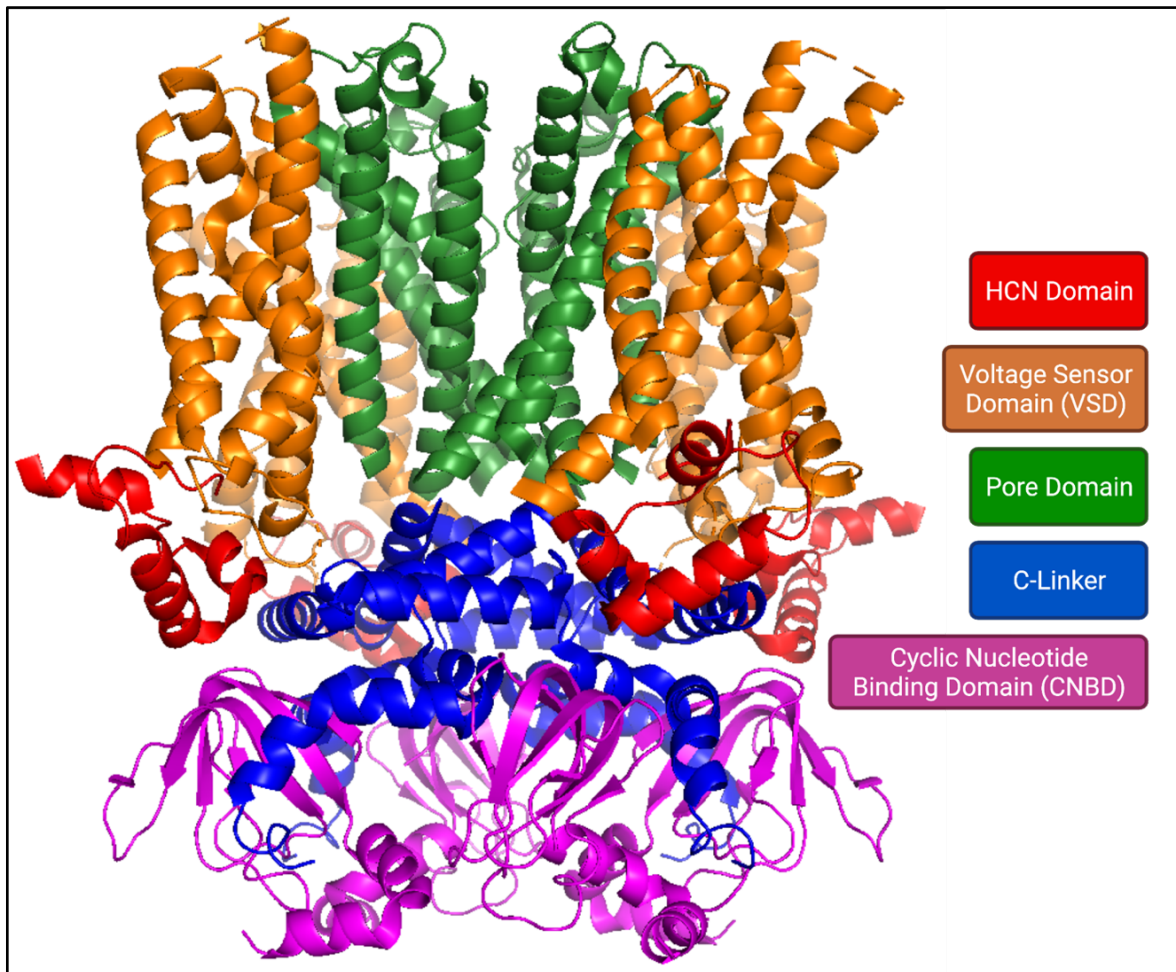


**Figure 6: Structure of human HCN1 channel** (Adapted from (Lee & Roderick, 2017))

Structural characteristics between the four isoforms are similar as they have a 60% sequence homology (Ludwig, 1999). However, the central portion of the sequence, which includes the pore, transmembrane and cyclic-nucleotide binding domains have a 90% sequence similarity. (Zagotta et al., 2003). All four isoforms have been isolated from human and mouse species. Recently, a construct of the human HCN1 isoform has been purified and studied by cryo-electron microscopy (cryo-EM) (Lee & MacKinnon, 2017) (Fig. 6). The structure of this construct has given us crucial knowledge about the channel's ion permeability, voltage sensing mechanism and cyclic-nucleotide binding domain structural conformity. The permeability of ion channels is quite important. Regulating the total number of ions and the type of ions which pass through the cell membrane is imperative to proper cellular function. HCN channels are semi-selective. However, after analyzing the pore, the reason why these channels are less selective for potassium (4:1) when compared to  $K_v$  channels (100:1) was uncovered. In contrast to other potassium channels, which have four binding sites within the selectivity filter, HCN channels only have two in the GYG (Glycine-Tyrosine-Glycine) selectivity filter (Lee & MacKinnon, 2017). This unique feature allows the permeation of other ions, in addition to potassium and sodium. HCN channels are voltage-dependent due to the ability of subunits S1-S4 to detect subtle changes in membrane voltages (Lee & MacKinnon, 2017). Most potassium channels have voltage-sensors which are domain swapped meaning the VSD of one subunit is in contact with PD of the neighboring subunit (Fig. 7A) (Mascarenhas & Gosavi, 2017). However, HCN channels are non-domain swapped, meaning the VSD of one subunit is in contact with the PD of the same subunit (Fig. 7B) (Lee & Roderick, 2017). Interestingly, the S4 helix in HCN channels is longer when compared to other cyclic-nucleotide gated channels and contains more positively charged amino acids (Lee & MacKinnon, 2017). Another interesting discovery which is unique to HCN channels is the fact that, in the hyperpolarized conformation, the S4 helix is speculated to interact and disturb the S5 and S6 domains which line the channel pore (Lee & MacKinnon, 2017). Since the interactions which regulate the S5-pore-S6 ensemble are disturbed, channel gating would be affected. Insights on the mode in which cAMP interacts with the CNBD portion of the channel was also examined. Overlaying the structure in the absence and presence of the ligand, identified conformational changes which occur within the binding site of the channel. A binding site which led to the opening of the channel through the propagation of the pore helices (Lee & MacKinnon, 2017). The

discovery of novel molecules which can directly or indirectly modulate HCN channels could play an integral role in finding potential therapeutics.

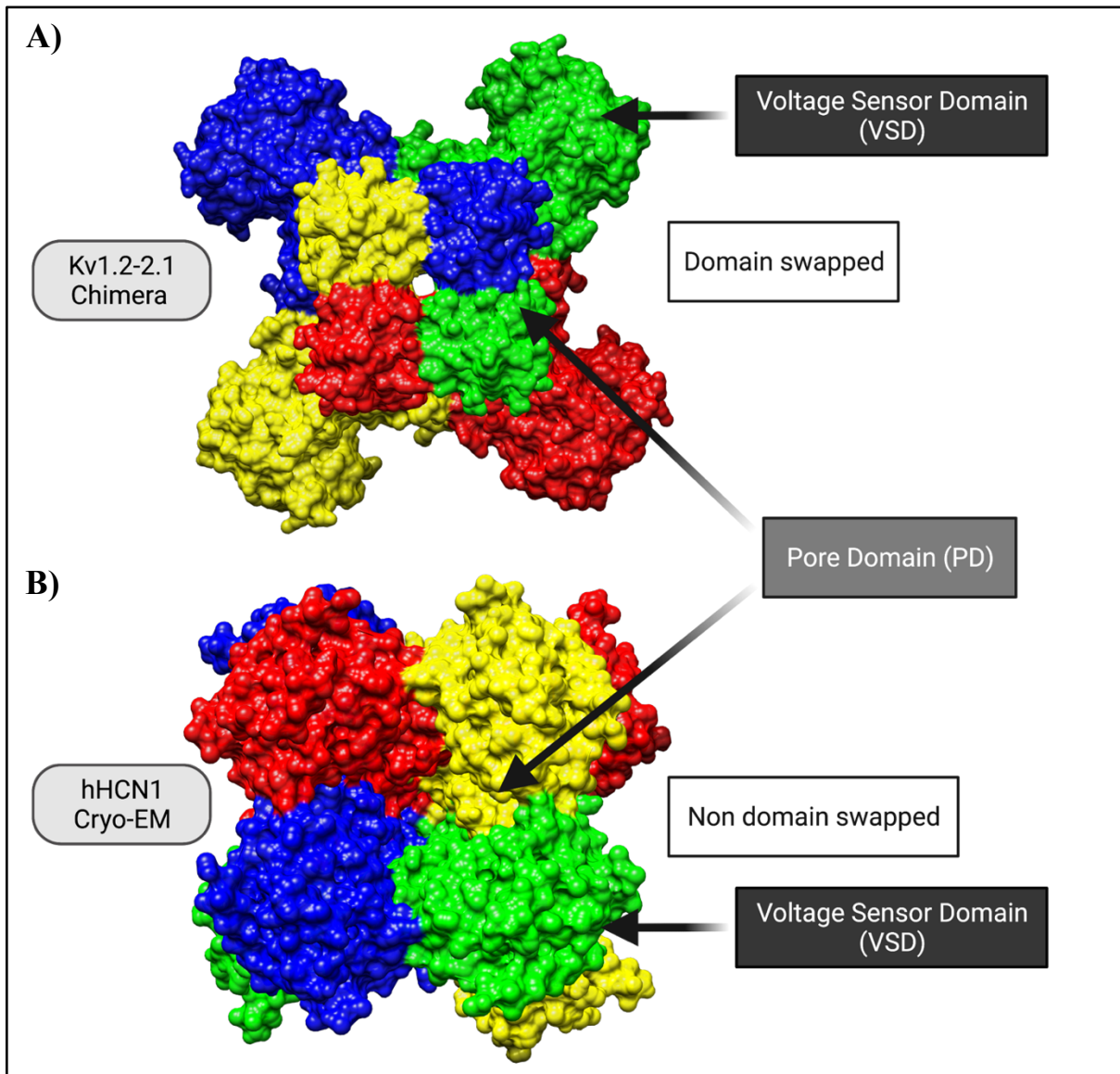


**Figure 7: Ion channel characteristic: Domain swapping** (Adapted from (Lee & Roderick, 2017; Matthies et al., 2018))

## 1.2. Cannabinoids

### 1.2.1. Origins and family of cannabinoids

#### i. Exogenous cannabinoids

Marijuana (hashish) was originally used medicinally 5000 years ago in China but, the active molecular constituents from the *cannabis sativa* plants have been studied only since the early to mid-1800's (Hanus, 2007). In addition to medical uses, the psychotropic effects from *cannabis sativa* plants also intrigued chemists in determining the plants molecular composition. Difficulties in properly identify these ambiguous molecular components was a problem up until the 1960's when cannabidiol (CBD) and  $\Delta^1$ -tetrahydrocannabidiol were isolated and characterized as non-psychoactive cannabinoids with the aid of nuclear magnetic resonance (NMR) (Gaoni & Mechoulam, 1971; R. Mechoulam & Shvo, 1963; Pertwee, 1988).

There are several other active ingredients which have been identified in cannabis plants, one of which being  $\Delta^9$ -tetrahydrocannabidiol (THC), which is the main psychoactive component (Gaoni & Mechoulam, 1971). The psychoactive (THC) and non-psychoactive (CBD) molecular constituents of *cannabis sativa* are represented in Figure 8 below. Since the discovery of CBD and THC, there have been approximately 120 different cannabinoids which have been isolated from *cannabis sativa* (Morales et al., 2017). Being one the first identified active ingredients in cannabis, CBD is classified as an exogenous cannabinoid since it is not naturally produced by humans. These cannabinoids are placed under the class of exogenous or phytocannabinoids (pCB) due to their link with its plant organism.

Cannabinoids share common structural characteristics. They have an aromatic (dibenzopyran) ring center and a hydrophobic alkyl chain (Fig. 8). However, pCBs differ when it comes to their substituent groups located on the dibenzopyran ring. Exogenous cannabinoids such as cannabidivarin (CBDV), tetrahydrocannabivarin (THCV) and cannabinol (CBN) have a different alkyl chain length or slight differences in their other aromatic ring. For example, CBD contains two separate alcohol groups in the *meta* positions on the benzene ring, as compared to THC which has an alcohol group on one end but a closed pyran ring containing an oxygen on the other end (R. Mechoulam & Shvo, 1963). The pyran ring moiety in THC makes the molecule more rigid,

compared to CBD. Another characteristic which is common amongst exogenous cannabinoids are the fact that they are highly lipophilic seeing as they are derived from oil specimens extracted from *cannabis sativa* (Raphael Mechoulam et al., 1998; Paton, 1975). The importance of the isolation of these molecules was imperative to determine their role in medicine for example, alleviating pain, stabilizing mood, antibacterial properties, and aid in neurological disorders.

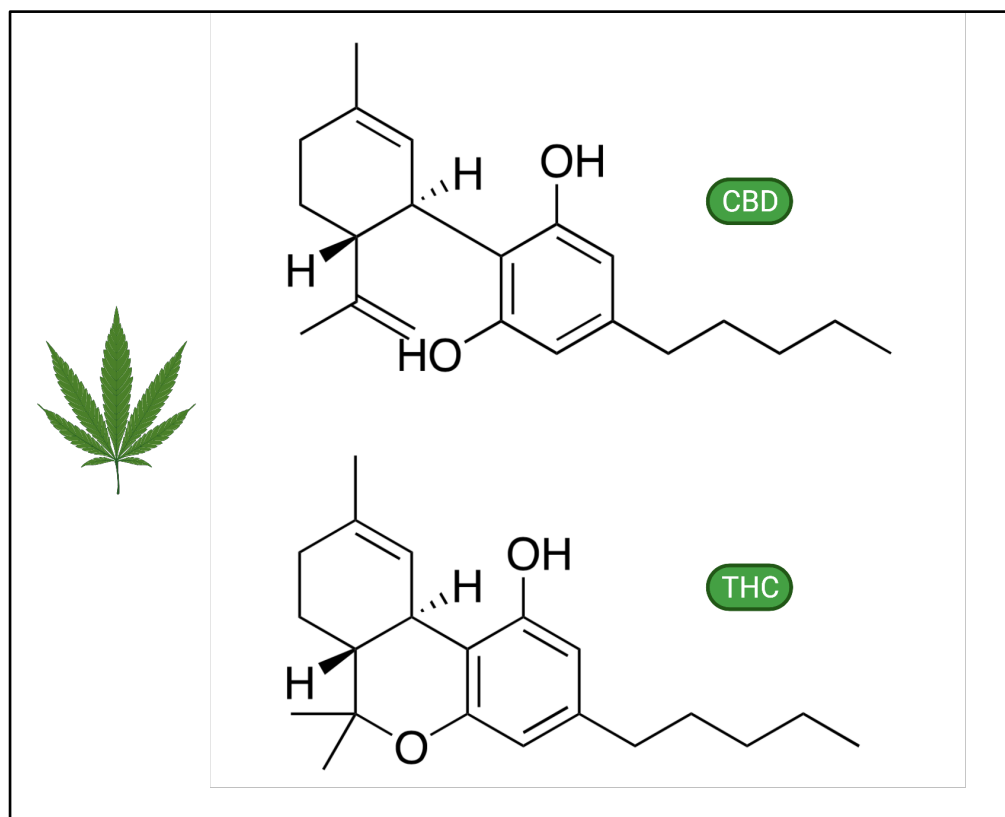


**Figure 8: Examples of exogenous cannabinoids**

## **ii. Endogenous cannabinoids**

Endogenous cannabinoids (eCBs) are defined as ligands which are produced naturally by humans and animals. Seeing as the lipophilicity of exogenous cannabinoids is high, endogenous cannabinoids which were isolated from human brain samples were also considered to be highly lipophilic (Devane et al., 1992; Raphael Mechoulam et al., 1998). The first endogenous cannabinoid isolated from porcine brain samples was arachidonylethanolamide (anandamide (AEA)) (Fig. 9) (Devane et al., 1992). Anandamide is a ligand which is highly lipophilic and

consists of a methyl, methylene, alcohol, and an amide group. However, the ligand differs from CBD and THC, as it does not contain a central aromatic ring and was found to be naturally produced in various mammalian tissues (Devane et al., 1992). Not much was known about the role of the receptors to which exogenous cannabinoids bind, however the discovery of pre-fabricated cannabinoids isolated from human brain tissue provided evidence for the existence of these receptors and hinted at their function (Devane et al., 1992).

Moreover, the endocannabinoid, 2-monoglyceride (or 2-arachidonyl glycerol (2-AG)) was isolated from the canine intestine (R. Mechoulam et al., 1995). Similar in structure to AEA, the molecule contains two adjacent alcohol groups connected to a carboxylate ester group rather than an amide group. Additionally, 2-AG produced similar effects to those of THC, with studies conducted in mice. This discovery gave rise to the idea of exogenous and endogenous cannabinoids working under a similar system. However, the receptor, signaling cascade and regulatory components of this cannabinoid system remained elusive.

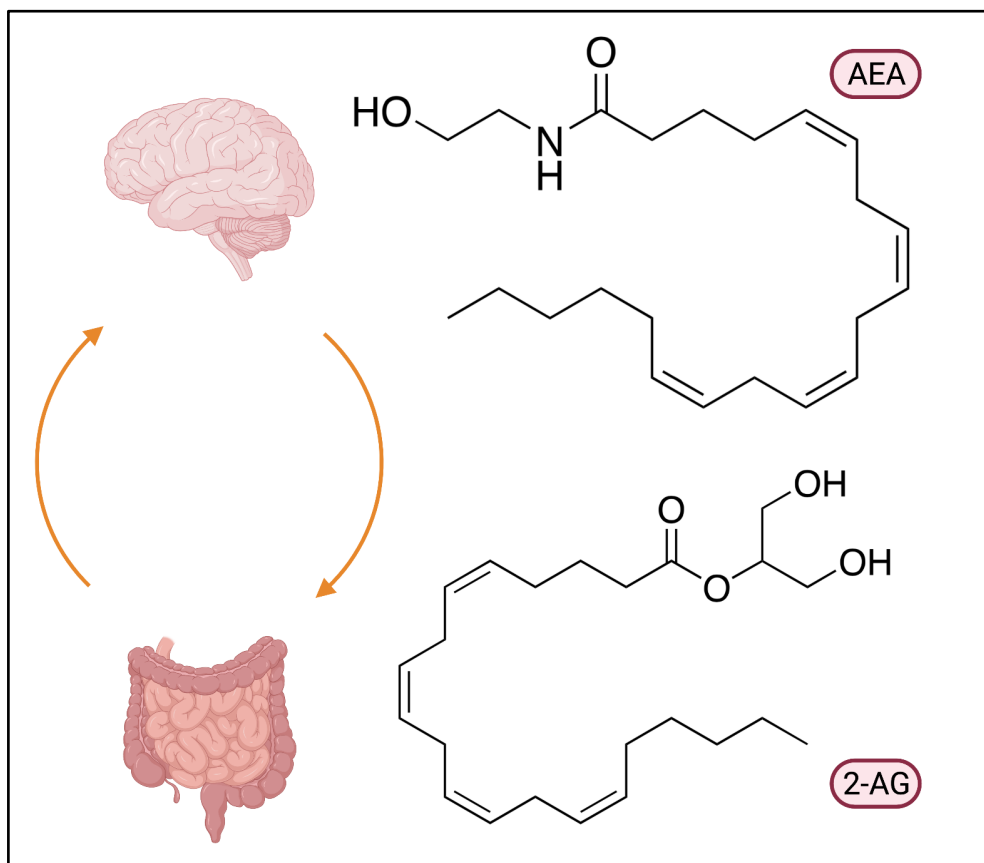


**Figure 9: Examples of endogenous cannabinoids**

### iii. Synthetic cannabinoids

Despite the discovery of several exogenous and endogenous cannabinoids, the development of synthetic cannabinoid mimics is ongoing. Being able to either block, enhance or compete with the activity of other cannabinoids, synthetic cannabinoids can be quite useful in several exploratory studies. For example, WIN55,212 (Niederhoffer & Szabo, 1999) and CP-55,940 (Wiley et al., 1995) were shown to act as potent cannabinoid receptor agonists (Fig. 10). They exhibit higher affinity and specificity (compared to endogenous and exogenous cannabinoids) to the newly discovered cannabinoid receptors (CBRs). The use of synthetic cannabinoids has expanded over the years. For example, covalent cannabinoid ligand, AM841 (Fig. 10) was developed to act as an irreversible CBR agonist (Keenan et al., 2015).

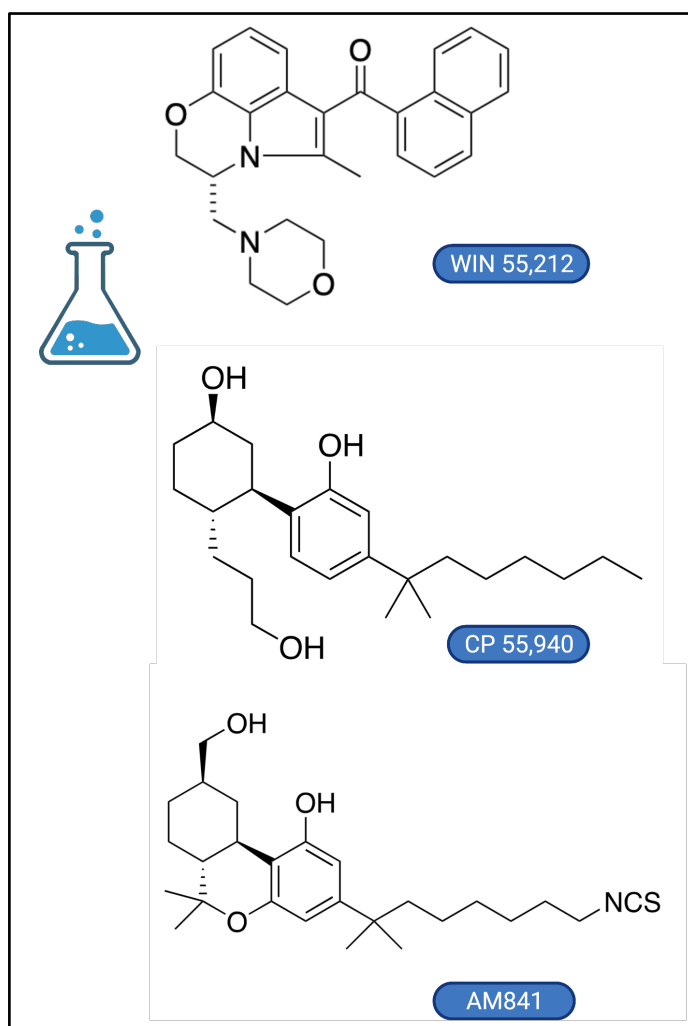


Figure 10: Examples of synthetic cannabinoids

## **1.2.2. Cannabinoid receptors**

### **i. Discovery of isoforms and unique characteristics**

Cannabinoids are flexible and lipophilic compounds. These ligands were originally shown to interact with the cell membrane, however, the primary target for cannabinoids was later determined to be to bind to cannabinoid receptors (CBRs). Like other receptors and ion channels, CBRs have different isoforms. Coming from the family of G protein-coupled receptors (GPCRs), the isoforms, CB1 and CB2 were subcloned, expressed and characterized (Matsuda et al., 1990; Munro et al., 1993). Cannabinoid-binding assays were used to determine that both isoforms are modulated by synthetic cannabinoid ligands such as CP55,940, HU-210 and WIN55-212 (Felder et al., 1992). Although CB1 and CB2 receptors experience similar modulation in the presence of cannabinoids, these isoforms are still distinct. Many amino acid residues were different when the amino acid sequence of the transmembrane portion for the two isoforms were compared (Munro et al., 1993). The CB1 receptor was isolated from brain tissue and are mainly expressed in neuronal cells (R. G. Pertwee, 2005). The CB2 receptor was isolated from the spleen and is predominantly expressed in immune cells (R. G. Pertwee, 2005). It was hypothesized that since the two isoforms were isolated from two different cell types, that there would also be differences in their physiological roles. Both psychoactive and non-psychoactive cannabinoids were shown to bind to both receptors. However, the CB1 receptor was shown to modulate the response upon psychoactive cannabinoid ligand binding (Ashton et al., 2008). The CB2 receptor on the other hand was shown to modulate the response after non-psychoactive cannabinoid ligand binding and the potential therapeutic target for inflammation and pain related ailments (Soethoudt et al., 2017). The structural details of the cannabinoid receptors were left uncharacterized, until they were found to be in the same family as a previously characterized receptor.

### **ii. Structural characteristics**

CBRs are part of two protein families, the G-protein-coupled and  $\alpha$ -rhodopsin (GPCR) families. These relationships helped in determining the structural details and characteristics of the CB1 and CB2 receptors. The isoforms share a poor sequence identity of about 44% (Munro et al.,

1993), although, when compared, they were recently shown to have similar tertiary structures (T. Hua et al., 2020). Previous studies of the bovine rhodopsin structure (Okada et al., 2000), computational modelling, and ligand binding assays, helped in determining the structure of the CB1 and CB2 receptors. CBRs, like other GPCRs, are composed of seven transmembrane domains (7-TM) (in which, CB1 and CB2 share a 68% sequence identity), three extracellular loops (ECL1-3), three intracellular loops (ICL1-3), a N-terminal domain and a C-terminal domain (Munro et al., 1993; Ye et al., 2019). Early studies have hypothesized that the interaction between CBRs and G-proteins ( $G_{\alpha i/o}$ ) occurred through the receptor's third intracellular loop (ICL3) and a putative fourth intracellular loop (ICL4) (Howlett, 2005). The putative ICL4 was identified through the palmitoylation of a cysteine residue located in the juxtamembrane C-terminal domain of CBRs (Howlett, 2005; Mukhopadhyay et al., 2000). Although interactions between CBRs and G-proteins were shown, the details of these interactions and specific structural changes which occurred upon ligand binding remained unclear. Recent studies have provided structural insights and a better understanding of the interactions between GPCRs (like CBRs) and G-proteins ( $G_{\alpha i/o}$ ). For instance, Kobilka and his group have recently determined the structure of an  $\mu$ -opioid receptor ( $\mu$ OR) bound to a G-protein ( $G_i$ ) heterotrimer complex (Koehl et al., 2018). The primary points of interactions between the GPCR and G-proteins occur specifically between the TM3, TM5, TM6, ICL2, and ICL3 of the GPCR ( $\mu$ OR) and the C-terminus of the  $G_{\alpha i}$  subunit (Koehl et al., 2018). Upon the binding of a ligand to a GPCR, the ICL2 and ICL3 undergo structural changes (parallel to outward movements of both TM5 and TM6) (Du et al., 2019). This structural arrangement provides a space (in between ICL2 and ICL3) in which the C-terminal domain ( $\alpha 5$ -helix) of the G-protein can insert and interact through multiple amino acid residues (Du et al., 2019; Koehl et al., 2018). CBRs and G-proteins were also found to exhibit similar interactions to those discovered in other GPCR- $G_i$  complexes. When the synthetic cannabinoid, AM841, was bound to CB1 and CB2, the receptors underwent structural changes (in ICL2 and ICL3) which allowed the interactions with the C-terminal domain of the  $G_{\alpha i}$  protein (Fig. 11) (T. Hua et al., 2020). These interactions led to the discovery of a larger protein complex which includes CBRs (CB1/CB2) and the heterotrimer  $G_i$  protein ( $G_{\alpha i}$ ,  $G_{\beta}$ , and  $G_{\gamma}$  subunits) (Fig. 11) (T. Hua et al., 2020; Xing et al., 2020). These structural studies pave the way to understanding how GPCRs like CBRs interact with other proteins and further modulate the effect of cannabinoids through various signalling pathways.

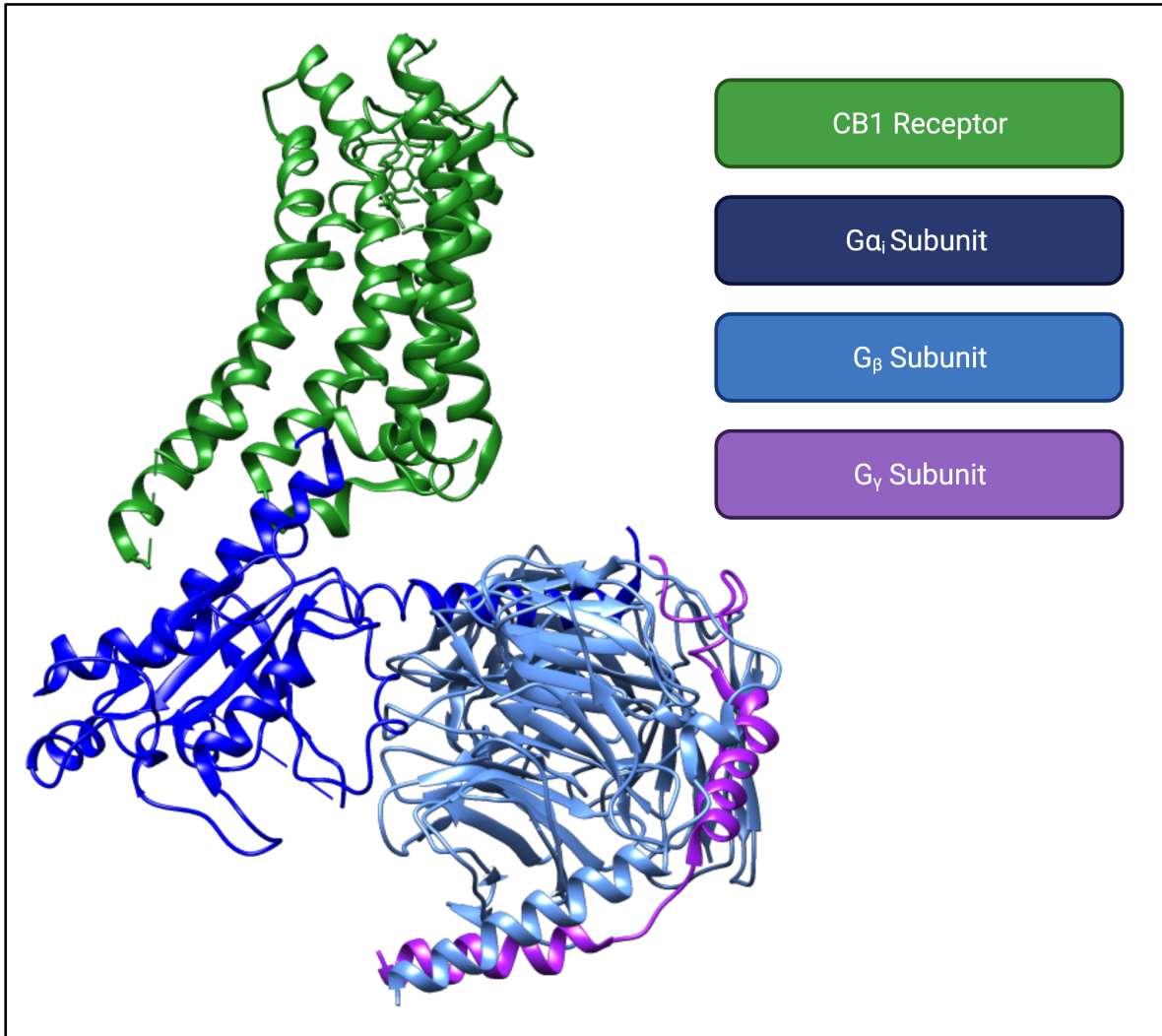


**Figure 11: Structure of human CB1 receptor bound to AM841 and G-protein coupled complex**  
(Adapted from (T. Hua et al., 2020))

### **iii. Cannabinoid receptor ligands**

In 1992, the first human cannabinoid receptor was isolated from neuronal cells and confirmation of receptor's activity was determined through binding assays with synthetic cannabinoids (Gérard, Mollereau, Vassart, & Parmentier, 1991). The binding affinities for the cannabinoids, THC and CBD are different for each of the isoforms of CBR. For example, THC and CBD exhibit binding affinities of 35.2 nM and 2860 nM, respectively, for the human CB2 receptor (Ashton et al., 2008; McPartland et al., 2007). CBD has been consistently shown to have

a weaker binding affinity for CBRs when compared to the binding affinity of THC (Ashton et al., 2008). THC or CBD can still bind either homolog of the receptor, therefore it is difficult to target one receptor over another. Endocannabinoids can also bind CBR. Studies of the structure of CB1 revealed the involvement of TM domains; 2, 3, 6 and 7 (TM2, 3, 6, 7) upon the binding of AEA. 2-AG was also shown to bind to the human CB1 receptor with a binding affinity of 3242.6 nM, compared to 239.2 nM for the binding affinity of AEA (7-fold difference) (Ashton et al., 2008; McPartland et al., 2007).

The binding site on CBRs and the specificity of cannabinoids remained elusive. Early modeling studies, proposed that CB2 receptors contained a hydrophobic pocket (comprising of a conserved lysine residue) in which CP 55,940 can bind (Q. Tao et al., 1999). However, recently, Tian Hua and his group were able to purify, isolate and crystalize the human CB1 receptor at a resolution of 2.8 Å (Tian Hua et al., 2016). A synthetic cannabinoid, AM6538, was used as a probe to determine the stability of an orthosteric binding site on the receptor. Structural components of the receptor were determined shortly after. In the same year, another group purified and crystalized the human CB1 receptor bound to taranabant (2.6 Å resolution), which is a CB1 antagonist (Shao et al., 2016). The study also revealed a unique CBR binding pocket. The binding pocket is considered orthosteric, making it highly specific to cannabinoid-like ligands (Shao et al., 2016). Additionally, the pocket is hydrophobic, as several hydrophobic amino acid residues are lining the site. These findings are in line to the study conducted by Tian and his group. Comparisons were made with the binding sites of other classes of GPCRs to reveal and characterize the orthosteric binding site of CB1. Conceptually, an extracellular loop (ECL2) and the N-terminal domain of TM1 in CB1 was shown to sequester taranabant or AM6538, further forming a “shield” over the binding pocket (Tian Hua et al., 2016; Shao et al., 2016).

### **1.2.3. Regulatory and signaling pathways**

As mentioned previously, both CBR isoforms are coupled to G-proteins. It was discovered that through the activation and binding of cannabinoids to the CBR that it would then couple to  $G_{i/o}$ -proteins and inhibit the production of cAMP (Childers & Deadwyler, 1996; Matsuda et al., 1990). The  $G_i$ -protein subunit in which directly interacts with CBRs is primarily the  $G_{\alpha i}$  subunit. This subunit was isolated from brain extracts and was found to have a canonical function in binding

and directly inhibiting adenylate cyclase, leading to a decrease in cAMP concentration (Bokoch et al., 1984; Sternweis & Robishaw, 1984). Interestingly, CB1 receptor activation upon the binding of the synthetic agonist WIN55,212 has recently been shown to increase cGMP production through activation of mitogen activated protein kinases (MAPKs), nitric oxide synthase (NOS) and stimulation of guanylyl cyclase (GC) (Maroso et al., 2016).

In addition to  $G_{\alpha i}$  signalling, the  $G_{\beta\gamma}$  subunits are also involved in other downstream signalling to regulate ion channels. Specifically, CBRs have been shown to mediate calcium ion channels via  $G_{\beta\gamma}$  subunits (Boczek & Zylinska, 2021; Mirotznik et al., 2000). For example, N- and P/Q-type calcium channels in rat hippocampal neurons have been shown to be inhibited in the presence of synthetic cannabinoid agonist, WIN55,212 (Twitchell et al., 1997).  $G_{\beta\gamma}$  subunits have also played a role in the regulation of other ion channels such as Kir3 potassium channels. Early studies have revealed the regulation of potassium currents by cannabinoids (WIN55,212) via a cAMP and G-protein coupled signalling pathway (Deadwyler et al., 1995; Vásquez et al., 2003). However, the details of the signalling pathway remained understudied. Later, inward rectifying potassium channels, Kir3 (GIRK) were shown to interact with  $G_{\beta\gamma}$  subunits (Lei et al., 2000; Zhao et al., 2003). Recent studies have further shed a light on this CBR, and G-protein coupled process. Using a real-time screening assay, the binding of cannabinoids (WIN55,212, AEA and CP55,940) to the CB1 receptor were shown to allow the dissociation of the  $G_{\beta\gamma}$  subunits from the  $G_{\alpha i}$  subunit, which then interact (and activate) GIRK channels (Andersen et al., 2018). These studies provide direct evidence for the link between the activation of potassium currents and cannabinoids.

Although both CBR isoforms have been shown to couple primarily with  $G_{i/o}$ -proteins, the CB1 receptor can also couple with  $G_s$  and  $G_q$  proteins. For instance, during the restricted availability of  $G_{i/o}$ -proteins, the binding of cannabinoids to CB1R has been shown to promote coupling to  $G_s$  (Caballero-Florán et al., 2016; Glass & Felder, 1997).  $G_q$  proteins have also been shown to interact with CB1R and further increase intracellular calcium levels (Lauckner et al., 2005; Navarrete & Araque, 2008). However, it has been suggested that G-protein coupling to CB1R can be biased toward different  $G_{\alpha}$ 's depending on their availability in different cell types (Ibsen et al., 2017). Like G-proteins, cannabinoid receptor interacting proteins (CRIP<sub>1a</sub> and CRIP<sub>1b</sub>) have been shown to interact with the C-terminal domain of CBRs (Niehaus et al., 2007). Although the predicted primary structures of CRIP<sub>1a</sub> and CRIP<sub>1b</sub> are highly conserved (Booth et al., 2019), little is known about the structural details of these proteins and how they regulate CBRs. However, hypotheses

have been made implicating CRIP<sub>1a</sub> and CRIP<sub>1b</sub> as possible competitors to certain G<sub>i/o</sub> protein subtypes such as G<sub>13</sub> and G<sub>o</sub> (Blume et al., 2015; Booth et al., 2019). Studies involving canonical and non-canonical signalling pathways by which CBRs are regulated are ongoing and can provide potential therapeutic targets such as G<sub>i/o</sub>-protein subunits, G<sub>s</sub> proteins, G<sub>q</sub> proteins and, CRIP<sub>1a/b</sub>.

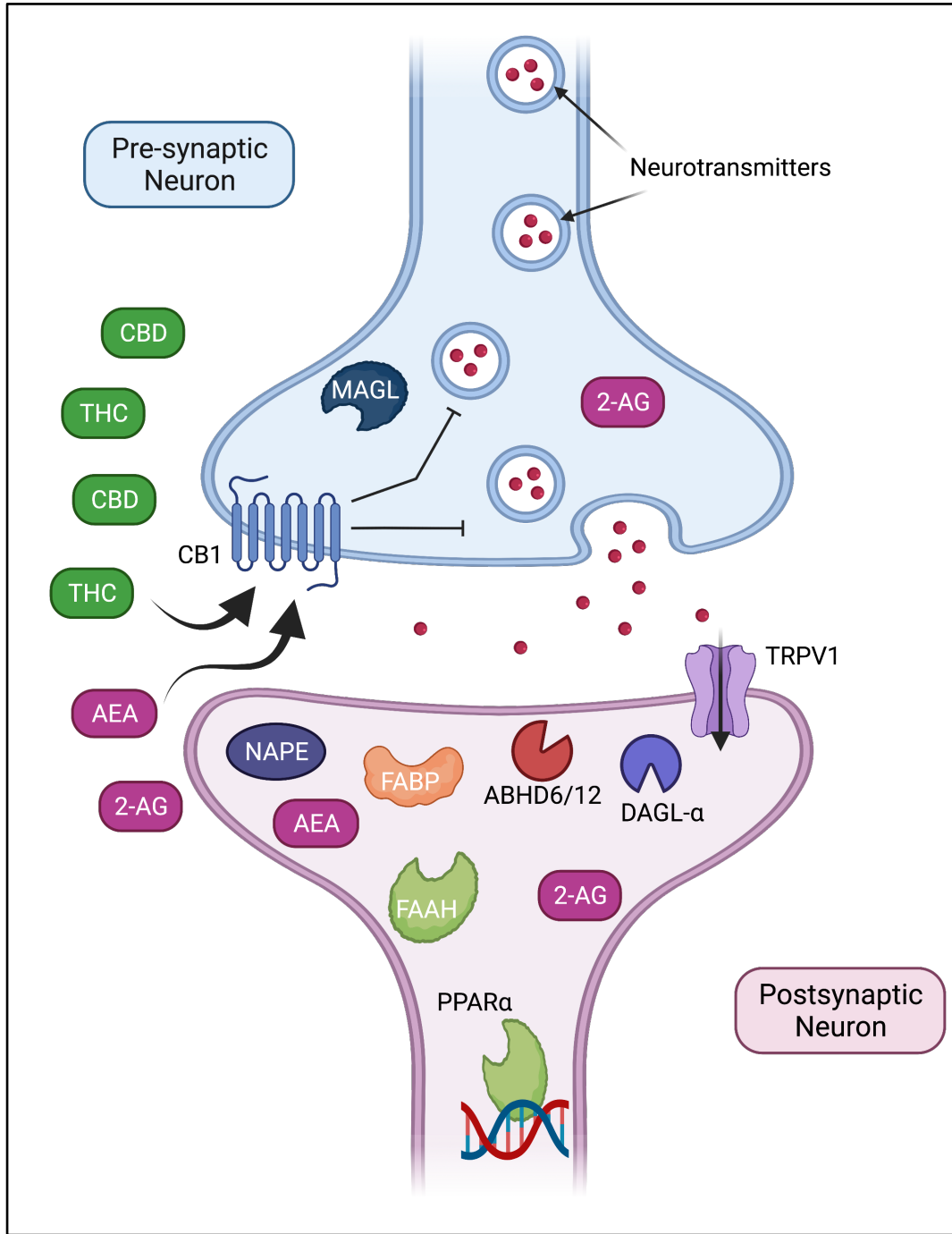


**Figure 12: Mechanics of the endocannabinoid system (ECS)** (Adapted from (Donvito et al., 2018))

In addition to the modulation of cannabinoid receptors by various cannabinoid ligands and auxiliary proteins, CBRs are well known for their integral role in the endocannabinoid system (ECS). CBRs are part of a complex signalling cascade involving:  $\alpha/\beta$ -hydrolase domain-6 (ABHD6),  $\alpha/\beta$ -hydrolase domain-12 (ABHD12), diacylglycerol lipase- $\alpha$  (DAGL- $\alpha$ ), fatty acid binding protein (FABP), fatty acid amide hydrolase (FAAH), monoacylglycerol lipase (MAGL) N-arachidonoyl phosphatidylethanolamine (NAPE) and *peroxisome proliferator-activated receptor alpha* (PPAR- $\alpha$ ) (Fig. 12). This signalling cascade is tightly regulated and controls the production rate of AEA and 2-AG in the brain (Donvito et al., 2018). Moreover, further brain signalling also controls the rate of production of these endocannabinoids in other regions of the body. The ECS is present in the central nervous system (CNS) and occurs during the communicating between the postsynaptic and presynaptic neuron. The system is modulated by endocannabinoids (AEA/2-AG) (Fig. 12). Exogenous cannabinoid (THC/CBD) can also modulate the ECS, when they are present in the system, either through administration or ingestion (Fig. 12). The ECS, gives us clearer insights on potential therapeutic applications such as direct drug targets (CBRs) and indirect drug target (G-proteins and ion channels).

#### **1.2.4. Physiological and therapeutic properties of cannabinoids**

Due to the structural differences between the classes of cannabinoids, these ligands exhibit dissimilar physiological effects. For instance, the two main constituents in naturally derived cannabinoids,  $\Delta^9$ -THC and CBD exhibit psychological and non-psychological activity, respectively (Gaoni & Mechoulam, 1971; Pertwee, 1988). The feeling of euphoria and being “high” stems primarily from the molecular component in cannabis,  $\Delta^9$ -THC. Additionally, the psychoactive compound impairs motor skills, memory and learning perception (Ameri, 1999). CBD tends to be the focus of discussion due to its non-psychological activity. CBD and many other non-psychoactive cannabinoids induce a sense of relaxation and are promising therapeutic agents for the treatment of depression. Knowledge on the physiological and neurological properties of cannabinoids are still ambiguous. We know that in various mammalian species, cannabinoids are able to modulate mood, appetite and induce relaxation (Pertwee, 1988). Concomitantly, the amygdala and hypothalamus are parts of the brain (also cannabinoid targets) in which cannabinoids regulate these physiological aspects (Fig. 13). For example, there is large distribution of CB1

receptors in the amygdala, which controls anxiety, emotion, and fear (Iversen, 2003; Katona et al., 2001). In human studies, cannabinoids such as THC and nabilone have been shown to produce anxiolytic effects (reduce anxiety) and decrease in social shyness (Viveros et al., 2007). In the same context of anxiety and mood disorders; HCN1 channels which regulate neuronal excitability have also been proven to regulate excitability in the basolateral amygdala (BLA) (Park et al., 2011).

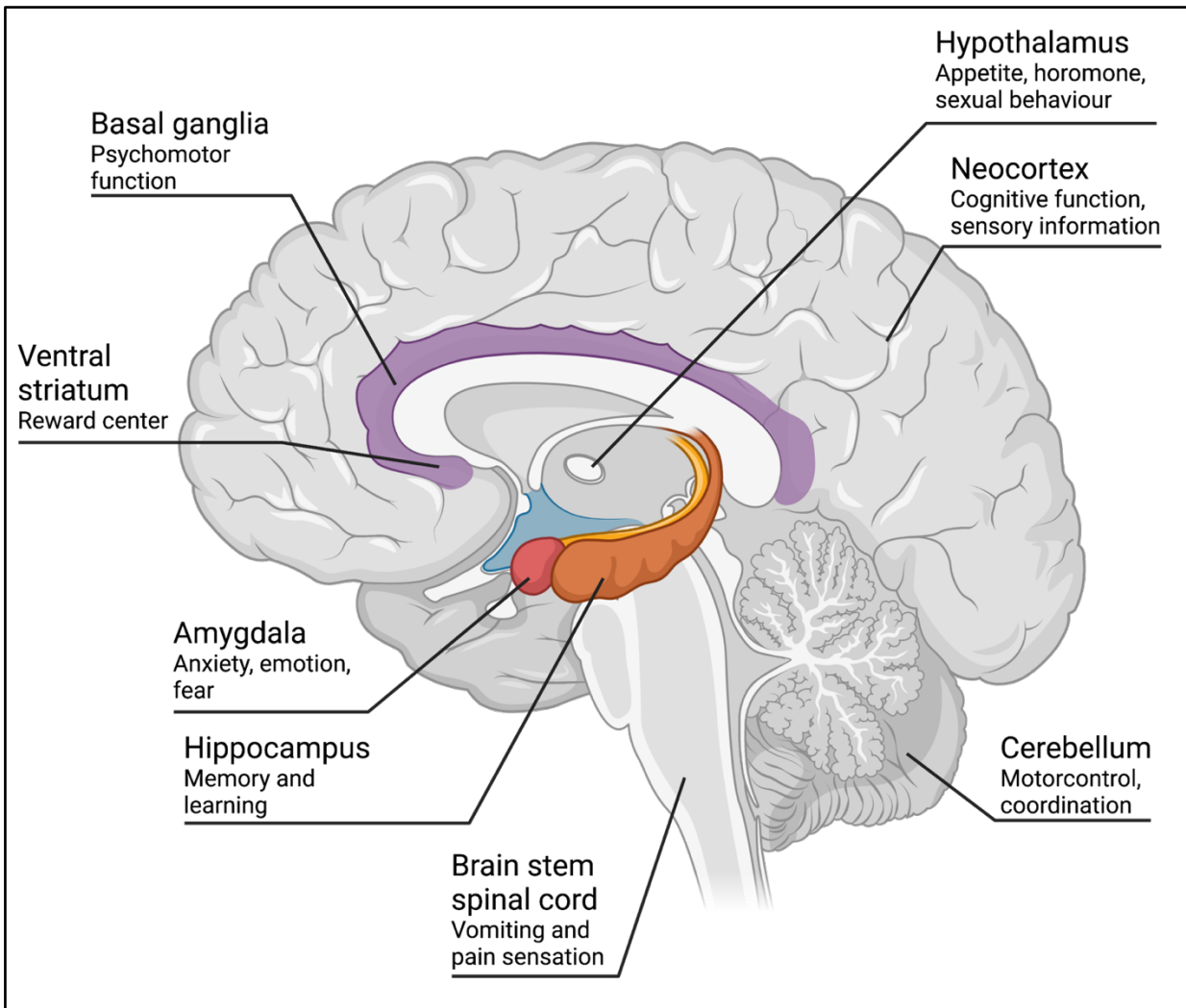


**Figure 13: Physiological avenues of cannabinoid modulation in various parts of the brain** (Adapted from (NIDA, 2021))

Common in various CNS disorders, epilepsy stems from abnormalities in neuronal cells and specifically leads to seizures. Human studies in children and teenagers diagnosed with epilepsy

revealed an 84% depletion in epileptic symptoms when administered CBD-enriched tablets (Porter & Jacobson, 2013). Learning and spatial memory, modulated by the hippocampus (Fig. 13) are cognitive aspects which can be altered by cannabinoids and in turn CBRs. Previous studies revealed that the ECS and exogenous cannabinoids significantly affect cognitive functions (Varvel & Lichtman, 2005). Additionally, cannabinoids have emerged as an anti-emetic drug. THC and CBD have been shown to reduce chemotherapy-induced vomiting and nausea which is a physiological aspect controlled by the brain stem and spinal cord (Fig. 13) (Parker et al., 2011). In parallel to cannabinoids and CBRs, HCN channels have also been studied as potential targets for CNS disorders. Epilepsy and Parkinson's disease have been speculated to be regulated by HCN channels (J. C. DiFrancesco & DiFrancesco, 2015). Additionally, it has been shown that by inhibiting HCN channels expressed in neurons, that there would be a prevention of neuropathic and inflammatory pain (J. C. DiFrancesco & DiFrancesco, 2015). The mechanism by which this selective HCN blocking occurs remains understudied. The roles of cannabinoids and CBRs are imperative in the CNS and peripheral nervous system (PNS). Various studies have hypothesized a link between ion channels which are also expressed in the CNS and the ECS (cannabinoids and CBRs).

### **1.2.5. Regulation of ion channels by cannabinoids**

#### **i. Transient receptor potential (TRP) channels**

Transient receptor potential (TRP) channels are essential ion channels in the CNS, PNS and the ECS which coordinate the passage of sodium and calcium ions. These channels have been studied for their potential therapeutic role in neurodegenerative diseases and pain sensation. Extensive studies with the isoforms of TRP and TRP-related channels, revealed their modulation by cannabinoids. For instance, both phytocannabinoids CBD and CBDV rapidly activate and desensitize rat TRPV1 channels which were expressed in HEK293 cells, in a dose-dependent manner (Iannotti et al., 2014). Recent studies into the putative binding sites of CBD on transient receptor potential vanilloid 2 (TRPV2) have provided insight on the channel's regulation by cannabinoids (Pumroy et al., 2019). A cryo-EM structure of TRPV2 bound to CBD revealed that the ligand interacts with the S5-S6 helical domains and promotes the opening of the pore (channel

activation) (Pumroy et al., 2019). Concomitantly, the TRP-related channels, TRPA1 and TRPM8 were also shown to be modulated by phytocannabinoids in HEK293 cells (De Petrocellis et al., 2008). Gaining insights into the direct modulation of TRP channels by cannabinoids can provide potential therapeutic treatments for pain perception related illnesses.

## **ii. Potassium channels**

Inward-rectifying potassium channels regulate the passage of potassium ions and provide the underlying basis for setting the resting membrane potential of excitable cells (repolarization). Some members of this channel family have been shown to be activated, indirectly by CBRs upon their binding of cannabinoids (Mackie et al., 1995). However, there have been studies which have proven the direct regulation of potassium channels by cannabinoids (McAllister et al., 1999). Through the utilization of a heterologous expression system in *Xenopus oocytes*, G-protein coupled inwardly rectifying (GIRK1/4) potassium channels and CB1 receptors were co-expressed (McAllister et al., 1999). The currents of GIRK1/4 were monitored to determine a unique dual effect of activation and deactivation by cannabinoids (McAllister et al., 1999). In the presence of 1  $\mu$ M AEA and 1  $\mu$ M CP 55,940, GIRK1/4 currents were enhanced (activated). Low concentrations of THC were also shown to partially activate GIRK1/4 currents. However, in the presence of low levels (1 nM) of synthetic cannabinoid, SR141716A, currents were inhibited (McAllister et al., 1999). Recent studies revealed a direct inhibition of the delayed rectifier potassium current ( $I_{Kr}$ ) in hERG channels by CBD at the low micromolar level (Orvos et al., 2020). Studies on understanding how potassium channels are directly and indirectly regulated by cannabinoids are ongoing.

## **iii. Sodium channels**

Sodium channels modulate the passage of sodium ions during rapid membrane depolarization. These channels exhibit quick (millisecond) kinetics. Sodium channels also play a large role in the CNS and the PNS. They channels can modulate various channelopathies such as pain related ailments and cardiac arrhythmias (de Lera Ruiz & Kraus, 2015). Early studies revealed the endocannabinoid, AEA and the synthetic cannabinoid AM404, were inhibiting depolarized

induced sodium channels (Nicholson et al., 2003). CBD and THC were also shown to inhibit sodium channel currents in human  $\text{Na}_v$  1.1 – 1.7 (Ghovanloo et al., 2018). The cannabinoids were prevented the opening of sodium channels and promoted a stable inactivated state. CBD was shown to bind to a hydrophobic pocket near the pore domain of the  $\text{Na}_v\text{M}$  (*M. marinus*) channel (Sait et al., 2020).

#### **iv. Calcium channels**

Similar to HCN channels, calcium ion channels are regulators of pacemaker activity and are integral membrane proteins expressed in neuronal and cardiac cells. An early study revealed the independent and direct inhibition of a T-type calcium ion channel in the presence of 1  $\mu\text{M}$  anandamide (AEA) (Chemin et al., 2001). Importantly, various control experiments revealed an interaction with the channel, which was independent of GCPRs, CBRs and a variety of signaling mediated cascades. Interactions between CBRs and ion channels have been shown. For example, upon binding of a cannabinoid, calcium ( $\text{Ca}^{2+}$ ) channels have been shown to be inhibited (indirectly), by a CBR-GCPR complex (Howlett, 2005). For instance, in a study which examined the effect of endogenous and synthetic cannabinoid, anandamide and WIN-55,212-2,  $\text{Ca}^{2+}$  channels currents were diminished. The inhibition was distinct, as an antagonist of CBRs, SR-141716A, was utilized in the presence of the two cannabinoids and no change in  $\text{Ca}^{2+}$  channels current was observed (Gebremedhin et al., 1999).

#### **v. Indirect modulation of HCN channels**

Seeing as cannabinoids play a role in the modulation of various areas of the brain, it was recently found that WIN55,212-2 modulates, through CBRs, the area of the brain which deals with learning and memory (Steinmetz & Freeman, 2016). However, the underlying mechanism by which this occurs remains obscure. A connection between CBRs and HCN ion channels has recently been shown to be the result of activation of a complex signaling cascade involving, c-Jun N-terminal kinases (JNKs), nitric oxide synthase (NOS), guanylyl cyclase (GC), and intracellular cGMP (Fig. 14) (Maroso et al., 2016). Thus, HCN channels are indirectly activated by cannabinoids via intracellular signaling pathways. It was hypothesized that impairments of

memory consolidation (converting short-term memories into long-term memories) in the brain may occur by the activation of HCN1 channels. To test the CBR-I<sub>h</sub> pathway and hypothesis in a pharmacological setting, a spatial memory task test in mice was conducted. It was determined that in the presence of WIN55,212, the CBR-I<sub>h</sub> pathway was responsible for the modulation of spatial memory.

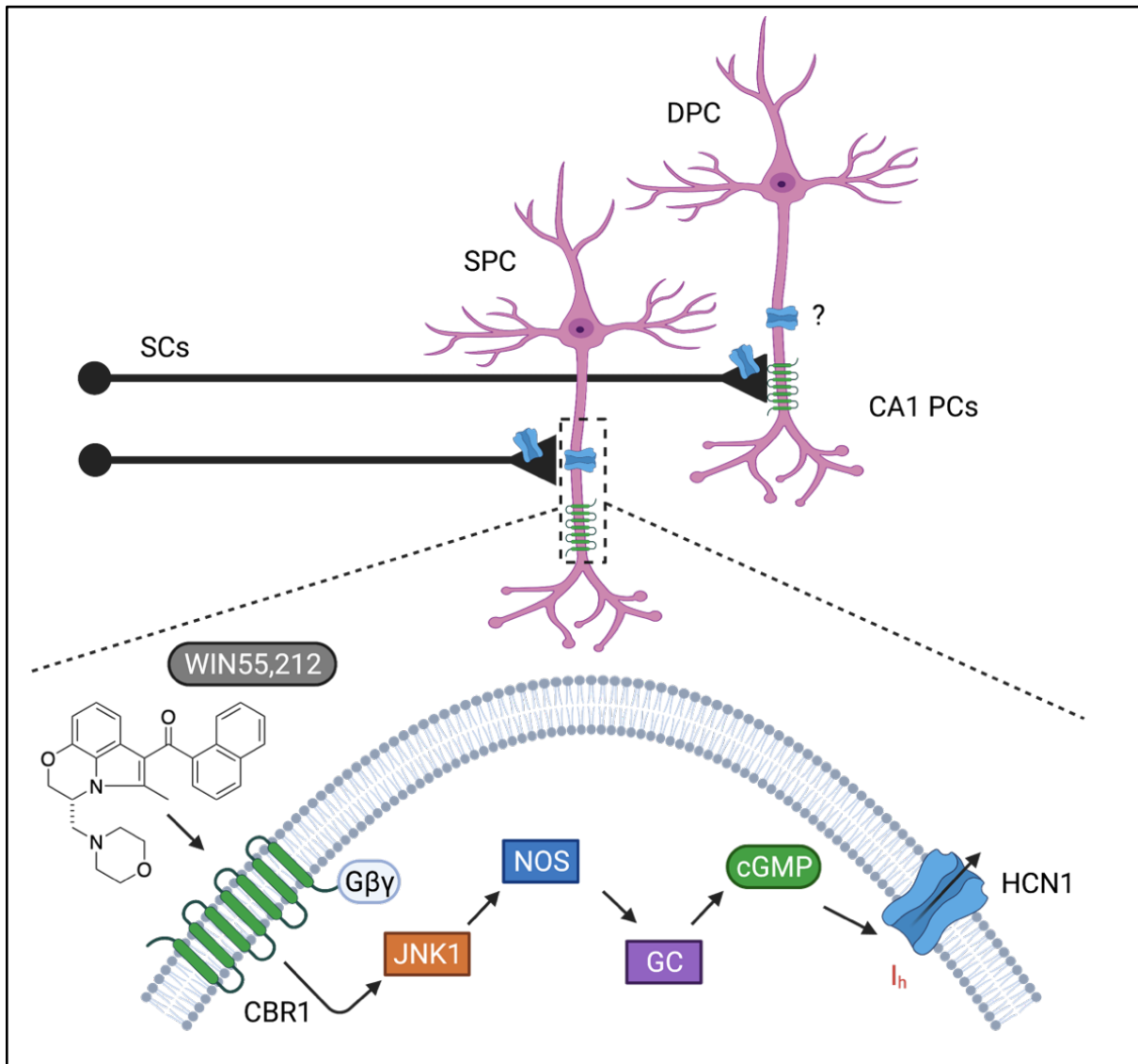


**Figure 14: Regulation of I<sub>h</sub> by activation of CBR1 (Adapted from (Vargish & McBain, 2016)).** CA1 PCs (pyramidal cells) were studied in the SPC (superficial PC) and DPC (deep PC) regions using SCs (Schaffer collaterals). Signalling cascade (right to left): JNK1: c-Jun N-terminal kinases, NOS: nitric oxide synthase, GC: guanylyl cyclase, cGMP: cyclic guanine monophosphate.

### 1.3. Objectives & Hypothesis

Ion channels coordinate the passage of ions through the cell membrane and mediate specificity of which ions can pass. Numerous intracellular and extracellular regulators affect these membrane proteins and their functional ability. Whether it be inhibitory, activation, deactivation or complete block of an ion channel, these effects are evident. Channels can be regulated by ligand binding, voltage changes, lipid constitution, intracellular ion concentrations, cyclic-nucleotide levels and signaling with other channels. Hence, there are several avenues in which the regulation of HCN channels can be explored. HCN channels are expressed in neurons and cardiac cells which are identical expression systems to CBRs. Additionally, CBRs and HCN channels have been proven to regulate several functions in neuronal cells which include excitability and synaptic plasticity. Several studies on both membrane proteins have shown modulation by molecules such as cAMP, lipids, and cannabinoids. These common characteristics make the two protein targets integral components in the central nervous system and in human physiology.

Although cannabinoids interact with cannabinoid receptors, these ligands can also directly modulate several ion channels through changes in membrane properties or through protein-ligand interactions (Ahrens et al., 2009; Chemin et al., 2001; Ghovanloo et al., 2021; Pumroy et al., 2019; Starkus et al., 2019). Cannabinoids can also affect several neuronal properties such as motor skills, spatial memory, and learning (Blázquez et al., 2020; Maroso et al., 2016) which are also dependent on proper HCN channel function. Cannabinoids are thought to be potential valuable therapeutics for several disorders that have been linked to HCN channel dysfunction. Therefore, we want to know if HCN channels can be directly regulated by cannabinoids independently of the CBRs.

Interplay between cannabinoids and HCN channels have been shown. However, the modulation is dependent on CBR activation by WIN55,212 (Maroso et al., 2016). To date, there has been no examination of a direct effect of cannabinoids on HCN channel function. Cannabinoids such as THC and CBD, like HCN channels, can therapeutically potentiate illnesses such as epilepsy, pain sensations, social anxiety disorders, and mood disorders. Given the potential therapeutic properties of cannabinoids and the potential therapeutic target in HCN channels, we aimed to determine if the molecular nature of cannabinoids can act as a direct modulator of HCN channels and its hyperpolarized  $I_h$  current. It will be important to study this possible pathway (directly) in the absence of cannabinoid receptors to avoid the signalling pathway previously

shown (Fig. 15). Altogether, determining a mode of regulation of cannabinoids on HCN channels would help in our understanding of how they can be therapeutically beneficial.

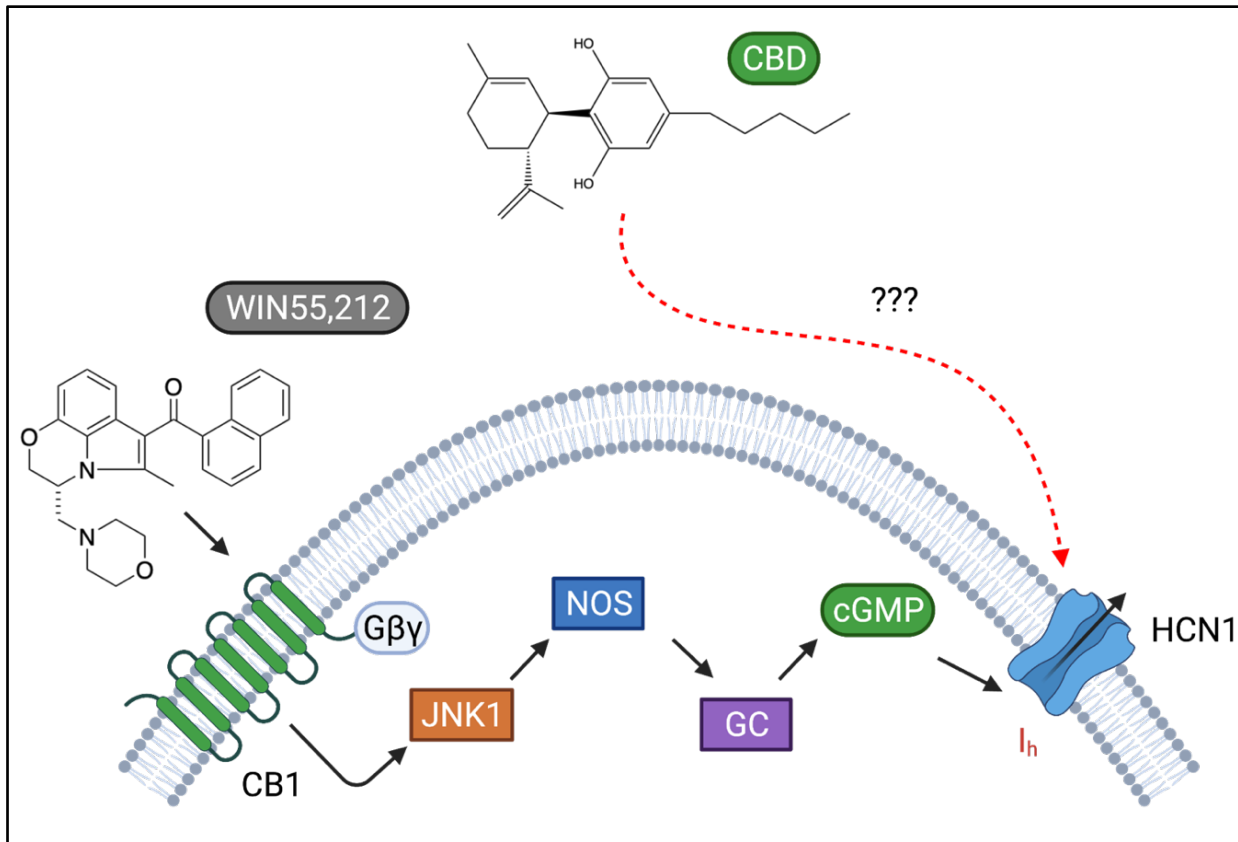


**Figure 15: Indirect and proposed direct regulation of CBD on HCN1 channels.** Signalling cascade adapted from (Vargish & McBain, 2016) (right to left): **JNK1**: c-Jun N-terminal kinases, **NOS**: nitric oxide synthase, **GC**: guanylyl cyclase, **cGMP**: cyclic guanine monophosphate.

## 2. Materials and Methods

### 2.1. Drugs and reagents

Cannabidiol (CBD) and (-)-trans- $\Delta^9$ -tetrahydrocannabinol (THC) were purchased pre-diluted in 99.8% methanol at a concentration of 1.0 mg/mL from Sigma-Aldrich. Triton™ X-100 (Sigma-Aldrich, USA) was diluted with distilled water from stock solution to a working concentration of 10 mM. Capsaicin ~95% (Sigma-Aldrich, USA) was diluted in 99.8% ethanol to a working concentration of 3200  $\mu$ M. AM251 ~98% (Sigma-Aldrich, USA) was diluted in 99.8% DMSO to a working concentration of 10 mM. Horse serum, penicillin-streptomycin and kanamycin stock solutions were used undiluted (Thermo Fisher Scientific, Gibco Cell Culture, USA).

### 2.2. Molecular biology and cell expression

Construct containing cDNA, rTRPV1, was previously subcloned into the *Xenopus* oocyte expression vector pBTSA (provided by Dr. Rikard Blunck, Université de Montréal, Quebec). cDNA coding for the mouse HCN1 gene was previously subcloned into expression vector pGH19 (provided by Dr. William N. Zagotta, University of Washington, Seattle, Washington). The mouse HCN1 $\Delta$ CNBD construct, previously named HCN1-CX5 (Bina Santoro et al., 2011b) was subcloned into expression vector pGH19 (provided by Bina Santoro, Columbia University, New York). The cDNA constructs mentioned were validated through Sanger sequencing (IRIC, Université de Montréal, Quebec).

Briefly, to obtain RNA, NotI (New England Biolabs) was used to linearize cDNA rTRPV1. NheI (New England Biolabs) was used to linearize both cDNA constructs of mHCN1. Standard *in vitro* transcription synthesis using ~1.0  $\mu$ g of linearized cDNA was conducted with the mMESAGE mMACHINE™ T7 Transcription kit (Thermo Fisher Scientific, Life Technologies, USA). Further, extracted, and purified RNA samples were validated by absorbance measurements at 260 nm and agarose gel electrophoresis.

All experiments were performed using unfertilized oocytes, extracted from anaesthetized female *Xenopus laevis* frogs. Oocytes were injected with 2.3 – 9.2 ng of mHCN1 (1.0  $\mu$ g/ $\mu$ L) or rTRPV1 mRNA (1.0  $\mu$ g/ $\mu$ L) using a Drummond Nanoject II injector (Drummond Scientific

Company). Prior to injection oocytes were subject to a controlled temperature of 17 – 19 °C and placed in vials containing Barth antibiotic solution (mM): 90 NaCl, 3 KCl, 0.82 MgSO<sub>4</sub>·7H<sub>2</sub>O, 0.41 CaCl<sub>2</sub>·2H<sub>2</sub>O, 0.33 Ca(NO<sub>3</sub>)<sub>2</sub>·4H<sub>2</sub>O and 5 HEPES supplemented with 100 U/mL of penicillin-streptomycin and 10 mg/mL of kanamycin stock (10 mg/mL). Post injection cells were incubated in Barth antibiotic serum solution supplemented with ~5% horse serum. Cells were expressed and ready to be used in electrophysiological recordings; 24 h (rTRPV1) or 2 – 3 days (mHCN1) post injection.

### 2.3. Electrophysiological recordings

Electrophysiological studies were conducted using the two-electrode voltage-clamp (TEVC) technique. Prior to recordings, borosilicate rapid fill microelectrode pipettes (1.0 mm OD X 0.5 mm ID/Fiber from FHC Inc., USA) were pulled to a final resistance of between 0.5 to 2 MΩ. using a P-97 Glaming/Brown Micropipette Puller (Sutter Instrument Company, USA). Pipettes were then filled with filtered 1 M KCL solution. Ag–AgCL ground pellets connected to the were placed the bath adjacent but connected to where the oocyte is placed. Macroscopic currents were recorded using Oocyte Voltage Clamp amplifier (OC-725C) (Warner Instruments, USA) and digitized using the Digidata 1322A data acquisition apparatus (Molecular Devices). All data were acquired using the software Clampex 10.5 at a sampling rate of 5 KHz with a filter of 1 KHz. Recordings were conducted at room temperature.

Oocytes expressing TPRV1 were recorded in a calcium-free external solution containing (mM) 100 NaOH, 2.5 mM KOH, 2 mM Mg (OH)<sub>2</sub>, 1 mM Ca (OH)<sub>2</sub>, 5 HEPES. The solution was adjusted to a pH of 7.35 with MES. For activation protocols, oocytes were held at 0 mV and then stepped to voltages with a range of –80 to +170 mV in steps of 10 mV, followed by a step to +50 mV before stepping back to 0 mV. In total cells were subject to a protocol lasting 600 ms.

Oocytes expressing wild type HCN1 and HCN-CX5 were recorded in a 100-K bath solution (mM) 89 KCl, 15 HEPES, 0.4 CaCl<sub>2</sub>, and 0.8 MgCl<sub>2</sub> (Männikkö et al., 2005). Repetitive pulse protocols involved holding oocytes at 0 mV and then applying a repetitive 2 s pulse to –130 mV voltage every 30 s. Activation protocols involved voltages stepped at every 10 mV. Briefly, oocytes were held at 0 mV, stepped to voltages ranging from –160 to –30 mV in incremental steps of +10 mV. Deactivation protocols involve holding oocytes at 0 mV, stepping to a pre-pulse

voltage of  $-130$  mV, and then stepping to test voltages from  $+50$  to  $-70$  mV ( $\Delta = 10$  mV). In all recordings, the cells were held at the holding potential for an interpulse time of 27s to allow the channels to fully recover between sweeps.

## 2.4. Data analysis and statistics

All recordings were analyzed offline using the Clampfit (Molecular Devices) software. Data was analyzed and plotted using Origin 8.0 software (Northampton, MA, USA) or GraphPad Prism (Version 8.1.1, San Diego, CA). Current-voltage (I-V) relationships were analyzed using built in software in pClamp, taking each respective voltage to an inquired current. The I-V relationship can be fit with the Boltzmann I-V equation (Equation 1):

$$I = \frac{(V_m - V_{rev})g_{max}}{1 - e^{-\frac{V_m - V_{1/2}}{k}}}$$

Equation 1

Where  $V_m$  corresponds to the test pulse,  $V_{rev}$  is the reversal potential ( $V_{rev} = 0$ , based on our recording solutions),  $g_{max}$  is the maximal conductance,  $V_{1/2}$  corresponds to the membrane potential at half activation and  $k$  is a slope factor to measure steepness of voltage dependence curve.

Steady-state activation curves were analyzed by fitting the adhered Boltzmann equation (Equation 2):

$$I/I_{Max} = \frac{1}{1 + e^{-\frac{V_m - V_{1/2}}{k}}}$$

Equation 2

Where 1 represents the maximal and normalized relative current,  $V_m$  corresponds to the test pulse,  $V_{1/2}$  corresponds to the midpoint voltage of activation and  $k$  is the slope factor.

Concentration dependence curves (relative current and remaining current) and  $EC_{50}/IC_{50}$  values were obtained by fitting the Hill equation (Equation 3):

$$I/I_{Max} = \frac{1}{1 + \left(\frac{EC_{50} \text{ or } IC_{50}}{[A]}\right)^n}$$

Equation 3

Where  $I/I_{Max}$  is the relative or remaining current,  $[A]$  is the concentration of MeOH, CBD or THC, and  $n$  is the Hill coefficient. To obtain time constants of activation ( $\tau_{act}$ ), the first 3600 ms of the test pulses were fit individually with a mono-exponential function after the initial lag. The test pulse for the time constants of deactivation ( $\tau_{deact}$ ) were also fit individually with a mono-exponential function.

Data are presented as means ( $\pm$ ) standard error. Statistical significance for I-V curves were determined measured using two-way ANOVA with Tukey HSD post-hoc analysis. The  $V_{1/2}$  values of the steady-state dependencies were determined for each recording and pooled for a given treatment then analyzed by one-way ANOVA with Tukey post-hoc analysis. Mean activation and deactivation kinetics (from  $-20\text{mV}$  to  $-70\text{mV}$ ) were analyzed using the Zar method for significance (Zar, 1984).

## 2.5. Intracellular cGMP Assay

Five uninjected oocytes were sorted for each given condition were placed and incubated for 20 min in the 100-K bath solution. Conditions were set as followed: untreated oocytes, methanol control, THC cannabinoid and CBD cannabinoid (varying micromolar concentrations). Post-incubation, cells for each condition were gathered and homogenized using 50  $\mu\text{L}$  of 0.1 N HCl and centrifuged at 12,000 rpm using a tabletop centrifuge. The supernatant was isolated placed in new Eppendorf tube and used for the assay within one hour of extraction.

Standards and oocyte samples and were used for the cGMP assay which was conducted using the protocol provided in the DetectX High Sensitivity Direct cGMP Chemiluminescent Immunoassay Kit (Arbor assays, USA). Using the 96-well white plate provided in the kit, chemiluminescence signals were read using the plate reader, TECAN Infinite® F200 PRO (Männedorf, Switzerland). During each run samples were ran in triplicates and standards in duplicates.

### 3. Results

#### 3.1. Cannabidiol activates TRPV1 channels

TRPV and TRP-related channels play an integral role in the CNS and are known to be modulated by heat, capsaicin, changes in pH and cannabinoids (Fig. 16A) (Kauer & Gibson, 2009). Studies in HEK293 cells revealed that with the application of increasing concentrations of CBD, rat TRPV1 channels are activated (Iannotti et al., 2014).

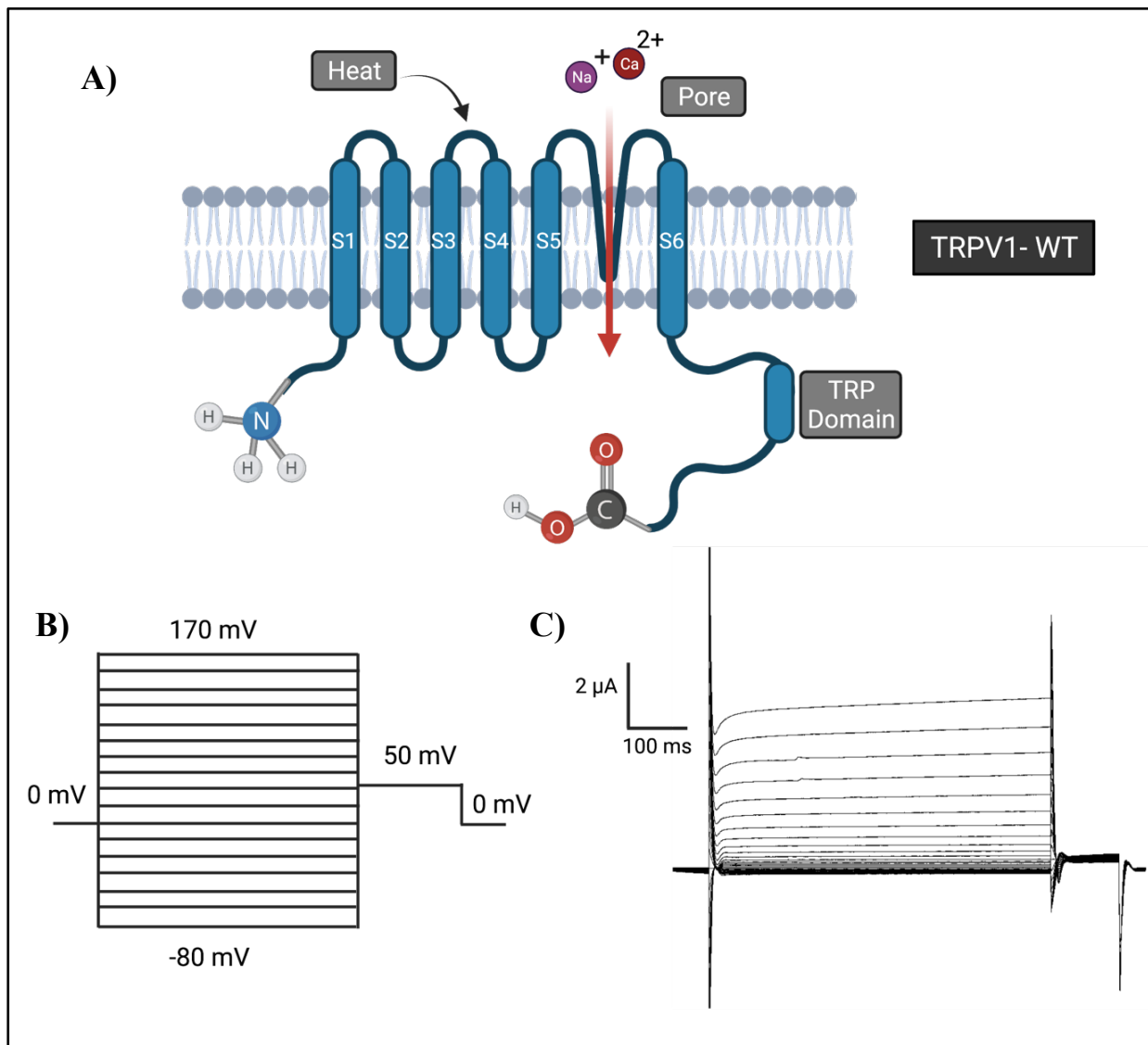


**Figure 16: Electrophysiological characteristics of TRPV1 ion channels.** A) Secondary structure of TRPV1 (Adapted from (Kauer & Gibson, 2009)). B) Stepwise protocol applied from -80 mV to +170 mV ( $\Delta 10$  mV) for 600 ms each C) Typical wild type rTRPV1 current traces.

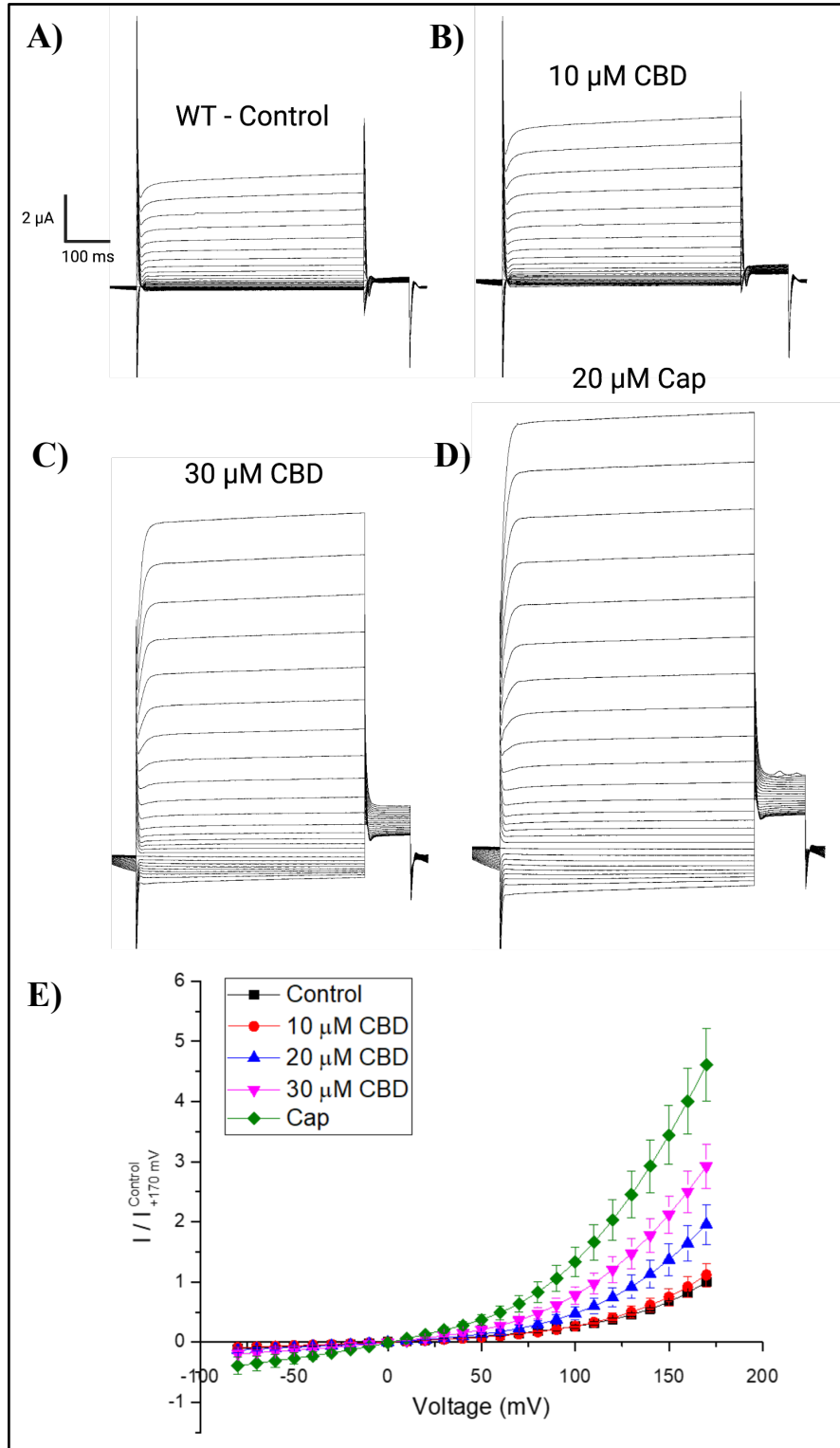


**Figure 17: Regulation of TRPV1 by cannabidiol (CBD).** A) Representative rTRPV1 control current in absence of drug. B) Current traces after applying 10  $\mu$ M CBD. C) Current traces after applying 30  $\mu$ M CBD. D) Current traces after the application of 20  $\mu$ M capsaicin. E) Normalized current voltage relationship ( $I/I_{Control +170 mV}$ ) after addition of increasing concentrations of CBD shown at voltages ranging from -80 to 170 mV. (n = 8; P < 0.05 for 20  $\mu$ M CBD, 30  $\mu$ M CBD and Cap vs. Control)

Prior to examining the effect of cannabinoids on HCN channels we wanted to validate our experimental approach using an ion channel previously shown to interact directly with CBD (Iannotti et al., 2014; Starkus et al., 2019). Using *Xenopus* oocytes as our cell model, because they lack CBRs (Peshkin et al., 2019), the rat TRPV1 isoform was expressed and currents were examined following increasing concentrations of CBD. Maximal TRPV1 current was elicited by the addition of 20  $\mu$ M capsaicin. Upon the addition of 10  $\mu$ M CBD we observe little activation in our TRPV1 currents compared to control (Fig. 17 A, B & E). However, upon the addition of 20  $\mu$ M and 30  $\mu$ M CBD we see an approximately 30% increase in outward rectifying current (Fig. 17 C & E). A large increase in the outward current is obtained upon the addition of 20  $\mu$ M of known agonist capsaicin (Fig. 17 D & E). Hence, our findings are in line with previous studies in discovering the activation of TRPV1 by CBD in *Xenopus* oocytes (Iannotti et al., 2014; Starkus et al., 2019). Therefore, TEVC and the application of our cannabinoids to the bath where oocytes were subject to test protocols is the experimental approach, we decided to use for studies in HCN1 channels.

### 3.2. Time dependent regulation of HCN1 by cannabinoids

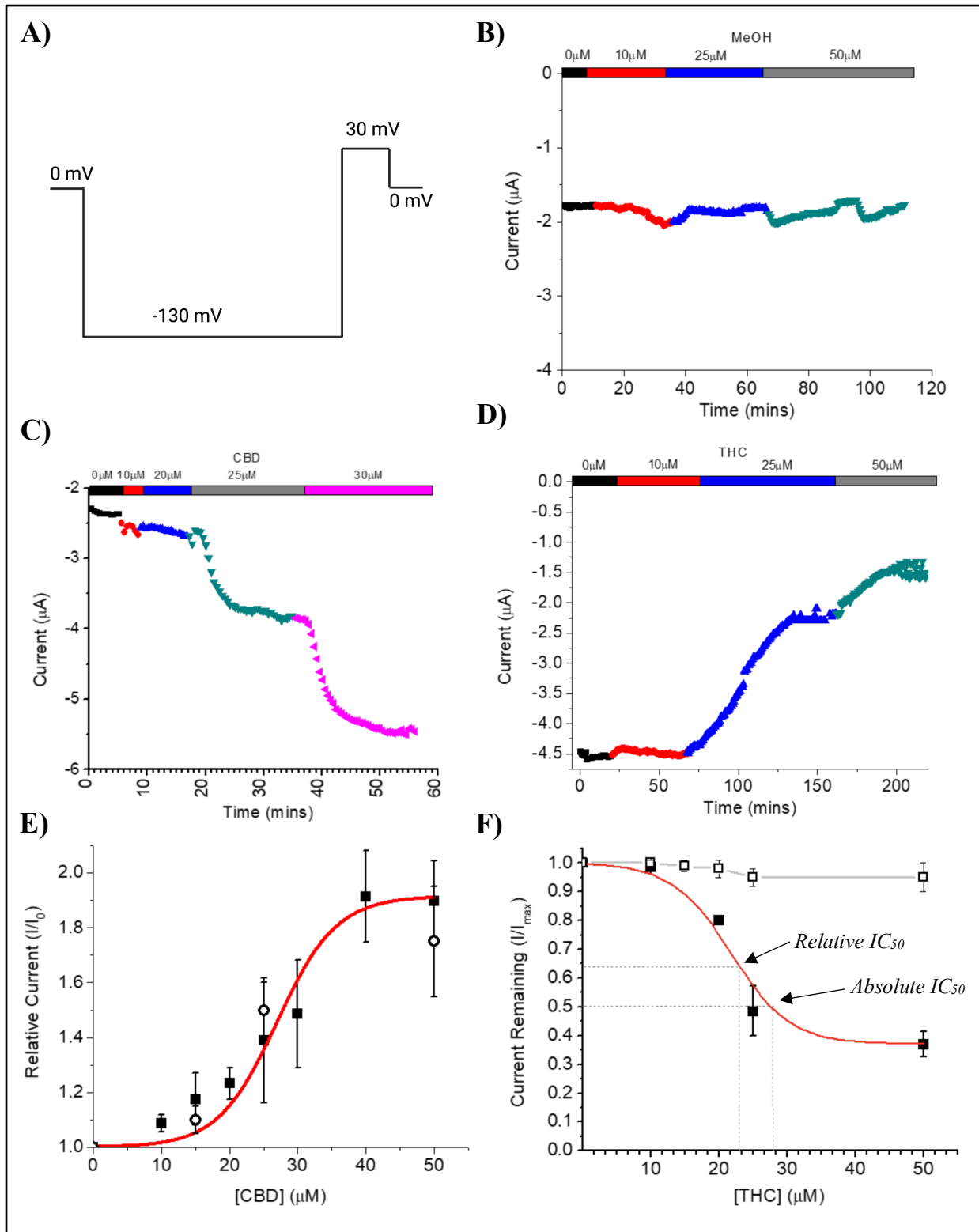


**Figure 18: Time and concentration dependent regulation of HCN1 by cannabinoids.** **A)** Constant pulse voltage protocol, holding at 0 mV, stepping to  $-130$  mV every 30 seconds. **B)** Representative recording of steady-state current versus time with varying concentrations of MeOH (concentration shown refers to the amount of vehicle used for that concentration of cannabinoid). **C)** Representative recording of steady-state current versus time with varying concentrations of CBD. **D)** Representative recording of steady-state current versus time with varying concentrations of THC. **E)** CBD concentration-dependent curve in the presence (*white circles*) and absence (*black squares*) of  $10 \mu\text{M}$  AM251 ( $n=13$  and  $5$  respectively). 50% Max response ( $\text{EC}_{50}$ ) for CBD is elicited at  $28.5 \mu\text{M}$ , with a 91% maximal increase in current. **F)** THC concentration-dependent curve (*black squares*) alongside concentration-dependency of vehicle (MeOH) (*white squares*). THC induces a 63% maximal block of HCN1 currents, with a half-maximal response (Relative  $\text{IC}_{50}$ ) of  $21.8 \mu\text{M}$  ( $n=5$ ). 50% block of total current (Absolute  $\text{IC}_{50}$ ) occurs at  $28.9 \mu\text{M}$ . Methanol induces less than a 5% decrease in current at concentrations above  $20 \mu\text{M}$  ( $n=4$ ).

To examine the potential effect of exogenous cannabinoids, cannabidiol (CBD) and  $\Delta^9$ -tetrahydrocannabinol (THC) on HCN1 channels expressed in *Xenopus* oocytes, we applied a repetitive pulse to  $-130$  mV every 30 seconds and applied CBD or THC to the bath solution. To ensure the effects of CBD and THC could be differentiated from the vehicle (methanol), we first examined the effects of equimolar quantities of methanol used to solvate the cannabinoids to their listed concentrations. We saw a negligible change (less than 5%) in overall current over the course of 120 minutes at varying concentrations (Fig. 18 B & F).

The phytocannabinoids, however, were shown to have dissimilar effects. CBD increases HCN1 currents in a concentration dependent manner when applying a repetitive pulse of  $-130$  mV over time (Fig. 18 C & E). Fits of the concentration dependence (Fig. 18 E) with the Hill equation, indicates a maximal response was calculated of 91% at saturating concentrations, with an  $\text{EC}_{50}$  (50% max response) value of  $28.5 \mu\text{M}$  and a slope coefficient of 0.1 (Fig. 18 E). This concentration dependence remains in the presence of AM251, a CB1R antagonist, providing further evidence that our findings are not the result of CB1R activation. In the presence of AM251, we saw a similar increase in current after the addition of  $30$ ,  $40$  and  $50 \mu\text{M}$  CBD (Fig. 18 E). Furthermore, no current is elicited by CBD in uninjected oocytes (Fig. 19 A), indicating that our results are specific to HCN1 channels. Moreover, currents activated by  $30 \mu\text{M}$  CBD could be inhibited by addition of well characterized HCN channel blocker, ZD7288 (Fig. 19 B).

We observed different effects on HCN1 currents with the addition of THC. HCN1 currents decreased, with the addition of THC in a concentration dependent manner between  $10$  and  $50 \mu\text{M}$ . (Fig. 18 D & F). A concentration dependence curve for THC, current was calculated using the Hill

equation. The maximal inhibitory response of THC was calculated to be 63% after the addition of 50  $\mu\text{M}$  THC (Fig. 18 F) with the half maximal response (relative  $\text{IC}_{50}$ ) of THC on HCN1 channels at 21.8  $\mu\text{M}$  (slope =  $-0.1$ ). Half the total HCN1 current is blocked at 28.9  $\mu\text{M}$  (absolute  $\text{IC}_{50}$ ) (Fig. 18 F).

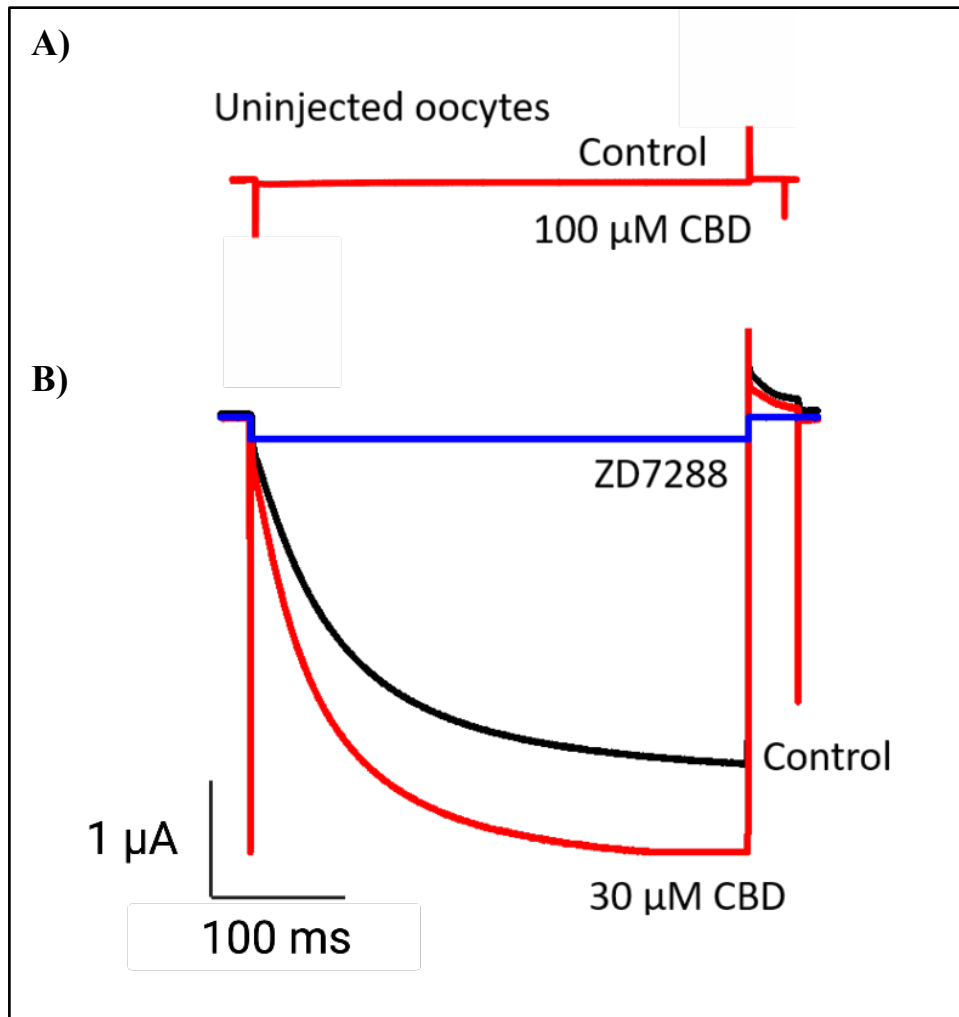


**Figure 19: Cannabidiol's distinct regulation in HCN1 channels.** **A)** Representative current output of non-injected oocytes in the presence of 100  $\mu\text{M}$  CBD. **B)** Representative  $I_h$  current before (*black sweep*), after (*red sweep*) the addition of 30  $\mu\text{M}$  CBD and after the addition of 900  $\mu\text{M}$  ZD7288 (*blue sweep*).

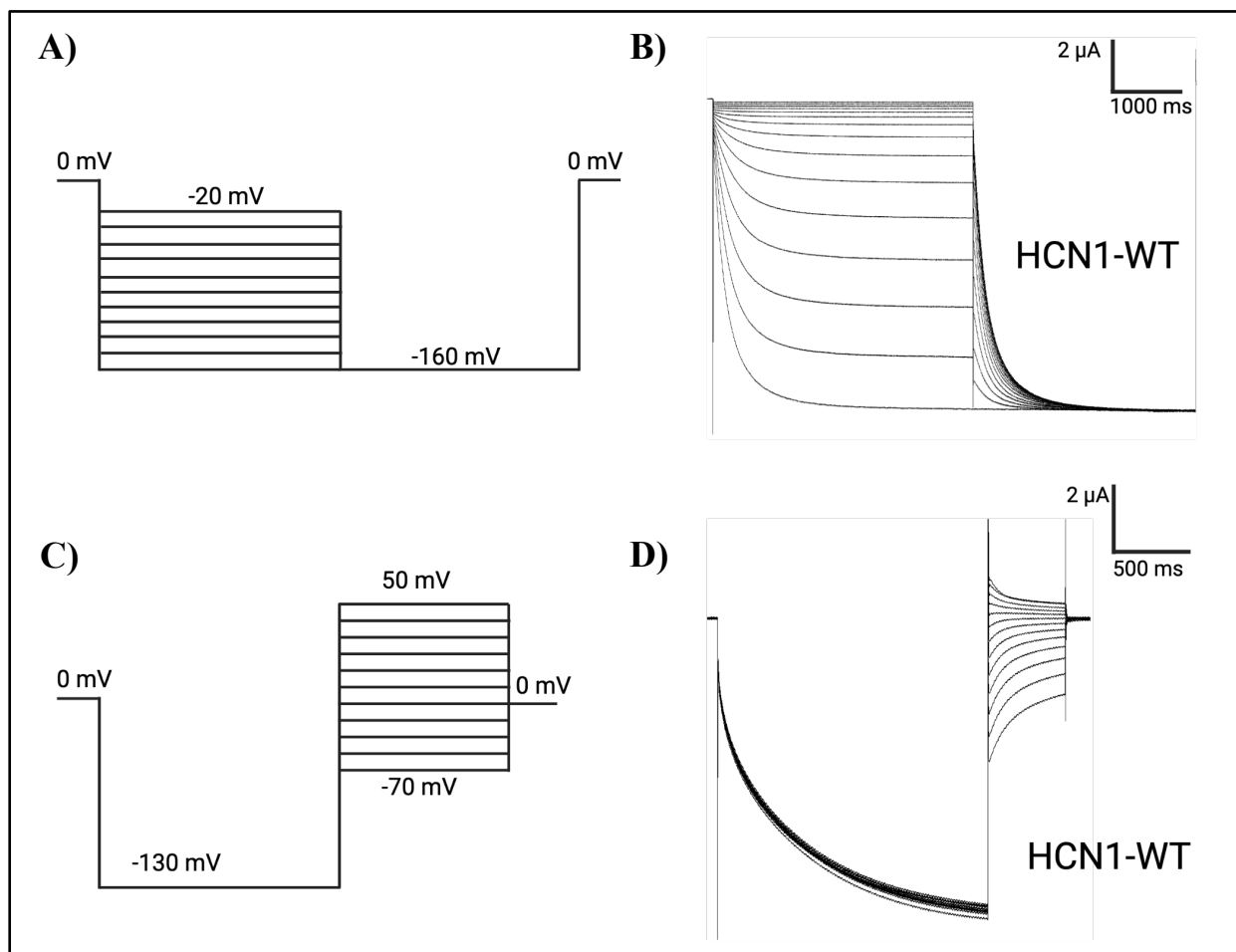


**Figure 20: HCN1 stepwise protocol.** **A)** Activation protocol. Channel opening from  $-160$  mV to  $-20$  mV ( $\Delta +10$  mV) and held at  $-160$  mV for maximal opening. **B)** Typical HCN1-WT current traces after implying activation protocol. **C)** Deactivation protocol. Channel opening to  $-130$  mV then stepwise closing  $+50$  to  $-70$  mV ( $\Delta -10$  mV). **D)** Typical HCN1-WT current traces after implying deactivation protocol.

To determine more specifically what properties of HCN1 channels are affected by CBD and THC, we applied specific step-wise protocols to assess activation and deactivation properties. (Fig. 20 A & C). By applying these protocols, we can monitor key changes in current-voltage relationship ( $I/V$ ), the voltage-dependence of activation at steady-state (which gives a measure of the probability of channel opening at a given voltage), activation time constants (speed of channel opening) and deactivation time constants (speed of channel closing). Assessing which of these properties are affected by the presence of CBD or THC may give us an indication of which conformational state(s) is/are affected by the given cannabinoid.

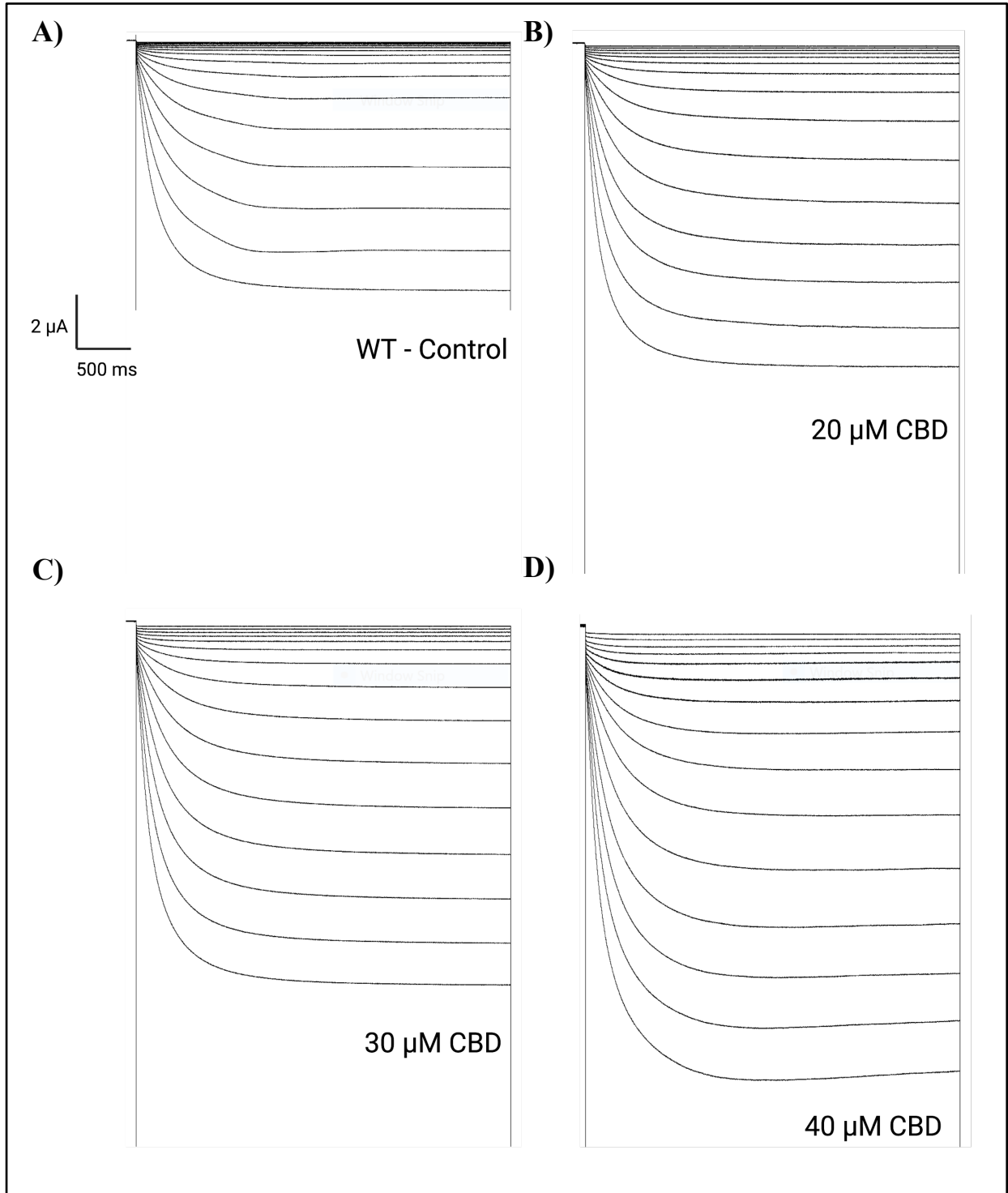


**Figure 21: HCN1-WT current in presence of cannabidiol (CBD).** A) Representative current traces in the absence of CBD. B) After addition of 20  $\mu$ M CBD. C) After 30  $\mu$ M CBD. D) After 40  $\mu$ M CBD.

Once we established stable HCN1 currents, we proceeded to add cannabidiol (CBD) in increments of 10  $\mu\text{M}$  to the bath solution, following stabilization of the current after each addition (normally between 15-30 mins post-application) (Fig. 21). We see an approximate 20% increase in overall current density, in comparison to our control after the addition of 30  $\mu\text{M}$  CBD and a nearly 40% increase in current density after the addition of 50  $\mu\text{M}$  CBD (Fig. 22 A). This reinforces our findings from our preliminary results demonstrating that CBD has the capacity to activate HCN1 channels.

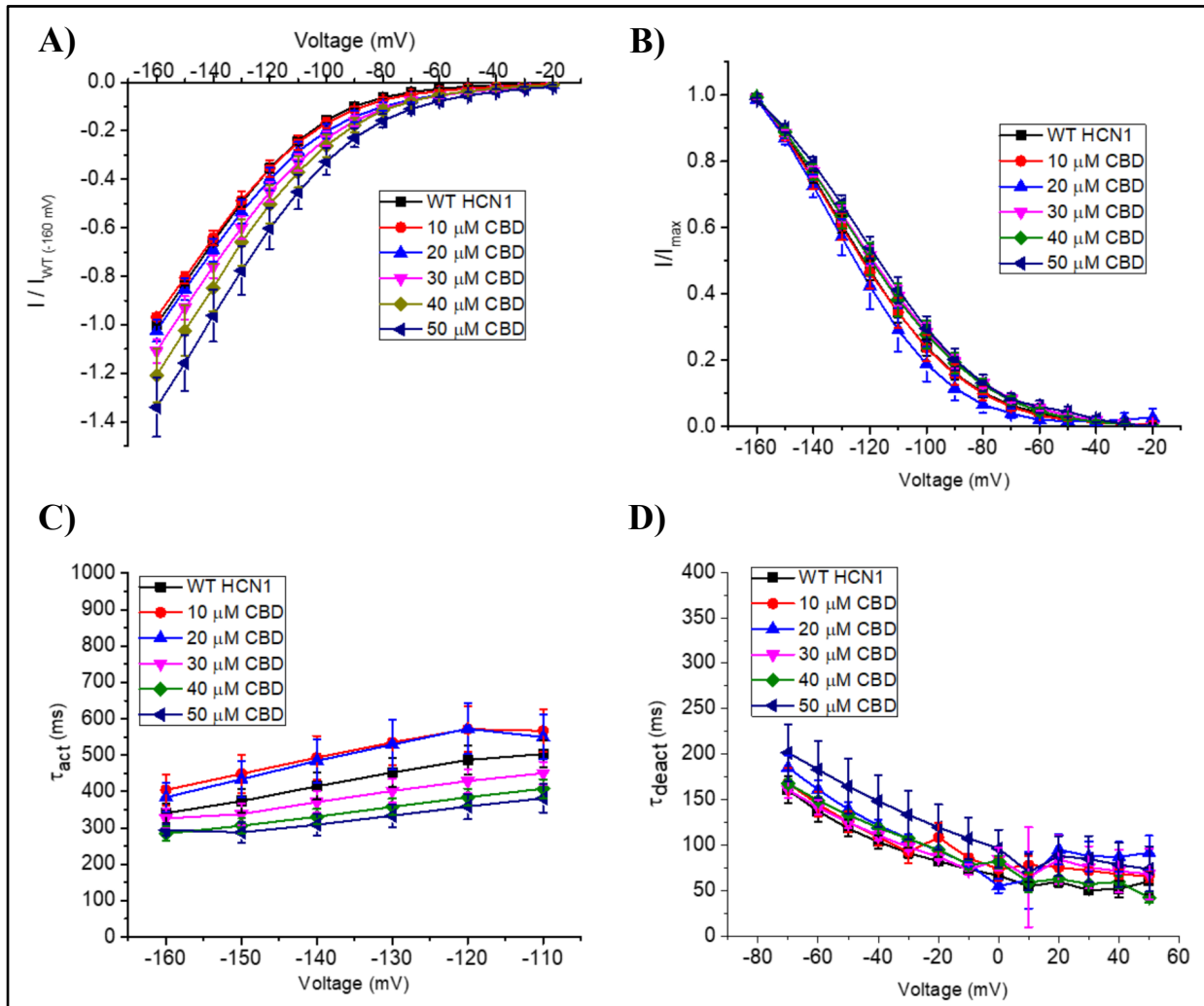


**Figure 22: Regulation of HCN1-WT by cannabidiol (CBD).** **A)** Current-voltage (I/V) relationship in presence of CBD normalized to maximal current ( $I_{WT(-160\text{ mV})}$ ). ( $5 < n < 18$  per condition;  $P < 0.05$  for 30 - 50  $\mu\text{M}$  CBD vs control) **B)** Steady state activation in presence of CBD. ( $P = 0.81$  for  $V_{1/2}$ ) **C)** Activation time constant ( $\tau$ ) kinetics in presence of CBD. ( $0.21 < P < 0.71$ ) **D)** Deactivation time constant ( $\tau$ ) kinetics in presence of CBD. ( $3 < n < 7$  per condition;  $0.09 < P < 0.65$ )

Additionally, the stepwise protocol allowed us to examine kinetic properties of the HCN1 channel in the presence of cannabinoids. The current-voltage relationship (Fig. 22 A), steady-state activation (Fig. 22 B and Table 1) and activation time constants (Fig. 22 C) as well as deactivation time constants (Fig. 22 D) in the presence of CBD were all quantified. Changes in HCN1 steady-state activation data (Table 1), activation time constants, and deactivation time constants, all showed statistically negligible changes after the addition of CBD.

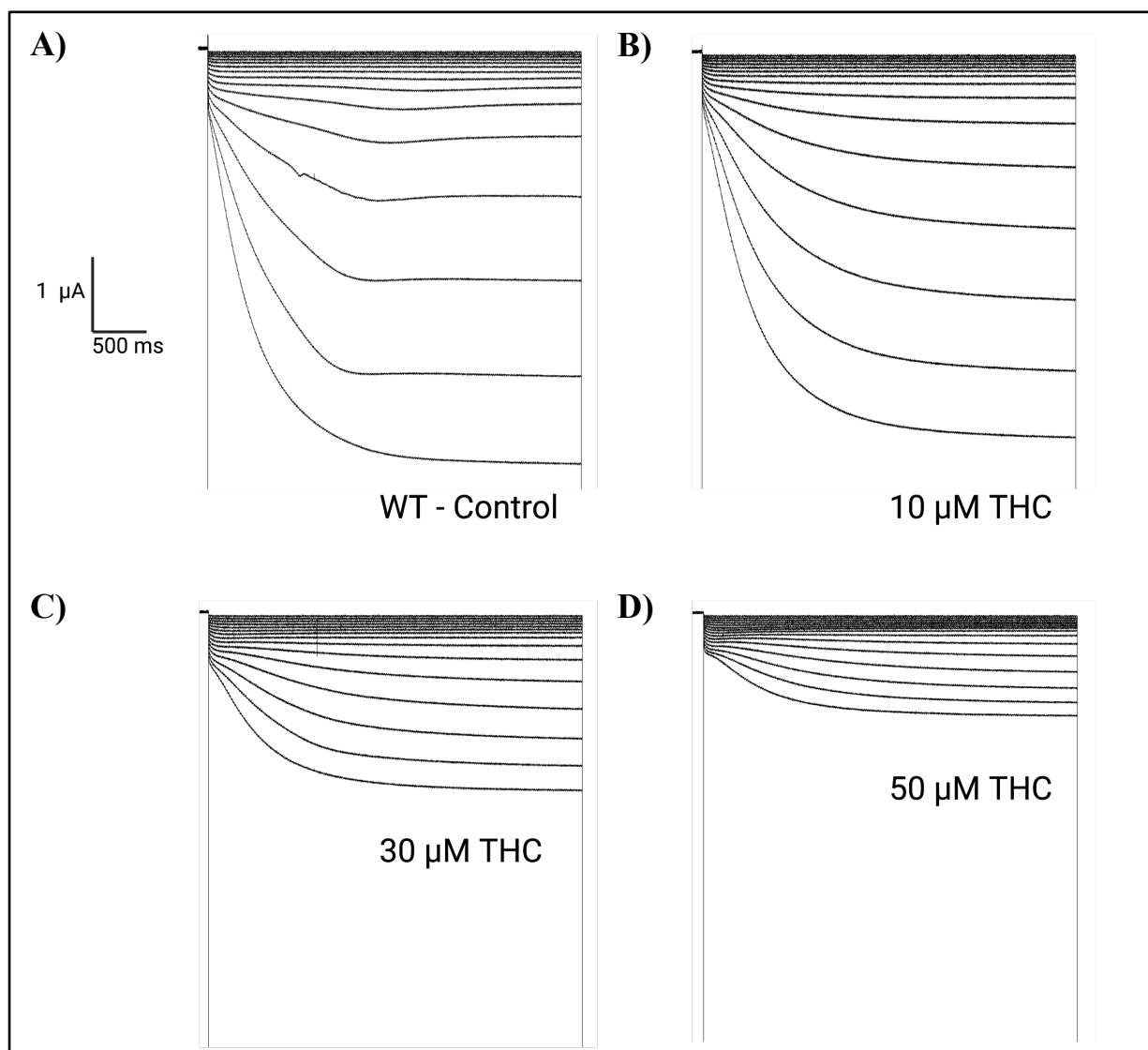


**Figure 23: HCN1-WT current in presence of  $\Delta^9$ -tetrahydrocannabinol (THC).** A) Representative current traces in the absence of THC. B) After addition of 10  $\mu\text{M}$  THC. C) After 30  $\mu\text{M}$  THC. D) After 40  $\mu\text{M}$  THC.

Next, we studied the effect of  $\Delta^9$ -tetrahydrocannabinidiol (THC) on HCN1 currents once again in the presence of 10  $\mu\text{M}$  increments of THC (Fig. 23). Based on our data, the addition of 10  $\mu\text{M}$  THC, we see the largest changes occurred following the addition of THC beyond 20  $\mu\text{M}$ . With the addition of 30  $\mu\text{M}$  THC, the HCN1 current was subject to close to a 50% inhibition of overall current density (Fig 24 A). 50  $\mu\text{M}$  THC produced close to a 75% inhibition the HCN1 current (Fig 24 A).

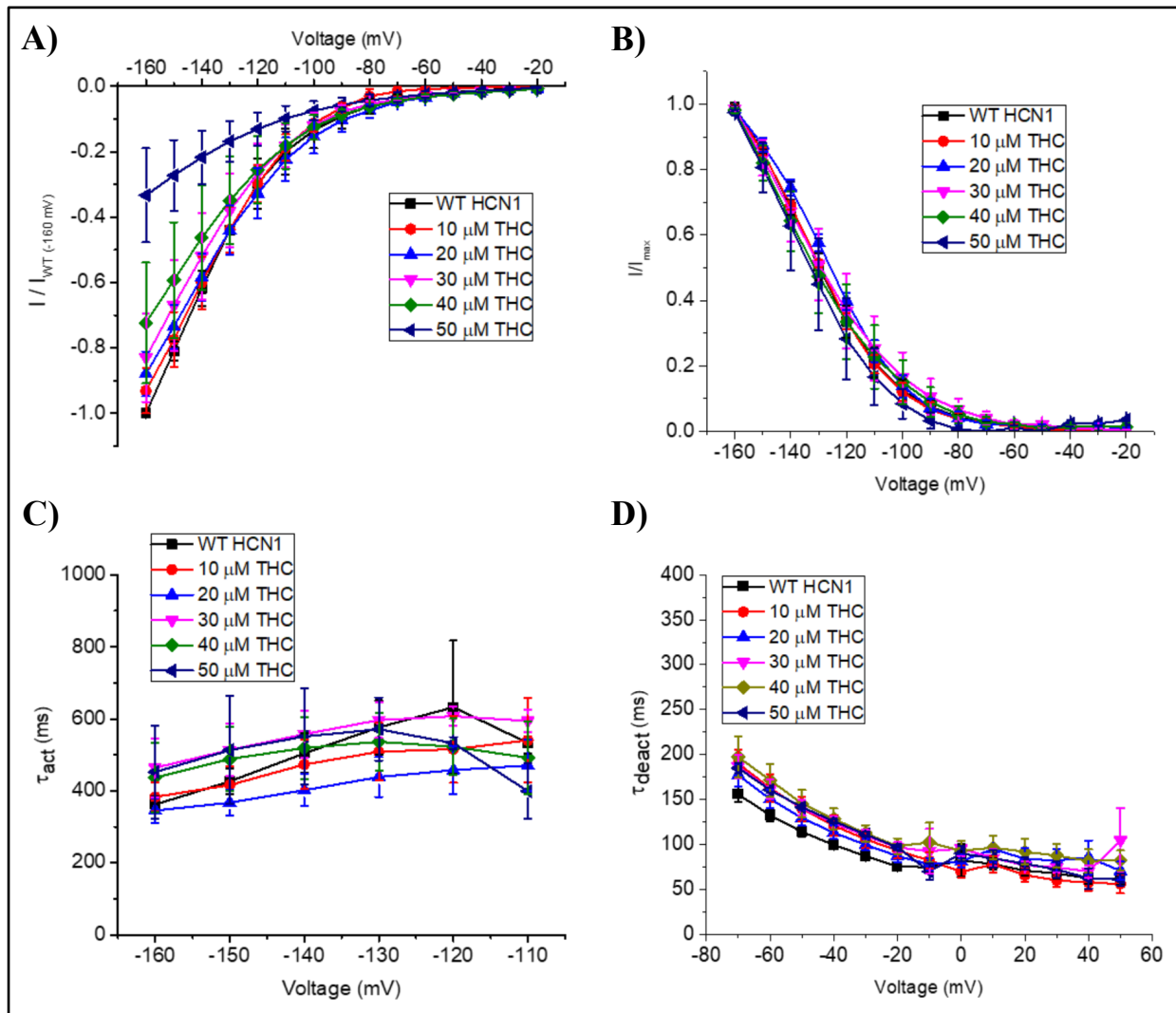


**Figure 24: Regulation of HCN1-WT by  $\Delta^9$ -tetrahydrocannabinidiol (THC).** **A)** Current-voltage ( $I/V$ ) relationship in presence of THC normalized to maximal current ( $I_{WT(-160\text{ mV})}$ ). ( $4 < n < 8$  per condition;  $P < 0.05$  for 20 - 50  $\mu\text{M}$  vs control) **B)** Steady state activation in presence of THC. ( $P = 0.49$  for  $V_{1/2}$ ) **C)** Activation time constant ( $\tau$ ) kinetics in presence of THC. ( $0.21 < P < 0.90$ ) **D)** Deactivation time constant ( $\tau$ ) kinetics in presence of THC. ( $3 < n < 8$  per condition;  $0.11 < P < 0.45$ )

Finally, we wanted to see if the addition of THC would change the kinetic properties of HCN1. Like CBD, changes in HCN1 steady-state activation (Fig. 24 B, Table 1), activation time constants (Fig. 24 C) and deactivation time constants (Fig. 24 D), revealed negligible changes in the presence of THC.

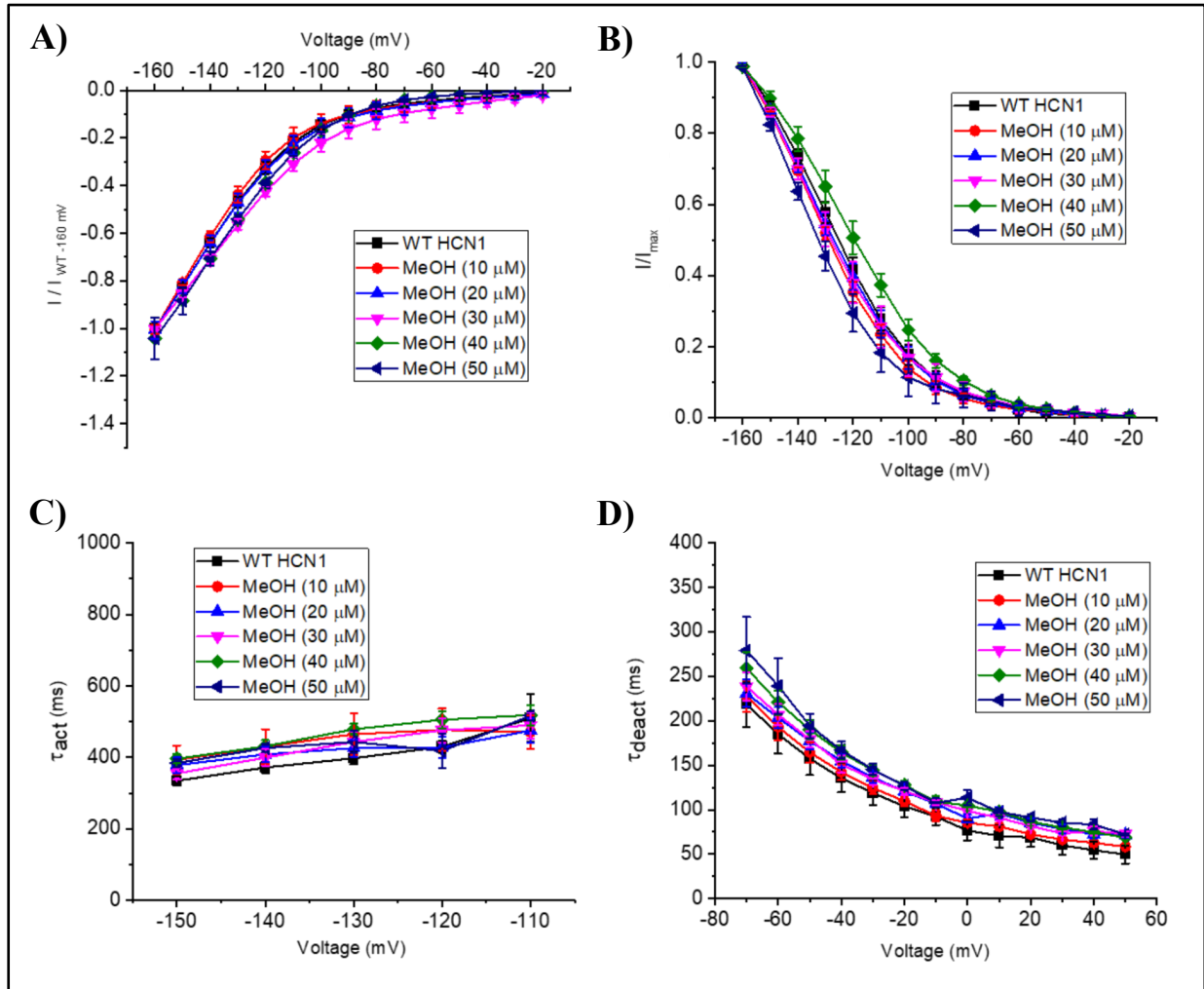


**Figure 25: Regulation of HCN1-WT by methanol (MeOH).** **A**) Current-voltage ( $I/V$ ) relationship in presence of MeOH normalized to maximal current ( $I_{WT(-160\text{ mV})}$ ). ( $4 < n < 10$  per condition;  $0.12 < P < 0.87$ ) **B**) Steady state activation in presence of MeOH. ( $P = 0.14$  for  $V_{1/2}$ ) **C**) Activation time constant ( $\tau$ ) kinetics in presence of MeOH. **D**) Deactivation time constant ( $\tau$ ) kinetics in presence of MeOH. ( $n = 3-4$  per condition;  $0.23 < P < 0.83$ )

Since CBD and THC are both dissolved in methanol (MeOH) we wanted to see if the vehicle altered the properties of HCN1 currents. As expected, MeOH had no effect to our HCN1 currents traces. The current-voltage relationship, steady-state activation data (Table 1), time activation and

deactivation constants were all shown to exhibited statistically negligible after the addition of the vehicle. It is important to mention, an equimolar volume of MeOH was added (Fig. 25 A, B, C & D). For example, 10  $\mu$ M of CBD is equivalent of adding 4.5  $\mu$ L (from stock). Hence, an equivalent volume of vehicle was added.

**Table 1: Steady state activation data for HCN1-WT in presence of cannabinoids**

Condition	$V_{1/2}$ (mV)	k
HCN1 Control	-125.2 $\pm$ 1.7	18.5 $\pm$ 0.3
HCN1 + MeOH (10 $\mu$ M)	-128.8 $\pm$ 2.3	17.6 $\pm$ 0.5
HCN1 + MeOH (20 $\mu$ M)	-127.1 $\pm$ 2.1	17.7 $\pm$ 0.7
HCN1 + MeOH (30 $\mu$ M)	-128.1 $\pm$ 1.2	18.5 $\pm$ 0.5
HCN1 + MeOH (40 $\mu$ M)	-119.7 $\pm$ 4.2	19.6 $\pm$ 1.0
HCN1 + MeOH (50 $\mu$ M)	-132.7 $\pm$ 6.6	16.9 $\pm$ 1.3
HCN1 Control	-129.8 $\pm$ 2.7	17.0 $\pm$ 0.3
HCN1 + 10 $\mu$ M THC	-129.2 $\pm$ 0.7	16.6 $\pm$ 0.5
HCN1 + 20 $\mu$ M THC	-125.9 $\pm$ 4.2	14.7 $\pm$ 0.6
HCN1 + 30 $\mu$ M THC	-129.3 $\pm$ 3.4	20.6 $\pm$ 1.3
HCN1 + 40 $\mu$ M THC	-131.8 $\pm$ 4.9	17.6 $\pm$ 1.0
HCN1 + 50 $\mu$ M THC	-132.8 $\pm$ 5.3	17.9 $\pm$ 1.1
HCN1 Control	-122.2 $\pm$ 0.4	21.1 $\pm$ 0.2
HCN1 + 10 $\mu$ M CBD	-122.8 $\pm$ 0.7	20.6 $\pm$ 0.5
HCN1 + 20 $\mu$ M CBD	-125.6 $\pm$ 2.8	17.6 $\pm$ 0.8
HCN1 + 30 $\mu$ M CBD	-118.9 $\pm$ 1.9	24.0 $\pm$ 0.3
HCN1 + 40 $\mu$ M CBD	-119.6 $\pm$ 1.5	22.9 $\pm$ 0.3
HCN1 + 50 $\mu$ M CBD	-116.8 $\pm$ 2.4	15.1 $\pm$ 1.9

\*Values for midpoint voltage of activation ( $V_{1/2}$ ) and k, the slope factor. Number of experiments and statistics are reported in respective figure legends.

### 3.3. Insights into the mechanism of cannabinoid regulation of HCN1 channels

#### 3.3.1. Role of cyclic-nucleotide binding domain (CNBD)

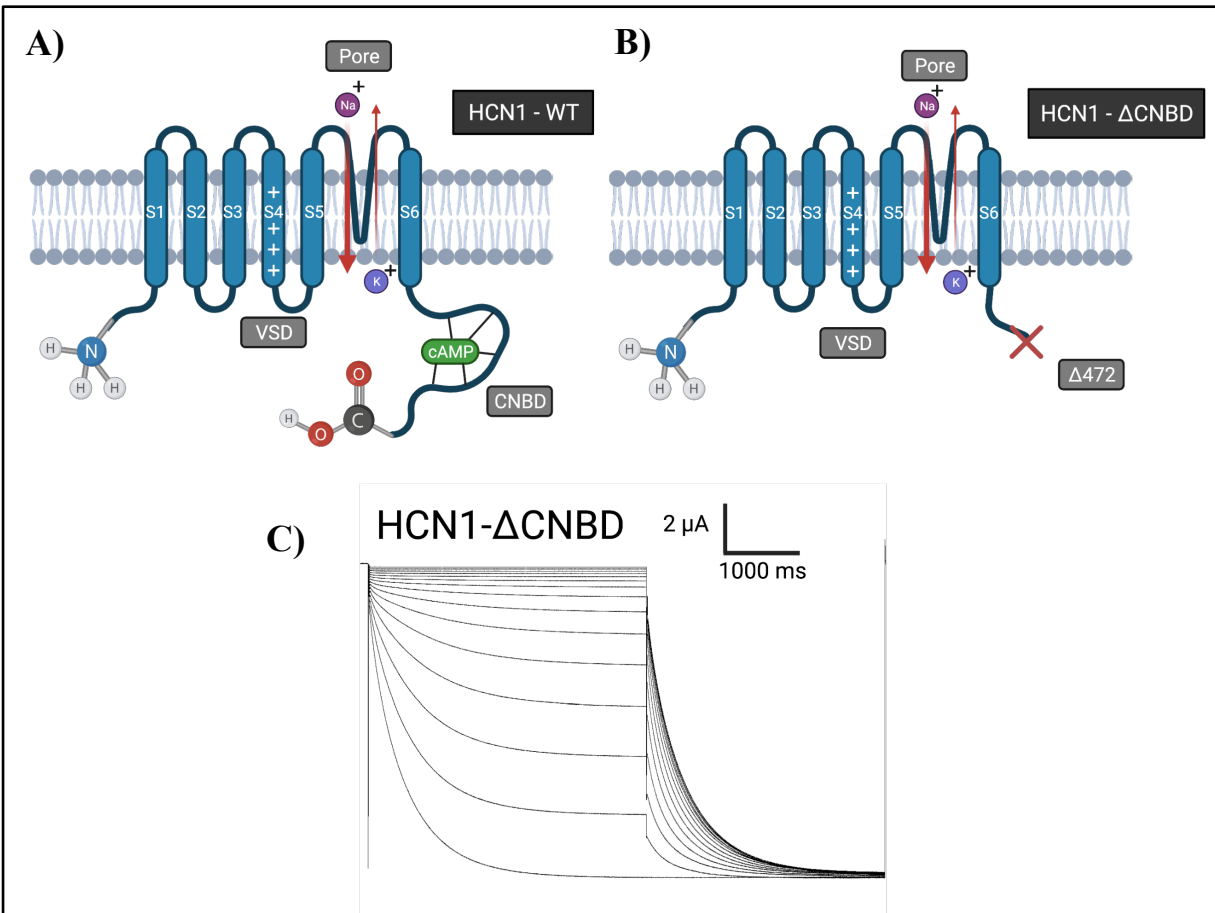


**Figure 26: Insights into the HCN1- $\Delta$ CNBD construct.** A) Secondary structure cartoon of HCN1-WT. B) Secondary structure cartoon of HCN1- $\Delta$ CNBD cut at  $\Delta$ 472 of the amino acid sequence. C) Typical hyperpolarized current traces of HCN1- $\Delta$ CNBD.

To address the mechanism(s) by which CBD and THC modulate HCN1 channels, the mHCN1 construct was altered to exclude the cyclic-nucleotide binding domain (HCN1 $\Delta$ CNBD) (B. Santoro et al., 2011a) (Fig. 26). This portion of the ion channel is the regulatory domain that allows these channels to respond to changes in cAMP and cGMP in the cell. We used this construct because previous work showed that HCN channels were affected by cannabinoids via activation of the cGMP pathway, and therefore, we wanted to know if the CNBD was a necessary domain for cannabinoid regulation in the absence of the CBR as well.

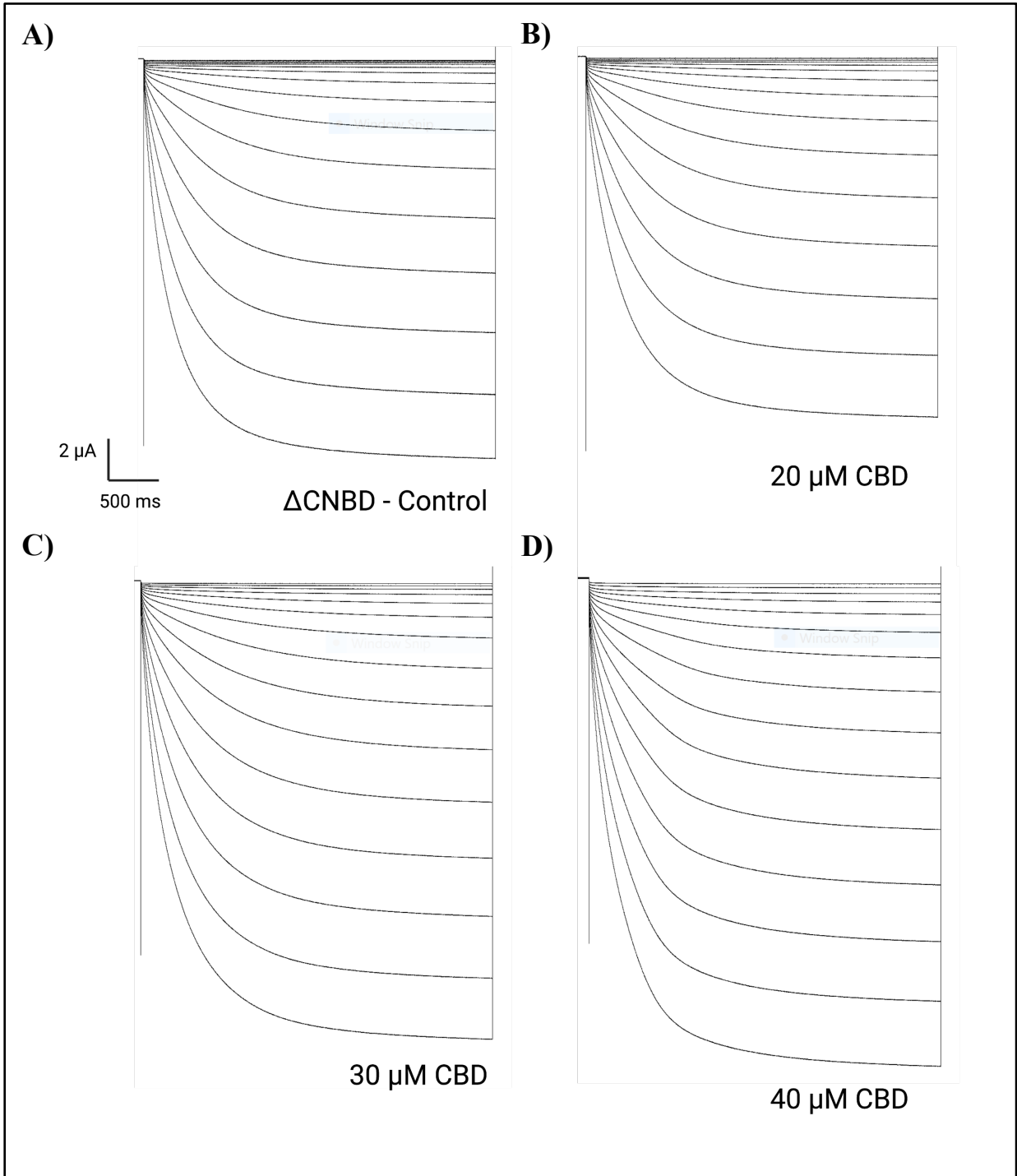


**Figure 27: HCN1- $\Delta$ CNBD current in presence of cannabidiol (CBD).** **A)** Representative current traces in the absence of CBD. **B)** After addition of 20  $\mu$ M CBD. **C)** After 30  $\mu$ M CBD. **D)** After 40  $\mu$ M CBD.

In the presence of either 10 or 20  $\mu$ M CBD we see little change in current traces compared to control (Fig. 27 A & B). Adding 30 or 40  $\mu$ M CBD increased HCN1 current density when

compared to control (Fig. 27 A, C & D). Hence, a total current increase of approximately 30%. HCN1 $\Delta$ CNBD kinetics were also studied. Current-voltage relationships showed close to a 40% increase after the addition of 50  $\mu$ M CBD (Fig. 28 A). Thus, CBD activates the whole cell current for both full-length (wild type) and HCN1 $\Delta$ CNBD. However, the voltage-dependence of steady-state activation (Table 2), and activation time constants showed negligible changes in the presence of CBD (Fig. 28 B & C). Interestingly, deactivation time constants are slowed in a concentration dependent manner by treatment with CBD (Fig. 28 D). Therefore, CBD treatment slows the closing of HCN1 $\Delta$ CNBD channels.

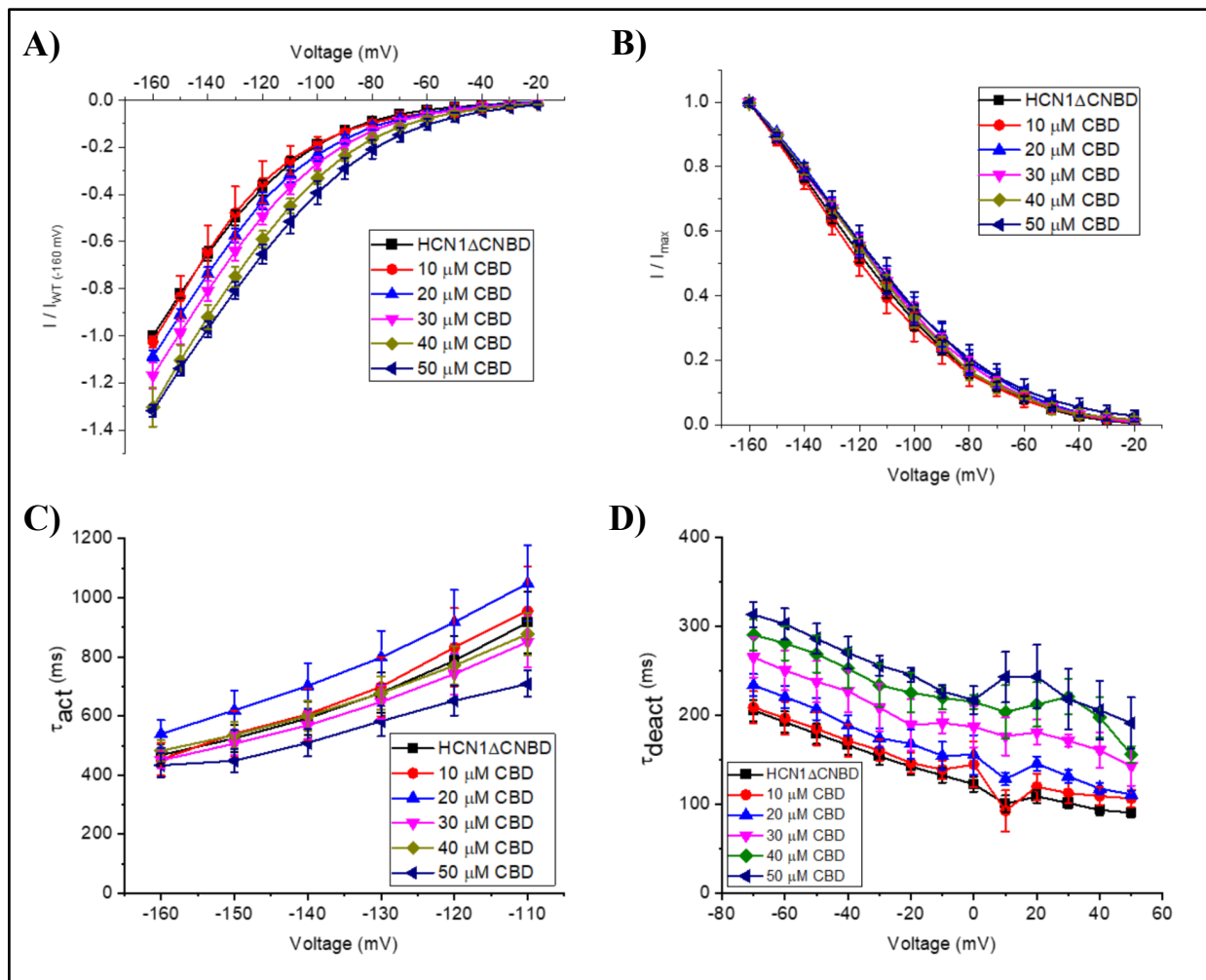


**Figure 28: Regulation of HCN1- $\Delta$ CNBD by cannabidiol (CBD).** **A)** Current-voltage (I/V) relationship in presence of CBD normalized to maximal current ( $I_{WT(-160\text{ mV})}$ ). ( $4 < n < 13$  per condition;  $P < 0.05$  for 20 - 50  $\mu$ M vs control) **B)** Steady state activation in presence of CBD. ( $P = 0.63$  for  $V_{1/2}$ ) **C)** Activation time constant ( $\tau$ ) kinetics in presence of CBD. ( $0.11 < P < 0.46$ ) **D)** Deactivation time constant ( $\tau$ ) kinetics in presence of CBD. ( $4 < n < 10$  per condition;  $P < 0.05$  for 20-50  $\mu$ M)

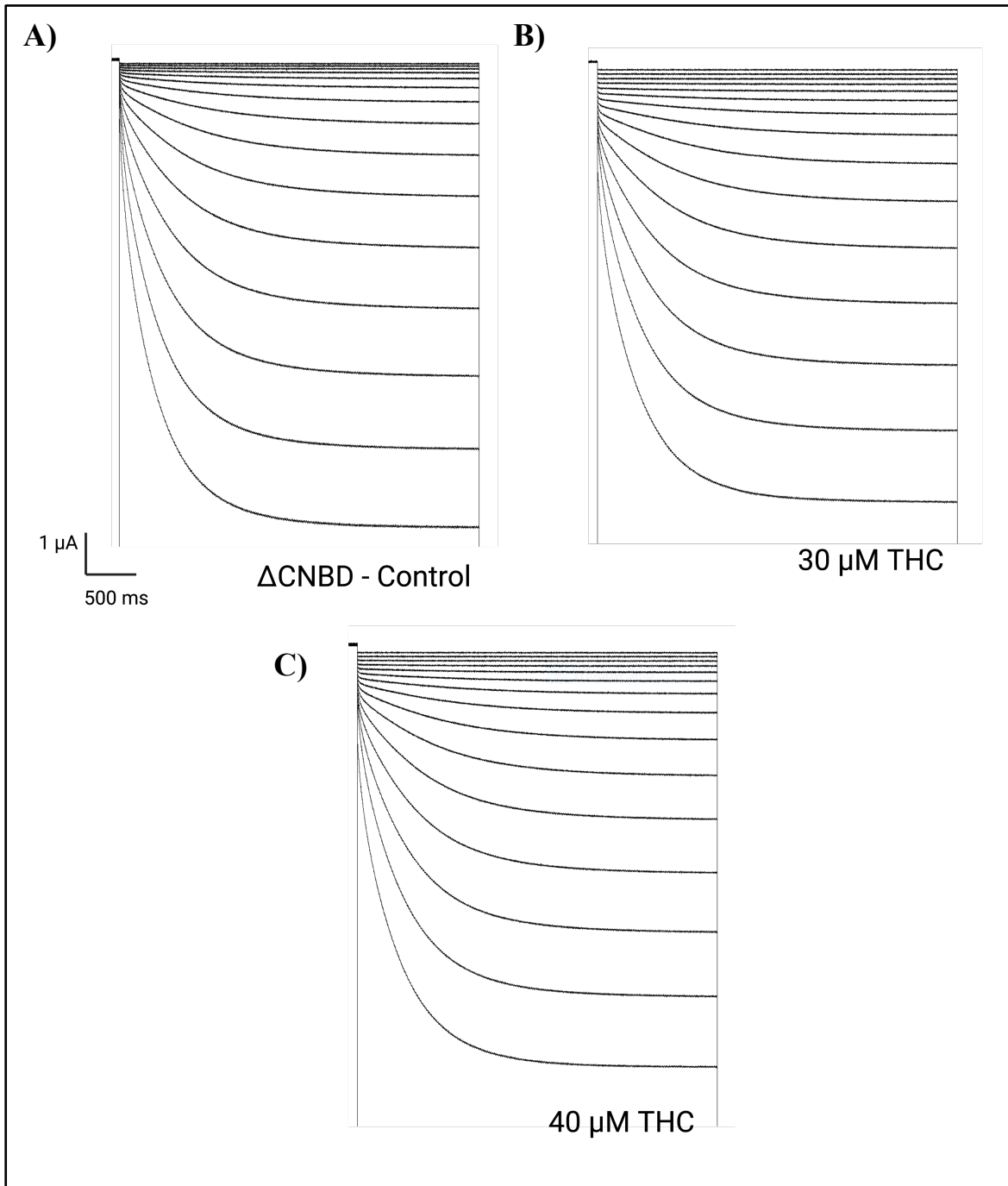


**Figure 29: HCN1-ΔCNBD current in presence of  $\Delta^9$ -tetrahydrocannabinidiol (THC).** A) Representative current traces in the absence of THC. B) After 30  $\mu\text{M}$  THC. C) After 40  $\mu\text{M}$  THC.

The modulation of HCN1-ΔCNBD channels were also monitored in the presence of THC. The addition of 30 or 40  $\mu\text{M}$  THC decreased HCN1 current density when compared to control (Fig. 29 A, B & C). The kinetics of the HCN1-ΔCNBD construct were also studied in the presence of THC.

The current-voltage relationships showed close to a 25% decreased in the presence of 50  $\mu\text{M}$  THC (Fig. 30 A), half of the inhibition shown with the full-length (wild type) (Fig. 24). Moreover, steady-state activation data (Table 2), activation time constants and deactivation time constants exhibited negligible changes in the presence of THC when compared to control (in absence of THC) (Fig. 30 B, C & D).

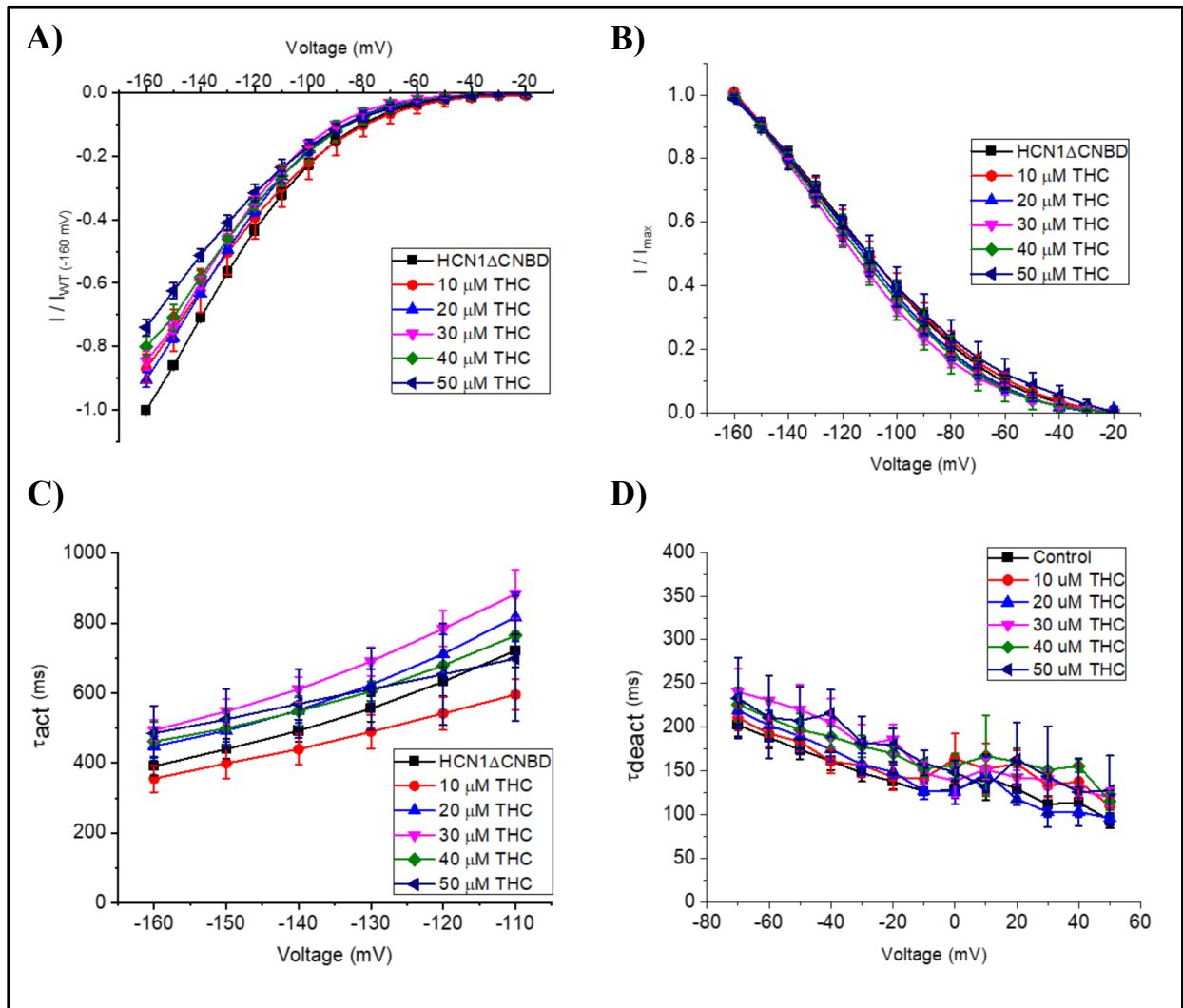


**Figure 30: Regulation of HCN1- $\Delta$ CNBD by  $\Delta^9$ -tetrahydrocannabinol (THC).** **A)** Current-voltage ( $I/V$ ) relationship in presence of THC normalized to maximal current ( $I_{WT(-160\text{ mV})}$ ). ( $4 < n < 12$  per condition;  $P < 0.05$  for 10 - 50  $\mu\text{M}$  vs control) **B)** Steady state activation in presence of THC. ( $P = 0.34$  for  $V_{1/2}$ ) **C)** Activation time constant ( $\tau$ ) kinetics in presence of THC. ( $0.12 < P < 0.46$ ) **D)** Deactivation time constant ( $\tau$ ) kinetics in presence of THC. ( $4 < n < 11$  per condition;  $0.23 < P < 0.84$ )

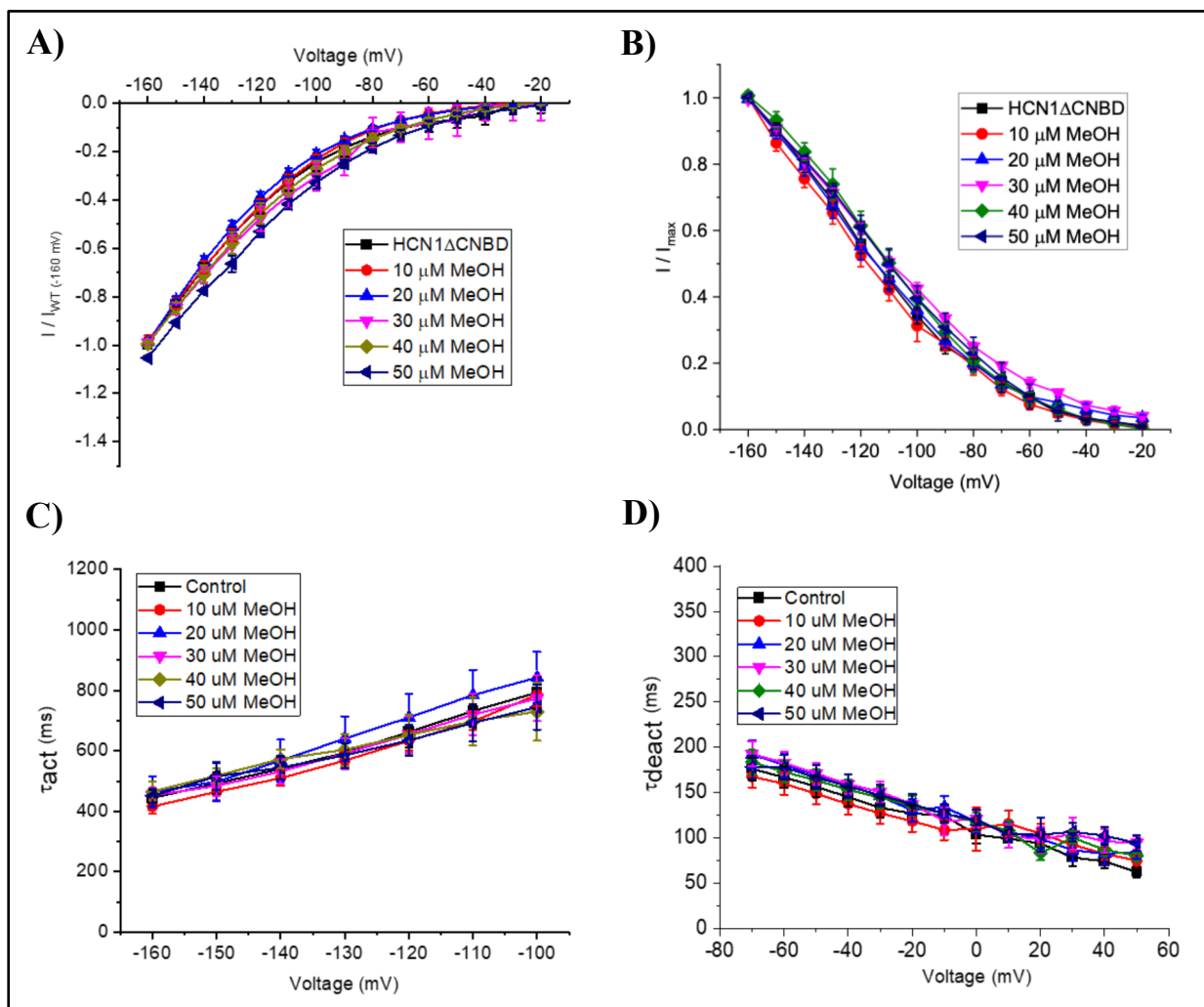


**Figure 31: Regulation of HCN1- $\Delta$ CNBD by methanol (MeOH).** **A)** Current-voltage ( $I/V$ ) relationship in presence of MeOH normalized to maximal current ( $I_{WT(-160\text{ mV})}$ ). ( $4 < n < 11$  per condition;  $0.16 < P < 0.93$ ) **B)** Steady state activation in presence of MeOH. ( $P = 0.89$  for  $V_{1/2}$ ) **C)** Activation time constant ( $\tau$ ) kinetics in presence of MeOH. **D)** Deactivation time constant ( $\tau$ ) kinetics in presence of MeOH. ( $4 < n < 6$  per condition;  $0.23 < P < 0.63$ )

To complete our understanding of the modulation of cannabidiol and  $\Delta^9$ -tetrahydrocannabinidiol on the HCN1- $\Delta$ CNBD construct we wanted to make sure our vehicle (MeOH) would produce no change to the overall current and kinetics. Following the addition of an equimolar volume (same volume as when adding CBD or THC) of MeOH to the bath containing the tested oocytes, we saw an insignificant change in current traces. Current voltage relationships ( $I/V$ ), steady-state activation (Table 2), time activation and deactivation constants were not affected by the addition of methanol (Fig. 31 A, B, C & D).

**Table 2: Steady state activation data for HCN1- $\Delta$ CNBD in presence of cannabinoids**

Condition	$V_{1/2}$ (mV)	k
HCN1 Control	$-115.9 \pm 2.1$	$22.6 \pm 0.5$
HCN1 + MeOH (10 $\mu$ M)	$-118.3 \pm 3.7$	$23.4 \pm 0.6$
HCN1 + MeOH (20 $\mu$ M)	$-115.2 \pm 2.3$	$22.9 \pm 0.8$
HCN1 + MeOH (30 $\mu$ M)	$-110.2 \pm 4.4$	$23.1 \pm 0.4$
HCN1 + MeOH (40 $\mu$ M)	$-111.5 \pm 2.7$	$22.8 \pm 0.3$
HCN1 + MeOH (50 $\mu$ M)	$-111.8 \pm 3.2$	$22.9 \pm 0.3$
HCN1 Control	$-117.8 \pm 3.6$	$24.4 \pm 0.3$
HCN1 + 10 $\mu$ M CBD	$-119.8 \pm 4.5$	$22.9 \pm 0.6$
HCN1 + 20 $\mu$ M CBD	$-115.3 \pm 2.5$	$23.5 \pm 0.8$
HCN1 + 30 $\mu$ M CBD	$-116.9 \pm 1.1$	$29.9 \pm 1.1$
HCN1 + 40 $\mu$ M CBD	$-114.3 \pm 1.8$	$25.3 \pm 2.3$
HCN1 + 50 $\mu$ M CBD	$-113.8 \pm 2.4$	$25.1 \pm 2.2$
HCN1 Control	$-113.9 \pm 5.4$	$28.6 \pm 0.6$
HCN1 + 10 $\mu$ M THC	$-114.3 \pm 4.8$	$28.5 \pm 0.5$
HCN1 + 20 $\mu$ M THC	$-115.2 \pm 1.3$	$26.9 \pm 1.2$
HCN1 + 30 $\mu$ M THC	$-116.2 \pm 3.4$	$26.2 \pm 0.4$
HCN1 + 40 $\mu$ M THC	$-115.2 \pm 2.7$	$27.6 \pm 1.0$
HCN1 + 50 $\mu$ M THC	$-112.8 \pm 3.2$	$25.3 \pm 0.6$

\*Values for midpoint voltage of activation ( $V_{1/2}$ ) and k, the slope factor. Number of experiments and statistics are reported in respective figure legends.

### 3.3.2. Manipulating membrane fluidity with Triton-X 100

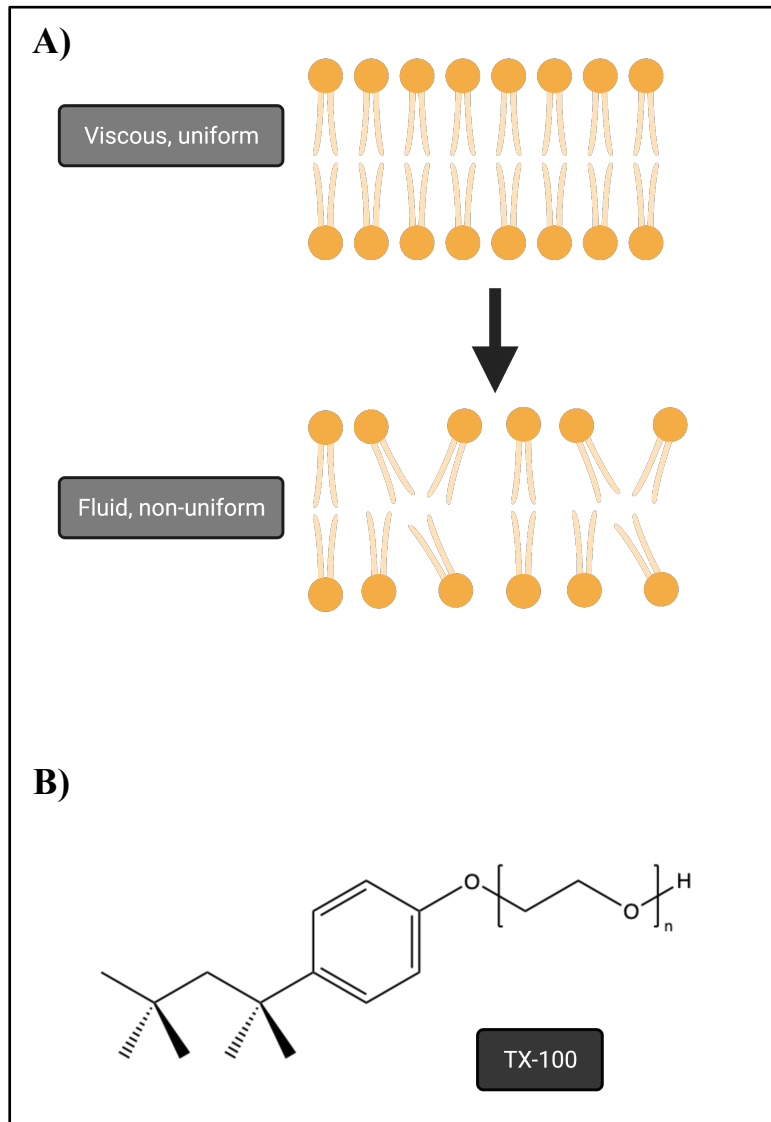


**Figure 32: Graphical representation of membrane fluidity. A)** Cartoon showing the difference between a uniform (viscous) compared to a non-uniform membrane (fluid). **B)** Structure of Triton-X 100 detergent.

Membrane fluidity is a property defined as how uniform, viscous, or fluid a lipid bilayer (Fig. 32 A). This property can be influenced by the packing, percentages, and composition of different lipids (cholesterol as an example) as well as the presence of various proteins (Tillman & Cascio, 2003). Other variables such as temperature and cannabinoids can also allow for regulating membrane fluidity. Since ion channels are embedded in the membrane, they are susceptible to changes in fluidity. HCN channels have already been shown to be modulated, in an isoform dependent manner, by cholesterol (Fürst & D'Avanzo, 2015), a small hydrophobic lipid known to

regulate the fluidity of cell membranes (Ikonen, 2008; Presti, 1985). To examine if CBD or THC regulate HCN channels by altering membrane fluidity, we compare their effects to the addition of TX-100 (Fig. 32 B), a detergent known to decrease membrane fluidity (Fig. 33 and 34). This approach has also been taken to study the mechanism of Nav channels regulation by CBD as well (Ghovanloo et al., 2021).

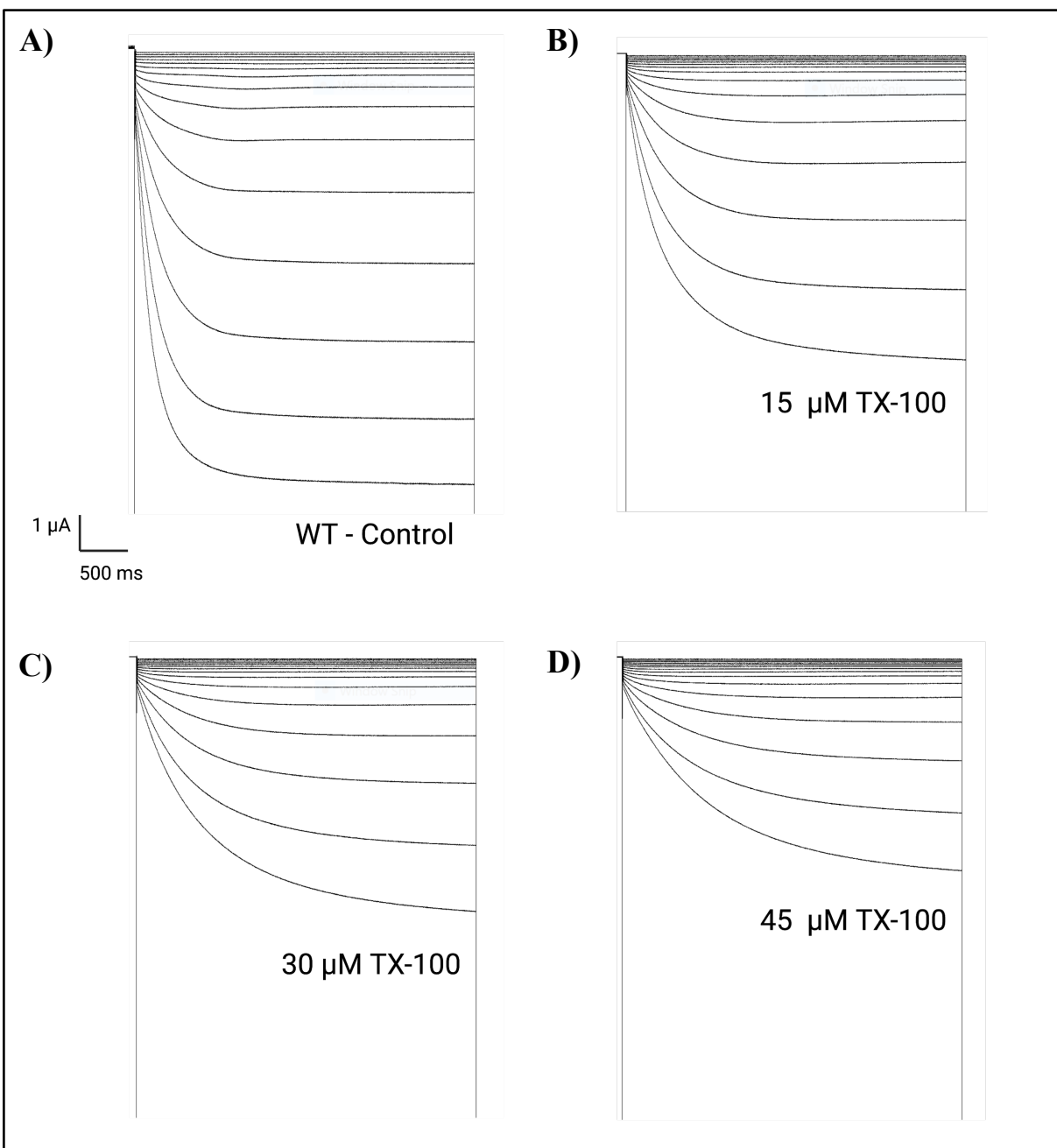


**Figure 33: HCN1-WT current in presence of Triton-X 100 (TX-100).** A) Representative current traces in the absence of TX-100. B) After 15  $\mu$ M TX-100. C) After 30  $\mu$ M TX-100. D) After 45  $\mu$ M TX-100.

After applying various concentrations of TX-100, we found a significant and quick change in the HCN1 current. The mere addition of 15  $\mu\text{M}$  TX-100 decreased HCN1 current density compared to control (Fig. 33 A & B). Addition of 30 or 45  $\mu\text{M}$  TX-100 further inhibited the HCN1 current by a total of more than 50% (Fig. 33 C & D). Notably, the effects of TX-100 treatment occurred much more rapidly (less than 5 mins) compared to the rate of cannabinoid treatment (15-30 mins).

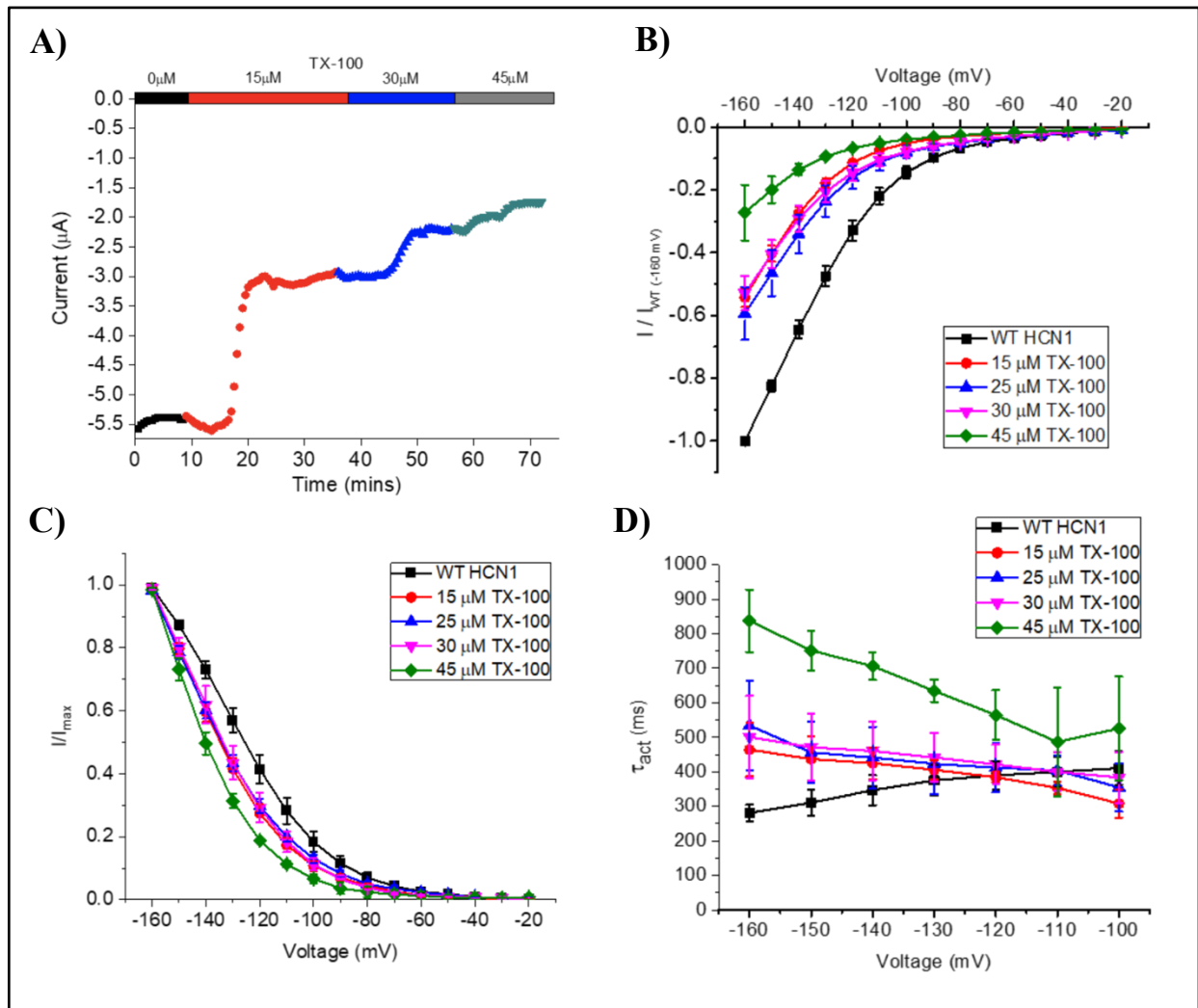


**Figure 34: Regulation of HCN1-WT by Triton-X 100 (TX-100).** A) Pulse protocol over time after addition of TX-100. B) Current-voltage (I/V) relationship in presence of TX-100 normalized to maximal current ( $I_{WT(-160\text{ mV})}$ ). ( $P < 0.05$  for all conditions vs control) C) Steady-state activation in presence of TX-100. ( $P < 0.05$  for all conditions vs. control) D) Activation time constant ( $\tau$ ) kinetics in presence of TX-100. ( $P < 0.05$  for all conditions vs. control) ( $3 < n < 9$  per condition)

Similar to THC, TX-100 also decreases HCN1 current, however, the effects on steady-state activation and gating kinetics are significantly different (for example  $P < 0.05$  for  $V_{1/2}$  of 30  $\mu\text{M}$  THC vs 30  $\mu\text{M}$  TX-100 using a two-sampled t-test). After the addition of 45  $\mu\text{M}$  TX-100, we see a leftward shift of about  $-15$  mV in our steady state, making it more difficult for HCN1 channels to open (Fig. 34 B, Table 3). Additionally, we see a change in our activation time constants, indicating that the channel opens slower at more hyperpolarized voltages (Fig. 34 C). Thus, since the effects of TX-100 do not resemble the modulation seen by either CBD or THC, it appears that the mechanism of HCN1 regulation by either of these cannabinoids cannot be completely described by the effects of altered membrane fluidity.

**Table 3: Steady state activation data for HCN1-WT in presence of TX-100**

Condition	$V_{1/2}$ (mV)	k
HCN1 Control	$-125.6 \pm 1.6$	$19.4 \pm 0.2$
HCN1 15 $\mu\text{M}$ TX-100	$-134.7 \pm 1.8$	$19.2 \pm 0.3$
HCN1 25 $\mu\text{M}$ TX-100	$-134.1 \pm 2.3$	$21.1 \pm 0.3$
HCN1 30 $\mu\text{M}$ TX-100	$-133.6 \pm 2.1$	$18.5 \pm 0.6$
HCN1 45 $\mu\text{M}$ TX-100	$-140.3 \pm 0.7$	$16.6 \pm 0.2$

\*Values for midpoint voltage of activation ( $V_{1/2}$ ) and k, the slope factor. Number of experiments and statistics are reported in respective figure legends.

## 4. Discussion

HCN channels generate the pacemaker current,  $I_h$ , predominantly found in a neuronal and cardiac setting, modulating various physiological aspects such as dendritic excitability, synaptic plasticity, and heart rhythmicity. However, HCN channels and in conjunction  $I_h$ , have been shown to be regulated by several external factors. Changes in membrane potential ( $V_m$ ), binding of cyclic-nucleotides, interactions with auxiliary proteins are all seen to alter the function, gating, and kinetics of HCN channels. Studying the direct interaction of HCN channels with small molecules, for instance the direct interaction and blocking mechanism of ivabradine on HCN1 (Bucchi et al., 2006) can pave the way to discovering potential therapeutic targets.

The vast molecular family of cannabinoids have been studied as potential therapeutic agents for epilepsy, mood, appetite, and sleep wake cycles. Concomitantly, HCN1 channels have also been shown to modulate the underline mechanisms of these physiological traits. So far, it is known that the  $I_h$  current is modulated, indirectly through a distinct signalling cascade involving CBRs (Maroso et al., 2016). Seeing as cannabinoids and the targeting of HCN1 channels share similar therapeutics roles, we aimed to determine if exogenous cannabinoids directly regulate HCN1 channels. Using electrophysiology and a model system which does not express CBRs, we sought to examine the effect of the cannabinoids, cannabidiol (CBD) and  $\Delta^9$ -tetrahydrocannabinol (THC) on HCN1 channels. We have also gained insights into the mechanistic details of the regulation of these cannabinoids. In discussing the findings of this study, we will in parallel compare them to previous studies with related ion channels and their modulation by cannabinoids.

### 4.1. Regulation of HCN1 channels by CBD and THC

As a starting point to the HCN1 study, we decided to reproduce the mechanism of action by which CBD activates TRPV1 ion channels. This stemmed from the fact that we wanted to prove the efficacy of our experimental approach, in using the electrophysiological technique, two-electrode voltage clamp (TEVC) on *Xenopus* oocytes. We saw a change and overall increase in the rTRPV1 current density after the addition of 10 to 30  $\mu$ M CBD. To maximize activation, we then applied 20  $\mu$ M of capsaicin, to the oocyte bath. Our findings coincide, with previous studies.

Using patch-clamp electrophysiology in HEK293 cells, CBD activated TRPV1 channels with an  $EC_{50}$  of 30  $\mu\text{M}$  (Starkus et al., 2019). Therefore, these results justified our use of TEVC electrophysiology on *Xenopus* oocytes which do not express CBRs (Peshkin et al., 2019). This was our experimental model going forward in studying HCN1 currents in the presence of cannabinoids.

In the study, we demonstrate direct modulatory action of exogenous cannabinoids; CBD and THC on HCN1 channels and its correlating  $I_h$  current. Our initial results revealed a concentration and time dependency for the cannabinoids to interact with the channel to alter current density. Although the two drugs altered HCN1 channel function, the vehicle had a negligible change on HCN1 channels. Cannabidiol increases HCN1 current density with an  $EC_{50}$  of 28.5  $\mu\text{M}$  and a 91% maximal response. Therefore, CBD acts as an activator, of HCN1, while THC inhibits HCN1. HCN1 regulation by CBD remains even in the presence of 10  $\mu\text{M}$  AM251, a potent antagonist of CB1 receptors (Gatley et al., 1996). On the other hand, THC inhibits the HCN1 current with an absolute  $IC_{50}$  of 28.9  $\mu\text{M}$ . At maximal inhibition, HCN1 currents decreased by 63%. Various ion channels have been shown to be modulated by CBD and THC within the concentration ranges used in this study. For example, the activation of TRPV1 by CBD. Similarly, studies revealed the direct activation of chloride ion channels ( $\alpha_1$  and  $\alpha_2\beta$  glycine receptors) by cannabidiol with an  $EC_{50}$  of 132.4 and 144.3  $\mu\text{M}$  (Ahrens et al., 2009). In another facet, sodium ion channels, NavMs, experience an inhibitory modulation upon binding of CBD with an  $IC_{50}$  of 17.8  $\mu\text{M}$  (Sait et al., 2020).  $\alpha_7$ -nicotinic acetylcholine ( $\alpha_7$ nACh) receptors which are ligand gated ion channels have also been seen to be inhibited by CBD having an  $IC_{50}$  of 11.3  $\mu\text{M}$  (Mahgoub et al., 2013). A similar response was found in an earlier study using Kv1.2 channels. The voltage and ligand gated potassium ion channel which is structurally similar to HCN channels was shown to be directly inhibited by THC and anandamide (AEA) (Poling et al., 1996). The electrophysiological study was conducted in murine fibroblast cells where THC inhibited potassium currents with an  $IC_{50}$  of 2.4  $\mu\text{M}$ . Additionally, a recent study has shown that THC inhibits human ether-à-go-go (hERG) potassium ion channels expressed in with an  $IC_{50}$  of 10.3  $\mu\text{M}$  in the HEK293 cell line (Orvos et al., 2020). Taking everything into consideration our findings indicate that CBD and THC can also modulate HCN1 channels within the concentration ranges observed for regulatory action on other channels and receptors, and that our results have physiological relevance.

The concentrations of CBD and THC necessary to affect HCN1 channels (in the mid-micromolar range) may be considered high for these molecules to have therapeutic actions through these channels. However, additional considerations may prove such concerns to be unwarranted. Single-dose administration of 10 mg CBD and THC generate serum levels of  $3.0 \pm 3.1 \mu\text{g/L}$  ( $=9.1 - 19.4 \mu\text{M}$ ) (Guy & Flint, 2004; Guy & Robson, 2004). Anticonvulsant effects of THC and CBD have an  $\text{ED}_{50} \sim 120 \text{ mg/kg}$  (Devinsky et al., 2014). Depending on the mode of administration, 120 mg/kg of CBD leads to concentrations of  $7 \mu\text{M}$  in serum and  $1.3 \mu\text{g/g}$  in brain; increased with IP administration to  $45 \mu\text{M}$  in serum and  $6.9 \mu\text{g/g}$  in brain (Deiana et al., 2012). Due to their high lipophilicity ( $K_{\text{octanol-water}} \sim 6-7$ ), there is preferential distribution to fat with rapid distribution in the brain, adipose tissue, and other organs (Ohlsson et al., 1984) with only 10% of administered CBD bound to circulating red blood cells (Williamson, 2004). Chronic administration may lead to further accumulation. It is important to also note the relative differences in  $\text{IC}_{50}$  and  $\text{EC}_{50}$  values between mammalian cell lines such as HEK or CHO cells and *Xenopus* oocytes observed for some drugs, including cannabinoids. This may be because, the lipid bilayer of *Xenopus* oocytes are rich in sphingomyelin with about a 25.8 mole percent (Hill et al., 2005). This, in addition to the vitelline membrane surrounding the cells and low membrane permeability would alter any mechanism of action by a ligand. Previous studies reveal  $\text{IC}_{50}$  and  $\text{EC}_{50}$  values which are significantly higher in *Xenopus* oocytes when compared to mammalian cells. Potassium channel (Kv1.1) blocker, aminopyridine (4-AP), was shown to inhibit channels expressed in mammalian Sol-8 cells with an  $\text{IC}_{50}$  value of  $88 \pm 5 \mu\text{M}$  (Castle et al., 1994). This value was more than 10 times higher in oocytes with  $\text{IC}_{50}$  values closer to 1 mM. Another study monitored the efficacy of various blocking agents on potassium channel, hERG. Again, there seems to be a significant difference in  $\text{IC}_{50}$  values which was 5 to 100 times higher in *Xenopus* oocytes when compared to mammalian HEK293 and CHO cells (Lacerda et al., 2001). Taking this into account, it is likely that the  $\text{IC}_{50}$  and  $\text{EC}_{50}$  values we observe for HCN1 channels in oocytes are not outside the therapeutic range, especially since they are comparable to those observed for other channels and receptors, and likely to be the same, if not even lower, in mammalian cells.

## 4.2. Mechanistic insights into the modulation of HCN1 by CBD and THC

All isoforms of HCN channels contain a cyclic-nucleotide binding domain (CNBD) which modulates channel gating and as the name suggests occurs upon binding of cyclic-nucleotides. cAMP and cGMP are two of the main cyclic-nucleotides which regulate and activate HCN channels. In the next part of the study, we wanted to see if following the removal of the CNBD from the HCN1 isoform and disabling its functionality (being regulated by cyclic-nucleotides), there would still be regulation by cannabinoids. We observed comparable effects of both CBD and THC on the HCN1- $\Delta$ CNBD as we did for the full-length HCN1 channels. We saw a close to a 40% increase in current density after the addition of 50  $\mu$ M CBD and a 25 to 30% decrease in current density after the addition of 50  $\mu$ M THC. Interestingly, HCN1 $\Delta$ CNBD channels are slowed by CBD, however, this is not the sole function of CBD on the CNBD. Therefore, we believe the CNBD in HCN1 channels is not a key contributor to the mechanism. These insights suggest a more direct interaction with the channel rather than through an increase in intracellular cyclic-nucleotide concentration. We also think the cannabinoids would likely interact with another part of the channel rather than through the CNBD.

As ion channels sit in the lipid bilayer, any alteration (change in shape and rigidity) to the membrane could modulate channel functionality, gating, and kinetics. Membrane lipids such as cholesterol and PIP<sub>2</sub>, have been shown to directly regulate HCN channels (Fürst & D'Avanzo, 2015; Pian et al., 2007). In a recent study, by altering cholesterol content (depleting and enriching) in CHO-K1 cells expressing HCN (1, 2 & 4) channels, it was shown that in a isoform dependent manner, the channels were susceptible to changes in both current density and kinetics (Fürst & D'Avanzo, 2015). Stretch activation (mechanical force) on the membrane has also been shown to modulate HCN channels. Using cell-attached oocyte electrophysiological recordings, it was shown that HCN currents were increased and accelerated due to stretch activation (Lin et al., 2007). Since cannabinoids have also been shown to effect membrane fluidity (Beiersdorf et al., 2020; Ghovanloo et al., 2021; Ghovanloo et al., 2018), we compared the regulation by cannabinoids to that of altering membrane fluidity. There are many ways to study the effects of changes in membrane fluidity on ion channels such as using amphiphiles (TX-100), which makes the membrane less stiff (increases fluidity) (Watkins, 2019). Previous studies have shown that TX-

100 inhibits skeletal-muscle sodium channels and L-type calcium channels expressed in mammalian cells (Lundbæk et al., 2004; Narang et al., 2013). Using a gramicidin-based fluorescence (GFA) assay to study changes in membrane fluidity, it was shown that TX-100 (increases membrane fluidity) and CBD (decreases membrane fluidity) have opposing effects on the membrane (Ghovanloo et al., 2020). Additionally, THC has been shown to increase membrane fluidity in neurons which occurs independently of CBRs (Beiersdorf et al., 2020). In this study we used TX-100 to examine current and kinetic changes in HCN1 channels. With the addition of TX-100, we observe a depletion of HCN1 current over time and changes in our kinetics that differs from the effects on HCN1 we observe with cannabinoid treatments. Instead, with TX-100, we observe a shift ( $-15$  mV) in steady state activation towards more (negative) hyperpolarized voltages and slower time activation constants. We observe CBD and TX-100 having distinct effects on HCN1 channels. This could indicate that CBD's mechanism is independent of changes in membrane fluidity. In the case of THC, HCN1 channels are inhibited on a slower timescale when compared to the inhibition in the presence of TX-100. Additionally, there are no changes in the kinetics when looking at the modulation by THC. Taking this into account, this could indicate that CBD and THC are directly binding and modulating HCN1 channels. Moreover, there is a need to explore different avenues by which these cannabinoids can bind HCN1 channels, whether through the pore or one of the transmembrane domains.

Various cannabinoids have been shown to directly bind different ion channels such as sodium and TRP channels. Cannabidiol was proposed to interact and inhibit the voltage gated sodium channels, Nav1.4 and NavM (Ghovanloo et al., 2020; Sait et al., 2020). Sodium channels, like HCN channels have four subunits each consisting of six transmembrane domains, a voltage sensor domain, and a pore domain. Docking simulations using the hNav1.4 cryo-EM structure revealed CBD to bind to a local anesthetic binding site in the S6 region and block the pore. Subsequent X-ray crystallography studies unravelled, the structure NavM bound to CBD (Sait et al., 2020). The ligand was revealed to bind to a hydrophobic cavity located on TM helices lining the pore. These openings in the intra-membranes are called fenestrations and modulate channel inactivation (Montini et al., 2018). However, contrary to HCN channels, sodium channels are domain-swapped. Therefore, the CBD binding mechanism described in sodium channels which require a domain swapped configuration, would not hold in HCN1 channels since the four subunits form the pore domain.

TRPV are essential ion channels (in the CNS and PNS) and have been shown to be regulated by CBD. Activation attained from binding of capsaicin to TRPV1 channels is similar but different from the activation induced by CBD binding. Capsaicin activation is observed when the channel undergoes pore dilation. In this dilated form, the channel rapidly allows passage of larger ions like NMDG and exhibits non-rectification (Starkus et al., 2019). CBD, however, does not cause TRPV1 channels to dilate, instead it activates the channel independently. Recently, the structure of TRPV2 bound to CBD was solved (Pumroy et al., 2019). It hypothesized that the mechanism by which CBD binds TRPV2 and TRPV1 were similar due to the ligand's interaction with equivalent aromatic residues. The TRPV2 channel undergoes conformational changes upon CBD binding to a hydrophobic pocket. Seeing as TRPV channels are also domain swapped, the binding pocket is found near the S5 and S6 TMs of adjacent subunits. Evidently, CBD or THC would have to bind HCN1 channels in another manner since the channels are non-domain swapped. This may indicate that CBD and THC could interact, extracellularly, with the channel through one of the transmembrane domains.

### **4.3. Physiological and therapeutic applications**

Cannabinoids and their distinct molecular attributes are already being used for studies in various neuropsychiatric and neurodegenerative disorders. Neuropathic pain and epileptic seizures, for example, are known to be mediated by TRP channels expressed in neurons. CBD and capsaicin, activate then rapidly desensitize these channels. Physiologically, an epileptic episode involves hyperexcitability in neurons (increased fire rate), however, studies have found CBD to reduce these overages in neuronal activity (Iannotti et al., 2014). Additionally, as the mechanistic behavior suggests, capsaicin creams have been used as a desensitizing therapeutic in relieving pain (Fischer et al., 2020). Similarly, HCN channels expressed in CA1 pyramidal neurons were also seen as therapeutic targets for the antiepileptic molecule, lamotrigine. Mechanistically, the drug reduced neuronal firing by increasing and activating the  $I_h$  current (Peng et al., 2010). Looking at the results we obtained for the regulation of HCN1 channels by CBD we believe the same may also be occurring in a neuronal setting. Therefore, cannabidiol may act as an  $I_h$  activator and could stabilize neuronal excitability.

Based on several studies, it has been suggested that cannabinoids can act as possible neuroprotective agents for Parkinson's disease (PD) and Alzheimer's disease (AD) (Cooray et al., 2020). However, the mechanism by which this occurs remains elusive. Also, it is believed that each cannabinoid can act differently. HCN channels have been recently linked to the possible underlying mechanism of both PD and AD. HCN channels were shown to regulate the rhythmicity and neuronal firing in different types of neurons in the brain. Damage to substantia nigra pars compacta (SNc) dopaminergic neurons are the basis of PD. HCN channels are shown to regulate these neurons. SNc neurons fire at faster rates and are correlated to the channels by their greater than normal  $I_h$  current (Chang et al., 2019). Therefore, a reduction or inhibition of HCN channels would prevent the underlying neuronal damage sustained with PD. Seeing as our findings suggest THC inhibits HCN1 currents, this could aid in solving the mechanistic nature linking cannabinoids, HCN channels and PD. THC could possibly reduce neuronal firing and the  $I_h$  current to prevent damage in a neuronal setting.

## **4.4. Future directions**

### **4.4.1. Short term**

#### **i. Other cannabinoids**

Cannabinoids are part of a large family of molecular entities which are either, isolated from plant extracts, found in mammalian tissue, or synthetically fabricated. One complimentary experiment which could be done would be to see whether if other exogenous cannabinoids such as tetrahydrocannabivarin (THCV), cannabinol (CBN) and cannabidivarin (CBDV) would also affect HCN1 currents (using electrophysiological recordings). The differences in molecular structure of these cannabinoids could change the way the ligand modulates HCN1. For instance, THC when compared to CBD contains a closed pyran ring. CBD does not have this ring formation, rather a free hydroxyl and alkene group. This makes CBD rotationally less rigid and has been modelled to have one more hydrogen bond interaction with the binding site of the sodium channel, NavM when compared to THC (Sait et al., 2020). Alternatively, endogenous cannabinoids such as 2-AG, AEA, 2-Arachidonyl glyceryl ether (2-AGE) and N-Arachidonoyl dopamine (NADA) may also be

studied to see their modulation on HCN1 channels. It would be interesting to see if certain structural moieties and groups in the various known cannabinoids would alter modulation of HCN1 channels. Additionally, the potency and concentration decency of each cannabinoid can also be compared.

## **ii. Monitor intracellular cGMP/cAMP in *Xenopus* oocytes**

To reinforce the direct modulation of CBD and THC on HCN1 currents, we monitored the concentration of cyclic-nucleotide, cGMP, in non-injected oocytes. It is known that by increasing the intracellular concentration of cGMP, HCN1 channels and the  $I_h$  current are activated. We incubated oocytes at two concentrations (30 and 50  $\mu\text{M}$ ) of CBD, THC and MeOH. These concentrations represent a range in which we saw the effect on HCN1 by cannabinoids. Next by homogenizing (vigorous pipetting with HCl) the grouped *Xenopus* oocytes we isolated the supernatant as previously described (Gao et al., 2015). Supernatants were then used in the cGMP assay alongside cGMP standards. Once the chemiluminescent substrate is added to the assay a light signal (luminescence) can be read by a plate reader and give a relative light unit (RLU). Any given light unit can then be correlated to a given cGMP concentration. This employs the use of the logarithmic standard curve which was created (Fig. 35 B).

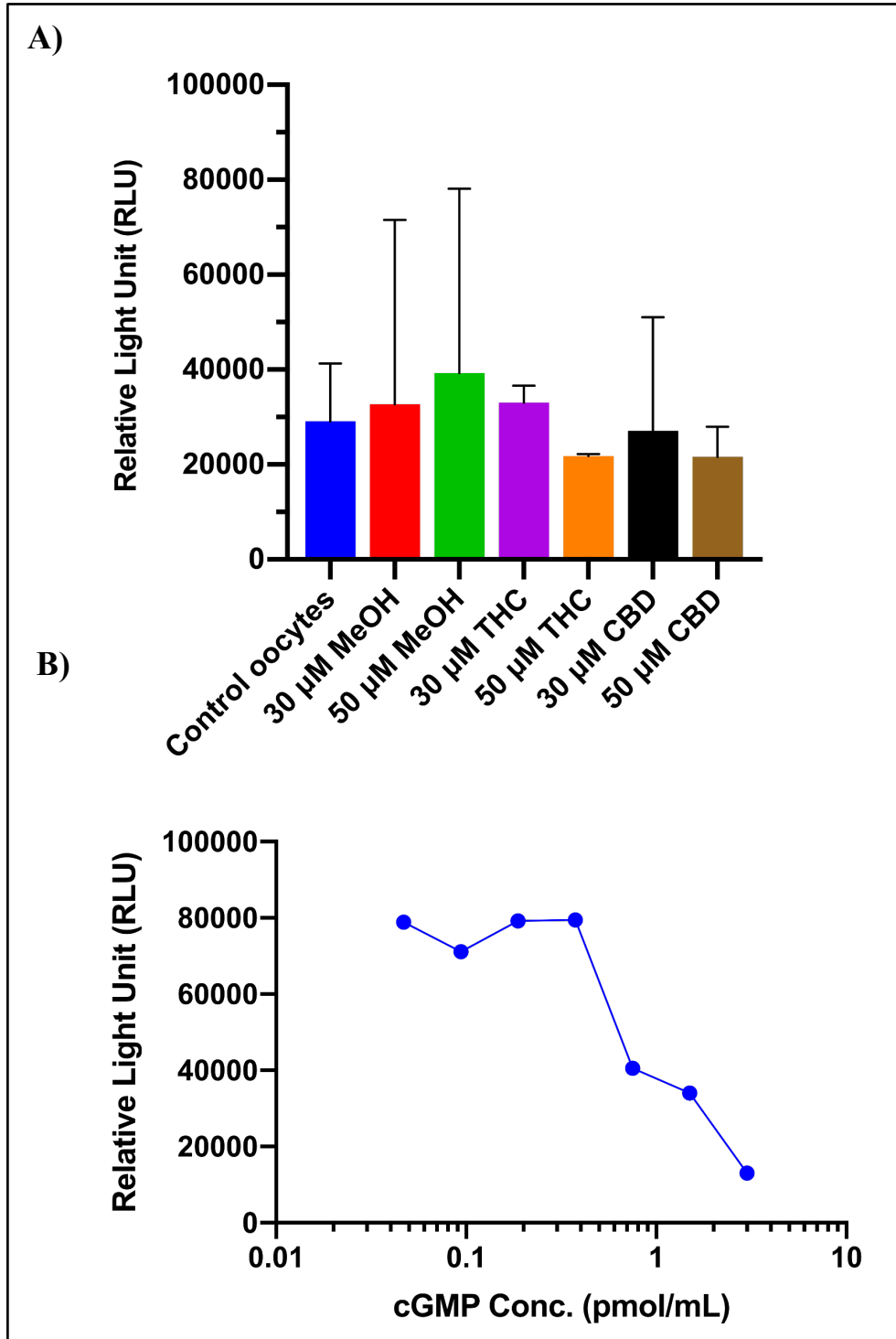


**Figure 35: Intracellular cGMP concentrations in *Xenopus* oocytes in presence of cannabinoids.** A) Bar graph of relative light unit (RLU) from homogenized control oocytes (blue), oocytes in presence of 30  $\mu$ M THC (red), 50  $\mu$ M THC (green), 30  $\mu$ M CBD (purple), 50  $\mu$ M CBD (orange), 30  $\mu$ M MeOH (black) and 50  $\mu$ M MeOH (brown). B) Logarithmic (scaled 10) standard cGMP concentration curve in correlation to relative light unit (RLU) (n=1 experiment, average of 5 oocytes each for each condition).

When comparing the RLU values for the various conditions we do not see much of a change, statistically, when compared to control oocytes (absence of drug or vehicle). cGMP concentrations stayed within a range of approximately  $\sim 0.9 - 2$  pmol/mL (Fig 35. A). Therefore, it seems as though cannabinoids have no influence on the intracellular cGMP concentrations in oocytes not expressing CBRs, and thus, this is not the mechanism involved in the altered HCN1 currents we observe with cannabinoid treatments. However, even though there are no apparent trends in RLU, the large error bars, indicate that more replicates are required to validate these findings. Concomitantly, another intracellular assay should be conducted to monitor changes in concentration of cAMP, in oocytes, as this ligand is also known to modulate HCN1 channels.

### **iii. FLIPR Potassium Assay**

HCN1 modulation by CBD and THC may also be studied with a Fluorescent Imaging Plate Reader (FLIPR) potassium assay. Originally developed to study the flux of calcium ions in GPCRs and related calcium ion channels, FLIPR has been modified over the years to accommodate the study of several other channels (Arkin et al., 2004). A potassium FLIPR assay provides a medium-throughput assay to assess screen a library of cannabinoids for their ability to modulate HCN1 function. Experimentally, HCN1 channels would be stably transfected, in CHO-K1 cells for plasmid incorporation into the genome. Once cells are expressed, they would be separated into a 96-well black-walled plate (equal quantity per well). Next, cells would be subject to 30-min incubations in a solution-based mixture of thallium ( $Tl^+$ ) dye with various concentrations of CBD, THC, and vehicle (MeOH). Control experiments with cells in the presence of ZD7288 (HCN1 inhibitor) would also be conducted. Thallium ions can mimic the action of potassium ions (Z. Tao et al., 2008). In this case,  $Tl^+$  ions would pass through the pore of HCN1 channels and then give off a fluorescence signal (RLU). This signal would be directly related to the rate of  $Tl^+$  ion influx (Weaver, 2018) and HCN1 channels in an open state, all in the presence of a cannabinoid over time. If a cannabinoid inhibits the channel,  $Tl^+$  ion influx rates would decrease and if a cannabinoid activates the channel, influx rates would increase (Zhang et al., 2010). Therefore, mechanistic behaviors of the channel upon interacting with cannabinoids could be unraveled. Cannabinoids which are identified by this screening would be further characterized with electrophysiological recordings.

## 4.4.2. Long term

### i. Patch-clamp electrophysiology

High fidelity electrophysiological measurements can be used to gain a better understanding of the effect of cannabinoids on HCN1 currents. A HCN1 cDNA construct can be expressed, exogenously in an expression system such as CHO-K1 or HEK293 cells (known for their low endogenous ion channel expression). More importantly, these cells have been shown through proteomic studies to not express cannabinoid receptors, endogenously (Baycin-Hizal et al., 2012; Lavado-García et al., 2020). These mammalian cell lines have been used to study various neurological diseases and can be used to examine  $I_h$  currents with an electrophysiological technique called patch-clamp. Briefly, a gigaohm seal would be formed between a glass pipette and cell membrane, the cell membrane then would be broken by suction to record whole-cell HCN1 currents (Kornreich, 2007). After this process, cells would be subject to either constant perfusion with a solution mixture of cannabinoid and extracellular solution or incubated with the cannabinoid prior to recording.

Alternatively, a neuronal cell-line can also be used to study the effect of cannabinoids on HCN1 channels. This would, experimentally, give us physiological insights. Mammalian neuronal cell line, Neuroblast-2a (N2a) isolated from *Mus musculus* is a prime cellular model for this study as HCN1 proteins are predominantly expressed in the brain. However, it is important to avoid the previously mentioned signalling cascade by which  $I_h$  is activated by CBRs. Since N2a cells highly expressed CBR1 proteins (Rouillard et al., 2016), we would have to either knock-out the gene or block CBR activity with AM251.

### ii. Structural studies

To gain insights into a possible binding site and structural changes upon binding of cannabinoids (CBD or THC) to HCN1, we can conduct cryogenic-electron microscopy studies. Purified HCN1 protein can be isolated using a heterologous expression system such as the BacMam method (using HEK293 cells) previously described in the determination of the structure of human HCN1 (Lee & Roderick, 2017). Alternatively, through an approach utilizing the *saccharomyces cerevisiae*

expression system previously used to purify human KCNJ channels (D'Avanzo et al., 2010). Once purified, and before preparing cryo-EM grids for data collection, a sample of the purified protein ( $\mu\text{g}$ ) would be incubated in CBD or THC ( $30 \mu\text{M}$ ) for approximately 20-30 minutes. Similar to the method employed in finding the cryo-EM structure of TRPV2 bound to CBD (Pumroy et al., 2019). To help us in determining subtle or large conformational changes upon cannabinoid binding we can solve structures in both the proteins apo form (ligand free) and the cannabinoid bound form.

### **iii. Putative binding site and computational studies**

Computational docking experiments can also shed a light on the putative binding site of cannabinoids on the HCN1 channel. Screening for these potential binding sites can be conducted using docking software such as Autodock and MOE-Dock (Corbeil et al., 2012; Österberg et al., 2002). Once potential targets are found, the various conformations of the HCN channel and cannabinoid ligands can be studied to determine which mutants could be created. These putative sites can then be examined experimentally again, using electrophysiology experiments (TEVC or patch-clamp) on channels with mutations introduced by site-directed mutagenesis.

Extensive computational experiments such as a combination of coarse grain with all-atom molecular dynamic (MD) simulations would aid in unravelling the local motions, global motions, and the folding behaviours of HCN1 in the presence of CBD or THC (Kmieciak et al., 2016). Using a combination of both MD simulations would give us insights in first, a global molecular model by which cannabinoids can bind the HCN1 structure and second, the way in which the cannabinoid would bind. These simulations may also be conducted at a longer time scale, allowing us to monitor the system in greater depth. This is due to the computational power behind coarse-grained MD. Validation of a binding site and mechanistic insights of a cannabinoid bound to HCN1 can give us knowledge on how these ligands can be used as potential therapeutics.

## Conclusion

Given the unique role of cannabinoids and their effects, we see a potential future for the use of these lipophilic molecular entities as therapeutic agents for several diseases. HCN channels and cannabinoids share similar roles as active members in the central nervous system. Regulating neuronal firing, stabilizing mood, and inducing appetite are some of the roles in which HCN channels and cannabinoids function upon. Strengthening the link, especially in a direct manner between cannabinoids and HCN channels would give us directionality on mediating the interaction. Determining new and direct ligand regulators for HCN channels expressed in neuronal cells can lead to possible therapeutic targets. Especially for neurodegenerative and neuropsychiatric diseases which predominantly involve irregularities in neuron firing. The importance linking cannabinoids and the physiological role of HCN channels is evident.

In this study, cannabidiol (CBD) and  $\Delta^9$ -tetrahydrocannabinol (THC), the primary molecular components in *cannabis sativa*, were used to study the effect on HCN1 channels. Using an electrophysiological technique, two-electrode voltage clamp (TEVC) on *Xenopus* oocytes, a concentration and time dependent modulation was unraveled with the micromolar addition of the drug. Vehicle, methanol was shown to leave macroscopic current and kinetics of HCN1 channels untouched. THC was shown to gradually inhibit the current and leave HCN1 kinetics the same. CBD had a dissimilar effect in gradually activating and increasing the  $I_h$  current while leaving the channel's kinetics unchanged. Manipulating membrane fluidity, inhibited the  $I_h$  current and altered HCN1 kinetics. The steady state activation voltage dependency shifted towards more negative potentials while proving to slow down the rate ( $\tau$ ) of channel activation. Taken together, we believe to have determined a plausible route to the direct regulation of HCN1 channels by cannabinoids, CBD, and THC.

## References

- Abbott, G. W. (2015). The KCNE2 K<sup>+</sup> channel regulatory subunit: Ubiquitous influence, complex pathobiology. *Gene*, 569(2), 162-172. doi:10.1016/j.gene.2015.06.061
- Ahrens, J., Demir, R., Leuwer, M., de la Roche, J., Krampfl, K., Foadi, N., . . . Haeseler, G. (2009). The Nonpsychotropic Cannabinoid Cannabidiol Modulates and Directly Activates Alpha-1 and Alpha-1-Beta Glycine Receptor Function. *Pharmacology*, 83(4), 217-222. doi:10.1159/000201556
- Ameri, A. (1999). The effects of cannabinoids on the brain. *Progress in Neurobiology*, 58(4), 315-348. doi:[https://doi.org/10.1016/S0301-0082\(98\)00087-2](https://doi.org/10.1016/S0301-0082(98)00087-2)
- Andersen, H. K., Piroli, G. G., & Walsh, K. B. (2018). A real time screening assay for cannabinoid CB1 receptor-mediated signaling. *Journal of Pharmacological and Toxicological Methods*, 94, 44-49. doi:<https://doi.org/10.1016/j.vascn.2018.05.001>
- Arkin, M. R., Connor, P. R., Emkey, R., Garbison, K. E., Heinz, B. A., Wiernicki, T. R., . . . Sittampalam, S. (2004). FLIPR™ Assays for GPCR and Ion Channel Targets. In S. Markossian, A. Grossman, K. Brimacombe, M. Arkin, D. Auld, C. P. Austin, J. Baell, T. D. Y. Chung, N. P. Coussens, J. L. Dahlin, V. Devanarayan, T. L. Foley, M. Glicksman, M. D. Hall, J. V. Haas, S. R. J. Hoare, J. Inglese, P. W. Iversen, S. C. Kales, M. Lal-Nag, Z. Li, J. McGee, O. McManus, T. Riss, P. Saradjian, G. S. Sittampalam, M. Tarselli, O. J. Trask, Jr., Y. Wang, J. R. Weidner, M. J. Wildey, K. Wilson, M. Xia, & X. Xu (Eds.), *Assay Guidance Manual*. Bethesda (MD): Eli Lilly & Company and the National Center for Advancing Translational Sciences.
- Ashton, J. C., Wright, J. L., McPartland, J. M., & Tyndall, J. D. (2008). Cannabinoid CB1 and CB2 receptor ligand specificity and the development of CB2-selective agonists. *Curr Med Chem*, 15(14), 1428-1443. doi:10.2174/092986708784567716
- Bader, C. R., Bertrand, D., & Schwartz, E. A. (1982). Voltage-activated and calcium-activated currents studied in solitary rod inner segments from the salamander retina. *The Journal of physiology*, 331(1), 253-284. doi:<https://doi.org/10.1113/jphysiol.1982.sp014372>
- Baruscotti, M. a. B. A. a. D. D. (2005). Physiology and pharmacology of the cardiac pacemaker (“funny”) current. *Pharmacology & Therapeutics*, 107(1), 59--79. doi:<https://doi.org/10.1016/j.pharmthera.2005.01.005>
- Baycin-Hizal, D., Tabb, D. L., Chaerkady, R., Chen, L., Lewis, N. E., Nagarajan, H., . . . Betenbaugh, M. (2012). Proteomic Analysis of Chinese Hamster Ovary Cells. *Journal of Proteome Research*, 11(11), 5265-5276. doi:10.1021/pr300476w
- Beiersdorf, J., Hevesi, Z., Calvigioni, D., Pyszkowski, J., Romanov, R., Szodorai, E., . . . Keimpema, E. (2020). Adverse effects of Δ9-tetrahydrocannabinol on neuronal bioenergetics during postnatal development. *JCI insight*, 5(23), e135418. doi:10.1172/jci.insight.135418

- Blázquez, C., Ruiz-Calvo, A., Bajo-Grañeras, R., Baufreton, J. M., Resel, E., Varilh, M., . . . Guzmán, M. (2020). Cannabinoid-induced motor dysfunction via autophagy inhibition. *Autophagy*, *16*(12), 2289-2291. doi:10.1080/15548627.2020.1827560
- Blume, L. C., Eldeeb, K., Bass, C. E., Selley, D. E., & Howlett, A. C. (2015). Cannabinoid receptor interacting protein (CRIP1a) attenuates CB1R signaling in neuronal cells. *Cell Signal*, *27*(3), 716-726. doi:10.1016/j.cellsig.2014.11.006
- Boczek, T., & Zylinska, L. (2021). Receptor-Dependent and Independent Regulation of Voltage-Gated Ca(2+) Channels and Ca(2+)-Permeable Channels by Endocannabinoids in the Brain. *International journal of molecular sciences*, *22*(15), 8168. doi:10.3390/ijms22158168
- Bokoch, G. M., Katada, T., Northup, J. K., Ui, M., & Gilman, A. G. (1984). Purification and properties of the inhibitory guanine nucleotide-binding regulatory component of adenylyate cyclase. *Journal of Biological Chemistry*, *259*(6), 3560-3567. doi:[https://doi.org/10.1016/S0021-9258\(17\)43131-0](https://doi.org/10.1016/S0021-9258(17)43131-0)
- Booth, W. T., Walker, N. B., Lowther, W. T., & Howlett, A. C. (2019). Cannabinoid Receptor Interacting Protein 1a (CRIP1a): Function and Structure. *Molecules (Basel, Switzerland)*, *24*(20), 3672. doi:10.3390/molecules24203672
- Brown, H., DiFrancesco, D., & Noble, S. (1979a). Cardiac pacemaker oscillation and its modulation by autonomic transmitters. *The Journal of Experimental Biology*, *81*, 175-204. Retrieved from <http://europepmc.org/abstract/MED/315983>
- Brown, H. a. D. D. a. N. S. (1979). Cardiac pacemaker oscillation and its modulation by autonomic transmitters. *The Journal of Experimental Biology*, *81*(1), 175 LP -- 204. Retrieved from <http://jeb.biologists.org/content/81/1/175.abstract>
- Brown, H. F., DiFrancesco, D., & Noble, S. J. (1979b). How does adrenaline accelerate the heart? *Nature*, *280*(5719), 235-236. doi:10.1038/280235a0
- Bucchi, A., Tognati, A., Milanesi, R., Baruscotti, M., & DiFrancesco, D. (2006). Properties of ivabradine-induced block of HCN1 and HCN4 pacemaker channels. *J Physiol*, *572*(Pt 2), 335-346. doi:10.1113/jphysiol.2005.100776
- Caballero-Florán, R. N., Conde-Rojas, I., Oviedo Chávez, A., Cortes-Calleja, H., Lopez-Santiago, L. F., Isom, L. L., . . . Florán, B. (2016). Cannabinoid-induced depression of synaptic transmission is switched to stimulation when dopaminergic tone is increased in the globus pallidus of the rodent. *Neuropharmacology*, *110*, 407-418. doi:<https://doi.org/10.1016/j.neuropharm.2016.08.002>
- Calejo, A. I., Reverendo, M., Silva, V. S., Pereira, P. M., Santos, M. A. S., Zorec, R., & Gonçalves, P. P. (2014). Differences in the expression pattern of HCN isoforms among mammalian tissues: sources and implications. *Molecular Biology Reports*, *41*(1), 297-307. doi:10.1007/s11033-013-2862-2

Callewaert, G. a. C. E. a. V. J. (1984). Single cardiac Purkinje cells: general electrophysiology and voltage-clamp analysis of the pace-maker current. *The Journal of physiology*, 349, 643--661. doi:10.1113/jphysiol.1984.sp015179

Campbell, N. A., Reece, J. B., Urry, L. A., Cain, M. L., Wasserman, S. A., Minorsky, P. V., & Jackson, R. B. (2008). *Biology, 8th Edition* (8 ed.): Pearson Benjamin Cummings.

Castle, N. A., Fadous, S., Logothetis, D. E., & Wang, G. K. (1994). Aminopyridine block of Kv1.1 potassium channels expressed in mammalian cells and *Xenopus* oocytes. *Molecular Pharmacology*, 45(6), 1242. Retrieved from <http://molpharm.aspetjournals.org/content/45/6/1242.abstract>

Chang, X., Wang, J., Jiang, H., Shi, L., & Xie, J. (2019). Hyperpolarization-Activated Cyclic Nucleotide-Gated Channels: An Emerging Role in Neurodegenerative Diseases. *Frontiers in Molecular Neuroscience*, 12(141). doi:10.3389/fnmol.2019.00141

Chemin, J., Monteil, A., Perez-Reyes, E., Nargeot, J., & Lory, P. (2001). Direct inhibition of T-type calcium channels by the endogenous cannabinoid anandamide. *The EMBO Journal*, 20(24), 7033-7040. doi:10.1093/emboj/20.24.7033

Childers, S. R., & Deadwyler, S. A. (1996). Role of cyclic AMP in the actions of cannabinoid receptors. *Biochemical Pharmacology*, 52(6), 819-827. doi:[https://doi.org/10.1016/0006-2952\(96\)00419-4](https://doi.org/10.1016/0006-2952(96)00419-4)

Cooray, R., Gupta, V., & Suphioglu, C. (2020). Current Aspects of the Endocannabinoid System and Targeted THC and CBD Phytocannabinoids as Potential Therapeutics for Parkinson's and Alzheimer's Diseases: a Review. *Molecular Neurobiology*, 57(11), 4878-4890. doi:10.1007/s12035-020-02054-6

Corbeil, C. R., Williams, C. I., & Labute, P. (2012). Variability in docking success rates due to dataset preparation. In (Vol. 26, pp. 775-786).

D'Avanzo, N., Cheng, W. W. L., Xia, X., Dong, L., Savitsky, P., Nichols, C. G., & Doyle, D. A. (2010). Expression and purification of recombinant human inward rectifier K<sup>+</sup> (KCNJ) channels in *Saccharomyces cerevisiae*. *Protein Expression and Purification*, 71(1), 115-121. doi:10.1016/j.pep.2010.01.010

de Lera Ruiz, M., & Kraus, R. L. (2015). Voltage-Gated Sodium Channels: Structure, Function, Pharmacology, and Clinical Indications. *Journal of Medicinal Chemistry*, 58(18), 7093-7118. doi:10.1021/jm501981g

De Petrocellis, L., Vellani, V., Schiano-Moriello, A., Marini, P., Magherini, P. C., Orlando, P., & Di Marzo, V. (2008). Plant-derived cannabinoids modulate the activity of transient receptor potential channels of ankyrin type-1 and melastatin type-8. *J Pharmacol Exp Ther*, 325(3), 1007-1015. doi:10.1124/jpet.107.134809

Deadwyler, S. A., Hampson, R. E., Mu, J., Whyte, A., & Childers, S. (1995). Cannabinoids modulate voltage sensitive potassium A-current in hippocampal neurons via a cAMP-dependent

process. *Journal of Pharmacology and Experimental Therapeutics*, 273(2), 734. Retrieved from <http://jpet.aspetjournals.org/content/273/2/734.abstract>

Decher, N. a. B. F. a. V. R. a. S. K. (2003). KCNE2 modulates current amplitudes and activation kinetics of HCN4: influence of KCNE family members on HCN4 currents. *Pflugers Arch-Eur J Physiol*, 446, 633--640. doi:10.1007/s00424-003-1127-7

Deiana, S., Watanabe, A., Yamasaki, Y., Amada, N., Arthur, M., Fleming, S., . . . Riedel, G. (2012). Plasma and brain pharmacokinetic profile of cannabidiol (CBD), cannabidivarin (CBDV),  $\Delta^9$ -tetrahydrocannabivarin (THCV) and cannabigerol (CBG) in rats and mice following oral and intraperitoneal administration and CBD action on obsessive-compulsive behaviour. *Psychopharmacology (Berl)*, 219(3), 859-873. doi:10.1007/s00213-011-2415-0

Devane, W., Hanus, L., Breuer, A., Pertwee, R., Stevenson, L., Griffin, G., . . . Mechoulam, R. (1992). Isolation and structure of a brain constituent that binds to the cannabinoid receptor. 258(5090), 1946-1949. doi:10.1126/science.1470919 %J Science

Devinsky, O., Cilio, M. R., Cross, H., Fernandez-Ruiz, J., French, J., Hill, C., . . . Friedman, D. (2014). Cannabidiol: pharmacology and potential therapeutic role in epilepsy and other neuropsychiatric disorders. *Epilepsia*, 55(6), 791-802. doi:10.1111/epi.12631

DiFrancesco, D. (1981). A new interpretation of the pace-maker current in calf Purkinje fibres. *The Journal of physiology*, 314(1), 359-376. doi:<https://doi.org/10.1113/jphysiol.1981.sp013713>

DiFrancesco, D. (1982). Block and activation of the pace-maker channel in calf purkinje fibres: effects of potassium, caesium and rubidium. *The Journal of physiology*, 329, 485-507. doi:10.1113/jphysiol.1982.sp014315

DiFrancesco, D. (1985). The cardiac hyperpolarizing-activated current, if. origins and developments. *Progress in Biophysics and Molecular Biology*, 46(3), 163--183. doi:[https://doi.org/10.1016/0079-6107\(85\)90008-2](https://doi.org/10.1016/0079-6107(85)90008-2)

DiFrancesco, D. (1993). Pacemaker Mechanisms in Cardiac Tissue. *Annual Review of Physiology*, 55(1), 455--472. doi:10.1146/annurev.ph.55.030193.002323

DiFrancesco, D., Noma, A., & Trautwein, W. (1979). Kinetics and magnitude of the time-dependent potassium current in the rabbit sinoatrial node. *Pflügers Archiv*, 381(3), 271-279. doi:10.1007/BF00583259

DiFrancesco, D., & Tortora, P. (1991). Direct activation of cardiac pacemaker channels by intracellular cyclic AMP. *Nature*, 351(6322), 145-147. doi:10.1038/351145a0

DiFrancesco, J. C., & DiFrancesco, D. (2015). Dysfunctional HCN ion channels in neurological diseases. *Frontiers in cellular neuroscience*, 6, 174-174. doi:10.3389/fncel.2015.00071

Donvito, G., Nass, S. R., Wilkerson, J. L., Curry, Z. A., Schurman, L. D., Kinsey, S. G., & Lichtman, A. H. (2018). The Endogenous Cannabinoid System: A Budding Source of Targets for

- Treating Inflammatory and Neuropathic Pain. *Neuropsychopharmacology*, 43(1), 52-79.  
doi:10.1038/npp.2017.204
- Draper, M. H., & Weidmann, S. (1951). Cardiac resting and action potentials recorded with an intracellular electrode. *The Journal of physiology*, 115(1), 74-94.  
doi:10.1113/jphysiol.1951.sp004653
- Du, Y., Duc, N. M., Rasmussen, S. G. F., Hilger, D., Kubiak, X., Wang, L., . . . Chung, K. Y. (2019). Assembly of a GPCR-G Protein Complex. *Cell*, 177(5), 1232-1242.e1211.  
doi:10.1016/j.cell.2019.04.022
- Fischer, M. J. M., Ciotu, C. I., & Szallasi, A. (2020). The Mysteries of Capsaicin-Sensitive Afferents. *Frontiers in Physiology*, 11(1587). doi:10.3389/fphys.2020.554195
- Fürst, O., & D'Avanzo, N. (2015). Isoform dependent regulation of human HCN channels by cholesterol. *Scientific Reports*, 5(1), 14270. doi:10.1038/srep14270
- Gao, S., Nagpal, J., Schneider, M. W., Kozjak-Pavlovic, V., Nagel, G., & Gottschalk, A. (2015). Optogenetic manipulation of cGMP in cells and animals by the tightly light-regulated guanylyl-cyclase opsin CycOp. *Nature communications*, 6(1), 8046. doi:10.1038/ncomms9046
- Gaoni, Y., & Mechoulam, R. (1971). Isolation and structure of .DELTA.+ tetrahydrocannabinol and other neutral cannabinoids from hashish. *Journal of the American Chemical Society*, 93(1), 217-224. doi:10.1021/ja00730a036
- Gatley, S. J., Gifford, A. N., Volkow, N. D., Lan, R., & Makriyannis, A. (1996). 123I-labeled AM251: a radioiodinated ligand which binds in vivo to mouse brain cannabinoid CB1 receptors. *European Journal of Pharmacology*, 307(3), 331-338. doi:[https://doi.org/10.1016/0014-2999\(96\)00279-8](https://doi.org/10.1016/0014-2999(96)00279-8)
- Gebremedhin, D., Lange, A. R., Campbell, W. B., Hillard, C. J., & Harder, D. R. (1999). Cannabinoid CB1 receptor of cat cerebral arterial muscle functions to inhibit L-type Ca<sup>2+</sup> channel current. *American Journal of Physiology-Heart and Circulatory Physiology*, 276(6), H2085-H2093. doi:10.1152/ajpheart.1999.276.6.H2085
- George, M. S., Abbott, L. F., & Siegelbaum, S. A. (2009). HCN hyperpolarization-activated cation channels inhibit EPSPs by interactions with M-type K(+) channels. *Nature neuroscience*, 12(5), 577-584. doi:10.1038/nn.2307
- Ghovanloo, M.-R., Choudhury, K., Bandaru, T. S., Fouda, M. A., Rayani, K., Rusinova, R., . . . Ruben, P. C. (2020). Mechanism and effects of the skeletal muscle Nav1.4 inhibition by cannabidiol. *bioRxiv*, 2020.2006.2030.180943. doi:10.1101/2020.06.30.180943
- Ghovanloo, M.-R., Choudhury, K., Bandaru, T. S., Fouda, M. A., Rayani, K., Rusinova, R., . . . Ruben, P. C. (2021). Cannabidiol inhibits the skeletal muscle Nav1.4 by blocking its pore and by altering membrane elasticity. *Journal of General Physiology*, 153(5).  
doi:10.1085/jgp.202012701

- Ghovanloo, M.-R., Shuart, N. G., Mezeyova, J., Dean, R. A., Ruben, P. C., & Goodchild, S. J. (2018). Inhibitory effects of cannabidiol on voltage-dependent sodium currents. *Journal of Biological Chemistry*, 293(43), 16546-16558. doi:<https://doi.org/10.1074/jbc.RA118.004929>
- Glass, M., & Felder, C. C. (1997). Concurrent Stimulation of Cannabinoid CB1 and Dopamine D2 Receptors Augments cAMP Accumulation in Striatal Neurons: Evidence for a Linkage to the CB1 Receptor. *The Journal of Neuroscience*, 17(14), 5327. doi:10.1523/JNEUROSCI.17-14-05327.1997
- Guy, G. W., & Flint, M. E. (2004). A Single Centre, Placebo-Controlled, Four Period, Crossover, Tolerability Study Assessing, Pharmacodynamic Effects, Pharmacokinetic Characteristics and Cognitive Profiles of a Single Dose of Three Formulations of Cannabis Based Medicine Extracts (CBMEs) (GWPD9901), Plus a Two Period Tolerability Study Comparing Pharmacodynamic Effects and Pharmacokinetic Characteristics of a Single Dose of a Cannabis Based Medicine Extract Given via Two Administration Routes (GWPD9901 EXT). *Journal of Cannabis Therapeutics*, 3(3), 35-77. doi:10.1300/J175v03n03\_03
- Guy, G. W., & Robson, P. J. (2004). A Phase I, Open Label, Four-Way Crossover Study to Compare the Pharmacokinetic Profiles of a Single Dose of 20 mg of a Cannabis Based Medicine Extract (CBME) Administered on 3 Different Areas of the Buccal Mucosa and to Investigate the Pharmacokinetics of CBME per Oral in Healthy Male and Female Volunteers (GWPK0112). *Journal of Cannabis Therapeutics*, 3(4), 79-120. doi:10.1300/J175v03n04\_01
- Hanus, L. O. (2007). Discovery and isolation of anandamide and other endocannabinoids. *Chem Biodivers*, 4(8), 1828-1841. doi:10.1002/cbdv.200790154
- He, C. a. C. F. a. L. B. a. H. Z. (2014). Neurophysiology of HCN channels: From cellular functions to multiple regulations. *Progress in Neurobiology*, 112, 1--23. doi:<https://doi.org/10.1016/j.pneurobio.2013.10.001>
- Hill, W. G., Southern, N. M., MacIver, B., Potter, E., Apodaca, G., Smith, C. P., & Zeidel, M. L. (2005). Isolation and characterization of the *Xenopus* oocyte plasma membrane: a new method for studying activity of water and solute transporters. *American Journal of Physiology-Renal Physiology*, 289(1), F217-F224. doi:10.1152/ajprenal.00022.2005
- Hodgkin, A. L., & Huxley, A. F. (1939). Action Potentials Recorded from Inside a Nerve Fibre. *Nature*, 144(3651), 710-711. doi:10.1038/144710a0
- Howlett, A. C. (2005). Cannabinoid Receptor Signaling. In (pp. 53-79). Berlin/Heidelberg: Springer-Verlag.
- Hua, T., Li, X., Wu, L., Iliopoulos-Tsoutsouvas, C., Wang, Y., Wu, M., . . . Liu, Z. J. (2020). Activation and Signaling Mechanism Revealed by Cannabinoid Receptor-G(i) Complex Structures. *Cell*, 180(4), 655-665.e618. doi:10.1016/j.cell.2020.01.008
- Hua, T., Vemuri, K., Pu, M., Qu, L., Han, G. W., Wu, Y., . . . Liu, Z.-J. (2016). Crystal Structure of the Human Cannabinoid Receptor CB1. *Cell*, 167(3), 750-762.e714. doi:<https://doi.org/10.1016/j.cell.2016.10.004>

- Hume, J. R., & Grant, A. O. (2015). Agents Used in Cardiac Arrhythmias. In B. G. Katzung & A. J. Trevor (Eds.), *Basic & Clinical Pharmacology, 13e*. New York, NY: McGraw-Hill Medical.
- Iannotti, F. A., Hill, C. L., Leo, A., Alhusaini, A., Soubrane, C., Mazzarella, E., . . . Stephens, G. J. (2014). Nonpsychotropic plant cannabinoids, cannabidivarin (CBDV) and cannabidiol (CBD), activate and desensitize transient receptor potential vanilloid 1 (TRPV1) channels in vitro: potential for the treatment of neuronal hyperexcitability. *ACS Chem Neurosci*, *5*(11), 1131-1141. doi:10.1021/cn5000524
- Ibsen, M. S., Connor, M., & Glass, M. (2017). Cannabinoid CB(1) and CB(2) Receptor Signaling and Bias. *Cannabis and cannabinoid research*, *2*(1), 48-60. doi:10.1089/can.2016.0037
- Ikonen, E. (2008). Cellular cholesterol trafficking and compartmentalization. *Nat Rev Mol Cell Biol*, *9*(2), 125-138. doi:10.1038/nrm2336
- Isenberg, G. (1976). Cardiac Purkinje fibers: Cesium as a tool to block inward rectifying potassium currents. *Pflügers Archiv*, *365*(2), 99-106. doi:10.1007/BF01067006
- Iversen, L. (2003). Cannabis and the brain. *Brain*, *126*(6), 1252-1270. doi:10.1093/brain/awg143
- Katona, I., Rancz, E. A., Acsady, L., Ledent, C., Mackie, K., Hajos, N., & Freund, T. F. (2001). Distribution of CB1 cannabinoid receptors in the amygdala and their role in the control of GABAergic transmission. *The Journal of neuroscience : the official journal of the Society for Neuroscience*, *21*(23), 9506-9518. doi:10.1523/jneurosci.21-23-09506.2001
- Kauer, J. A., & Gibson, H. E. (2009). Hot flash: TRPV channels in the brain. *Trends Neurosci*, *32*(4), 215-224. doi:10.1016/j.tins.2008.12.006
- Keenan, C. M., Storr, M. A., Thakur, G. A., Wood, J. T., Wager-Miller, J., Straiker, A., . . . Sharkey, K. A. (2015). AM841, a covalent cannabinoid ligand, powerfully slows gastrointestinal motility in normal and stressed mice in a peripherally restricted manner. *British journal of pharmacology*, *172*(9), 2406-2418. doi:10.1111/bph.13069
- Kmiecik, S., Gront, D., Kolinski, M., Wieteska, L., Dawid, A. E., & Kolinski, A. (2016). Coarse-Grained Protein Models and Their Applications. *Chemical Reviews*, *116*(14), 7898-7936. doi:10.1021/acs.chemrev.6b00163
- Koch, U., & Grothe, B. (2003). Hyperpolarization-Activated Current (I<sub>h</sub>) in the Inferior Colliculus: Distribution and Contribution to Temporal Processing. *Journal of Neurophysiology*, *90*(6), 3679-3687. doi:10.1152/jn.00375.2003
- Koehl, A., Hu, H., Maeda, S., Zhang, Y., Qu, Q., Paggi, J. M., . . . Kobilka, B. K. (2018). Structure of the  $\mu$ -opioid receptor–Gi protein complex. *Nature*, *558*(7711), 547-552. doi:10.1038/s41586-018-0219-7

- Kornreich, B. G. (2007). The patch clamp technique: Principles and technical considerations. *Journal of Veterinary Cardiology*, 9(1), 25-37. doi:<https://doi.org/10.1016/j.jvc.2007.02.001>
- Ku, S. M., & Han, M.-H. (2017). HCN Channel Targets for Novel Antidepressant Treatment. *Neurotherapeutics : the journal of the American Society for Experimental NeuroTherapeutics*, 14(3), 698-715. doi:10.1007/s13311-017-0538-7
- Lacerda, A. E., Kramer, J., Shen, K. Z., Thomas, D., & Brown, A. M. (2001). Comparison of block among cloned cardiac potassium channels by non-antiarrhythmic drugs. *European Heart Journal Supplements*, 3(suppl\_K), K23-K30. doi:10.1016/S1520-765X(01)90003-3
- Lauckner, J. E., Hille, B., & Mackie, K. (2005). The cannabinoid agonist WIN55,212-2 increases intracellular calcium via CB1 receptor coupling to Gq/11 G proteins. *Proc Natl Acad Sci U S A*, 102(52), 19144-19149. doi:10.1073/pnas.0509588102
- Lavado-García, J., Jorge, I., Cervera, L., Vázquez, J., & Gòdia, F. (2020). Multiplexed Quantitative Proteomic Analysis of HEK293 Provides Insights into Molecular Changes Associated with the Cell Density Effect, Transient Transfection, and Virus-Like Particle Production. *Journal of Proteome Research*, 19(3), 1085-1099. doi:10.1021/acs.jproteome.9b00601
- Lee, C.-H., & Roderick, M. (2017). Structures of the Human HCN1 Hyperpolarization-Activated Channel. *Cell*, 168(1), 111--120.e111. doi:10.1016/j.cell.2016.12.023
- Lei, Q., Jones, M. B., Talley, E. M., Schrier, A. D., McIntire, W. E., Garrison, J. C., & Bayliss, D. A. (2000). Activation and inhibition of G protein-coupled inwardly rectifying potassium (Kir3) channels by G protein  $\beta\gamma$  subunits. *Proceedings of the National Academy of Sciences*, 97(17), 9771. doi:10.1073/pnas.97.17.9771
- Lin, W., Laitko, U., Juranka, P. F., & Morris, C. E. (2007). Dual Stretch Responses of mHCN2 Pacemaker Channels: Accelerated Activation, Accelerated Deactivation. *Biophysical Journal*, 92(5), 1559-1572. doi:<https://doi.org/10.1529/biophysj.106.092478>
- Ludwig, A. a. Z. X. a. H. F. a. B. M. (1999). Structure and Function of Cardiac Pacemaker Channels. *Cellular Physiology and Biochemistry*, 9(4-5), 179--186. doi:10.1159/000016315
- Lundbæk, J. A., Birn, P., Hansen, A. J., Søgaard, R., Nielsen, C., Girshman, J., . . . Andersen, O. S. (2004). Regulation of Sodium Channel Function by Bilayer Elasticity : The Importance of Hydrophobic Coupling. Effects of Micelle-forming Amphiphiles and Cholesterol. *Journal of General Physiology*, 123(5), 599-621. doi:10.1085/jgp.200308996
- Lussier, Y., Fürst, O., Fortea, E., Leclerc, M., Priolo, D., Moeller, L., . . . D'Avanzo, N. (2019). Disease-linked mutations alter the stoichiometries of HCN-KCNE2 complexes. *Sci Rep*, 9(1), 9113. doi:10.1038/s41598-019-45592-3
- Mackie, K., Lai, Y., Westenbroek, R., & Mitchell, R. (1995). Cannabinoids activate an inwardly rectifying potassium conductance and inhibit Q-type calcium currents in AtT20 cells transfected

with rat brain cannabinoid receptor. *The Journal of neuroscience : the official journal of the Society for Neuroscience*, 15(10), 6552-6561. doi:10.1523/JNEUROSCI.15-10-06552.1995

Mahgoub, M., Keun-Hang, S. Y., Sydorenko, V., Ashoor, A., Kabbani, N., Al Kury, L., . . . Oz, M. (2013). Effects of cannabidiol on the function of  $\alpha 7$ -nicotinic acetylcholine receptors. *European Journal of Pharmacology*, 720(1), 310-319. doi:<https://doi.org/10.1016/j.ejphar.2013.10.011>

Männikkö, R., Pandey, S., Larsson, H. P., & Elinder, F. (2005). Hysteresis in the voltage dependence of HCN channels: conversion between two modes affects pacemaker properties. *J Gen Physiol*, 125(3), 305-326. doi:10.1085/jgp.200409130

Maroso, M., Szabo, G. G., Kim, H. K., Alexander, A., Bui, A. D., Lee, S.-H., . . . Soltesz, I. (2016). Cannabinoid Control of Learning and Memory through HCN Channels. *Neuron*, 89(5), 1059-1073. doi:10.1016/j.neuron.2016.01.023

Mascarenhas, N. M., & Gosavi, S. (2017). Understanding protein domain-swapping using structure-based models of protein folding. *Progress in Biophysics and Molecular Biology*, 128, 113-120. doi:<https://doi.org/10.1016/j.pbiomolbio.2016.09.013>

Matsuda, L. A., Lolait, S. J., Brownstein, M. J., Young, A. C., & Bonner, T. I. (1990). Structure of a cannabinoid receptor and functional expression of the cloned cDNA. *Nature*, 346(6284), 561-564. doi:10.1038/346561a0

Matthies, D., Bae, C., Toombes, G. E., Fox, T., Bartesaghi, A., Subramaniam, S., & Swartz, K. J. (2018). Single-particle cryo-EM structure of a voltage-activated potassium channel in lipid nanodiscs. *eLife*, 7, e37558. doi:10.7554/eLife.37558

McAllister, S. D., Griffin, G., Satin, L. S., & Abood, M. E. (1999). Cannabinoid Receptors Can Activate and Inhibit G Protein-Coupled Inwardly Rectifying Potassium Channels in a *Xenopus* Oocyte Expression System. *Journal of Pharmacology and Experimental Therapeutics*, 291(2), 618. Retrieved from <http://jpet.aspetjournals.org/content/291/2/618.abstract>

McPartland, J. M., Glass, M., & Pertwee, R. G. (2007). Meta-analysis of cannabinoid ligand binding affinity and receptor distribution: interspecies differences. *British journal of pharmacology*, 152(5), 583-593. doi:10.1038/sj.bjp.0707399

Mechoulam, R., Ben-Shabat, S., Hanus, L., Ligumsky, M., Kaminski, N. E., Schatz, A. R., . . . et al. (1995). Identification of an endogenous 2-monoglyceride, present in canine gut, that binds to cannabinoid receptors. *Biochem Pharmacol*, 50(1), 83-90. doi:10.1016/0006-2952(95)00109-d

Mechoulam, R., Fride, E., & Di Marzo, V. (1998). Endocannabinoids. *European Journal of Pharmacology*, 359(1), 1-18. doi:[https://doi.org/10.1016/S0014-2999\(98\)00649-9](https://doi.org/10.1016/S0014-2999(98)00649-9)

Mechoulam, R., & Shvo, Y. (1963). Hashish—I: The structure of Cannabidiol. *Tetrahedron*, 19(12), 2073-2078. doi:[https://doi.org/10.1016/0040-4020\(63\)85022-X](https://doi.org/10.1016/0040-4020(63)85022-X)

- Mirotznik, R. R., Zheng, X., & Stanley, E. F. (2000). G-Protein Types Involved in Calcium Channel Inhibition at a Presynaptic Nerve Terminal. *The Journal of Neuroscience*, 20(20), 7614. doi:10.1523/JNEUROSCI.20-20-07614.2000
- Molnar, C. (2019). *Concepts of Biology - 1st Canadian Edition*.
- Monteggia, L. M., Eisch, A. J., Tang, M. D., Kaczmarek, L. K., & Nestler, E. J. (2000). Cloning and localization of the hyperpolarization-activated cyclic nucleotide-gated channel family in rat brain. *Brain Res Mol Brain Res*, 81(1-2), 129-139. doi:10.1016/s0169-328x(00)00155-8
- Montini, G., Booker, J., Sula, A., & Wallace, B. A. (2018). Comparisons of voltage-gated sodium channel structures with open and closed gates and implications for state-dependent drug design. *Biochemical Society Transactions*, 46(6), 1567-1575. doi:10.1042/BST20180295
- Morales, P., Hurst, D. P., & Reggio, P. H. (2017). Molecular Targets of the Phytocannabinoids: A Complex Picture. In A. D. Kinghorn, H. Falk, S. Gibbons, & J. i. Kobayashi (Eds.), *Phytocannabinoids: Unraveling the Complex Chemistry and Pharmacology of Cannabis sativa* (pp. 103-131). Cham: Springer International Publishing.
- Mukhopadhyay, S., McIntosh, H. H., Houston, D. B., & Howlett, A. C. (2000). The CB(1) cannabinoid receptor juxtamembrane C-terminal peptide confers activation to specific G proteins in brain. *Mol Pharmacol*, 57(1), 162-170.
- Munro, S., Thomas, K. L., & Abu-Shaar, M. (1993). Molecular characterization of a peripheral receptor for cannabinoids. *Nature*, 365(6441), 61-65. doi:10.1038/365061a0
- Narang, D., Kerr, P. M., Baserman, J., Tam, R., Yang, W., Searle, G., . . . Plane, F. (2013). Triton X-100 inhibits L-type voltage-operated calcium channels. *Canadian Journal of Physiology and Pharmacology*, 91(4), 316-324. doi:10.1139/cjpp-2012-0257
- Navarrete, M., & Araque, A. (2008). Endocannabinoids Mediate Neuron-Astrocyte Communication. *Neuron*, 57(6), 883-893. doi:<https://doi.org/10.1016/j.neuron.2008.01.029>
- Nicholson, R. A., Liao, C., Zheng, J., David, L. S., Coyne, L., Errington, A. C., . . . Lees, G. (2003). Sodium channel inhibition by anandamide and synthetic cannabimimetics in brain. *Brain Research*, 978(1), 194-204. doi:[https://doi.org/10.1016/S0006-8993\(03\)02808-7](https://doi.org/10.1016/S0006-8993(03)02808-7)
- NIDA. (2021). *How does marijuana produce its effects?* Retrieved from National Institute on Drug Abuse: <https://www.drugabuse.gov/publications/research-reports/marijuana/how-does-marijuana-produce-its-effects>
- Niederhoffer, N., & Szabo, B. (1999). Effect of the cannabinoid receptor agonist WIN55212-2 on sympathetic cardiovascular regulation. *British journal of pharmacology*, 126(2), 457-466. doi:10.1038/sj.bjp.0702337
- Niehaus, J. L., Liu, Y., Wallis, K. T., Egertová, M., Bhartur, S. G., Mukhopadhyay, S., . . . Lewis, D. L. (2007). CB1 Cannabinoid Receptor Activity Is Modulated by the Cannabinoid

Receptor Interacting Protein CRIP 1a. *Molecular Pharmacology*, 72(6), 1557.  
doi:10.1124/mol.107.039263

Noble, D., & Tsien, R. W. (1968). The kinetics and rectifier properties of the slow potassium current in cardiac Purkinje fibres. *J Physiol*, 195(1), 185-214.  
doi:10.1113/jphysiol.1968.sp008454

Noma, A., & Irisawa, H. (1976). Membrane currents in the rabbit sinoatrial node cell as studied by the double microelectrode method. *Pflugers Arch*, 364(1), 45-52. doi:10.1007/bf01062910

Ohlsson, A., Lindgren, J. E., Andersson, S., Agurell, S., Gillespie, H., & Hollister, L. E. (1984). SINGLE DOSE KINETICS OF CANNABIDIOL IN MAN1. In S. Agurell, W. L. Dewey, & R. E. Willette (Eds.), *The Cannabinoids: Chemical, Pharmacologic, and Therapeutic Aspects* (pp. 219-225): Academic Press.

Okada, T., Le Trong, I., Fox, B. A., Behnke, C. A., Stenkamp, R. E., & Palczewski, K. (2000). X-Ray diffraction analysis of three-dimensional crystals of bovine rhodopsin obtained from mixed micelles. *J Struct Biol*, 130(1), 73-80. doi:10.1006/jsbi.1999.4209

Orvos, P., Pászti, B., Topal, L., Gazdag, P., Prorok, J., Polyák, A., . . . Csupor, D. (2020). The electrophysiological effect of cannabidiol on hERG current and in guinea-pig and rabbit cardiac preparations. *Scientific Reports*, 10(1), 16079. doi:10.1038/s41598-020-73165-2

Österberg, F., Morris, G. M., Sanner, M. F., Olson, A. J., & Goodsell, D. S. (2002). Automated docking to multiple target structures: Incorporation of protein mobility and structural water heterogeneity in autodock. *Proteins: Structure, Function and Genetics*, 46(1), 34-40.  
doi:10.1002/prot.10028

Pape, H. C. (1996). Queer Current and Pacemaker: The Hyperpolarization-Activated Cation Current in Neurons. *Annual Review of Physiology*, 58(1), 299--327.  
doi:10.1146/annurev.ph.58.030196.001503

Park, K., Yi, J. H., Kim, H., Choi, K., Kang, S. J., & Shin, K. S. (2011). HCN channel activity-dependent modulation of inhibitory synaptic transmission in the rat basolateral amygdala. *Biochem Biophys Res Commun*, 404(4), 952-957. doi:10.1016/j.bbrc.2010.12.087

Parker, L. A., Rock, E. M., & Limebeer, C. L. (2011). Regulation of nausea and vomiting by cannabinoids. *British journal of pharmacology*, 163(7), 1411-1422. doi:10.1111/j.1476-5381.2010.01176.x

Paton, W. D. M. (1975). *PHARMACOLOGY OF MARIJUANA*. Retrieved from [www.annualreviews.org](http://www.annualreviews.org)

Peng, B.-W., Justice, J. A., Zhang, K., He, X.-h., & Sanchez, R. M. (2010). Increased Basal Synaptic Inhibition of Hippocampal Area CA1 Pyramidal Neurons by an Antiepileptic Drug that Enhances IH. *Neuropsychopharmacology*, 35(2), 464-472. doi:10.1038/npp.2009.150

- Pertwee, R. G. (1988). The central neuropharmacology of psychotropic cannabinoids. *Pharmacology & Therapeutics*, 36(2), 189-261. doi:[https://doi.org/10.1016/0163-7258\(88\)90106-4](https://doi.org/10.1016/0163-7258(88)90106-4)
- Peshkin, L., Lukyanov, A., Kalocsay, M., Gage, R. M., Wang, D., Pells, T. J., . . . Kirschner, M. W. (2019). The protein repertoire in early vertebrate embryogenesis. *bioRxiv*, 571174. doi:10.1101/571174
- Pettersen, E. F., Goddard, T. D., Huang, C. C., Couch, G. S., Greenblatt, D. M., Meng, E. C., & Ferrin, T. E. (2004). UCSF Chimera—A visualization system for exploratory research and analysis. *Journal of Computational Chemistry*, 25(13), 1605-1612. doi:<https://doi.org/10.1002/jcc.20084>
- Pian, P., Bucchini, A., Decostanzo, A., Robinson, R. B., & Siegelbaum, S. A. (2007). Modulation of cyclic nucleotide-regulated HCN channels by PIP(2) and receptors coupled to phospholipase C. *Pflugers Arch*, 455(1), 125-145. doi:10.1007/s00424-007-0295-2
- Pian, P., Bucchini, A., Robinson, R. B., & Siegelbaum, S. A. (2006). Regulation of gating and rundown of HCN hyperpolarization-activated channels by exogenous and endogenous PIP2. *J Gen Physiol*, 128(5), 593-604. doi:10.1085/jgp.200609648
- Poling, J. S., Rogawski, M. A., Salem, N., & Vicini, S. (1996). Anandamide, an Endogenous Cannabinoid, Inhibits Shaker-related Voltage-gated K<sup>+</sup> Channels. *Neuropharmacology*, 35(7), 983-991. doi:[https://doi.org/10.1016/0028-3908\(96\)00130-X](https://doi.org/10.1016/0028-3908(96)00130-X)
- Porter, B. E., & Jacobson, C. (2013). Report of a parent survey of cannabidiol-enriched cannabis use in pediatric treatment-resistant epilepsy. *Epilepsy & Behavior*, 29(3), 574-577. doi:<https://doi.org/10.1016/j.yebeh.2013.08.037>
- Presti, F. T. (1985). The role of cholesterol in regulating membrane fluidity. *Membrane fluidity in biology*, 4, 97-145.
- Pumroy, R. A., Samanta, A., Liu, Y., Hughes, T. E., Zhao, S., Yudin, Y., . . . Moiseenkova-Bell, V. Y. (2019). Molecular mechanism of TRPV2 channel modulation by cannabidiol. *eLife*, 8, e48792. doi:10.7554/eLife.48792
- Ramírez, D., Zúñiga, R., Concha, G., & Zúñiga, L. (2018). HCN Channels: New Therapeutic Targets for Pain Treatment. *Molecules (Basel, Switzerland)*, 23(9), 2094. doi:10.3390/molecules23092094
- Rouillard, A. D., Gundersen, G. W., Fernandez, N. F., Wang, Z., Monteiro, C. D., McDermott, M. G., & Ma'ayan, A. (2016). The harmonizome: a collection of processed datasets gathered to serve and mine knowledge about genes and proteins. *Database (Oxford)*, 2016. doi:10.1093/database/baw100
- Sait, L. G., Sula, A., Ghovanloo, M.-R., Hollingworth, D., Ruben, P. C., & Wallace, B. A. (2020). Cannabidiol interactions with voltage-gated sodium channels. *eLife*, 9, e58593. doi:10.7554/eLife.58593

- Santoro, B., Grant, S. G., Bartsch, D., & Kandel, E. R. (1997). Interactive cloning with the SH3 domain of N-src identifies a new brain specific ion channel protein, with homology to eag and cyclic nucleotide-gated channels. *Proc Natl Acad Sci U S A*, *94*(26), 14815-14820. doi:10.1073/pnas.94.26.14815
- Santoro, B., Hu, L., Liu, H., Saponaro, A., Pian, P., Piskorowski, R. A., . . . Siegelbaum, S. A. (2011a). TRIP8b regulates HCN1 channel trafficking and gating through two distinct C-terminal interaction sites. *The Journal of neuroscience : the official journal of the Society for Neuroscience*, *31*(11), 4074-4086. doi:10.1523/jneurosci.5707-10.2011
- Santoro, B., Hu, L., Liu, H., Saponaro, A., Pian, P., Piskorowski, R. A., . . . Siegelbaum, S. A. (2011b). TRIP8b regulates HCN1 channel trafficking and gating through two distinct C-terminal interaction sites. *The Journal of neuroscience : the official journal of the Society for Neuroscience*, *31*(11), 4074-4086. doi:10.1523/JNEUROSCI.5707-10.2011
- Santoro, B., Liu, D. T., Yao, H., Bartsch, D., Kandel, E. R., Siegelbaum, S. A., & Tibbs, G. R. (1998). Identification of a Gene Encoding a Hyperpolarization-Activated Pacemaker Channel of Brain. *Cell*, *93*(5), 717--729. doi:[https://doi.org/10.1016/S0092-8674\(00\)81434-8](https://doi.org/10.1016/S0092-8674(00)81434-8)
- Shao, Z., Yin, J., Chapman, K., Grzemska, M., Clark, L., Wang, J., & Rosenbaum, D. M. (2016). High-resolution crystal structure of the human CB1 cannabinoid receptor. *Nature*, *540*, 602. doi:10.1038/nature20613
- Starkus, J., Jansen, C., Shimoda, L. M. N., Stokes, A. J., Small-Howard, A. L., & Turner, H. (2019). Diverse TRPV1 responses to cannabinoids. *Channels (Austin, Tex.)*, *13*(1), 172-191. doi:10.1080/19336950.2019.1619436
- Steinmetz, A. B., & Freeman, J. H. (2016). Cannabinoid modulation of memory consolidation within the cerebellum. *Neurobiology of Learning and Memory*, *136*, 228-235. doi:<https://doi.org/10.1016/j.nlm.2016.11.002>
- Sternweis, P. C., & Robishaw, J. D. (1984). Isolation of two proteins with high affinity for guanine nucleotides from membranes of bovine brain. *J Biol Chem*, *259*(22), 13806-13813.
- Tao, Q., McAllister, S. D., Andreassi, J., Nowell, K. W., Cabral, G. A., Hurst, D. P., . . . Abood, M. E. (1999). Role of a conserved lysine residue in the peripheral cannabinoid receptor (CB2): evidence for subtype specificity. *Mol Pharmacol*, *55*(3), 605-613.
- Tao, Z., Gameiro, A., & Grewer, C. (2008). Thallium ions can replace both sodium and potassium ions in the glutamate transporter excitatory amino acid carrier 1. *Biochemistry*, *47*(48), 12923-12930. doi:10.1021/bi8017174
- Tillman, T. S., & Cascio, M. (2003). Effects of membrane lipids on ion channel structure and function. *Cell Biochem Biophys*, *38*(2), 161-190. doi:10.1385/cbb:38:2:161
- Twitchell, W., Brown, S., & Mackie, K. (1997). Cannabinoids inhibit N- and P/Q-type calcium channels in cultured rat hippocampal neurons. *J Neurophysiol*, *78*(1), 43-50. doi:10.1152/jn.1997.78.1.43

- Vargish, Geoffrey A., & McBain, Chris J. (2016). The Hyperpolarization-Activated Cation Current Ih: The Missing Link Connecting Cannabinoids to Cognition. *Neuron*, 89(5), 889-891. doi:<https://doi.org/10.1016/j.neuron.2016.02.027>
- Varvel, S. A., & Lichtman, A. H. (2005). Role of the endocannabinoid system in learning and memory. In (pp. 111-140). Basel: Birkhäuser-Verlag.
- Vásquez, C., Navarro-Polanco, R. A., Huerta, M., Trujillo, X., Andrade, F., Trujillo-Hernández, B., & Hernández, L. (2003). Effects of cannabinoids on endogenous K<sup>+</sup> and Ca<sup>2+</sup> currents in HEK293 cells. *Canadian Journal of Physiology and Pharmacology*, 81(5), 436-442. doi:10.1139/y03-055 %M 12774849
- Viveros, M.-P., Marco, E.-M., Llorente, R., & López-Gallardo, M. (2007). Endocannabinoid System and Synaptic Plasticity: Implications for Emotional Responses. *Neural Plasticity*, 2007, 052908. doi:10.1155/2007/52908
- Watkins, A. R. (2019). Cannabinoid interactions with ion channels and receptors. *Channels (Austin, Tex.)*, 13(1), 162-167. doi:10.1080/19336950.2019.1615824
- Weaver, C. D. (2018). Thallium Flux Assay for Measuring the Activity of Monovalent Cation Channels and Transporters. In S.-L. Shyng, F. I. Valiyaveetil, & M. Whorton (Eds.), *Potassium Channels: Methods and Protocols* (pp. 105-114). New York, NY: Springer New York.
- Wiley, J. L., Barrett, R. L., Lowe, J., Balster, R. L., & Martin, B. R. (1995). Discriminative stimulus effects of CP 55,940 and structurally dissimilar cannabinoids in rats. *Neuropharmacology*, 34(6), 669-676. doi:10.1016/0028-3908(95)00027-4
- Williamson, E. M. (2004). The Medicinal Uses of Cannabis and Cannabinoids. Edited by G. W. Guy, B. A. Whittle and P. J. Robson. Pharmaceutical Press: London, 2004. Pages: 448. ISBN: 0-85369-517-2. Price £39.95. *Human Psychopharmacology: Clinical and Experimental*, 19(8), 589-589. doi:<https://doi.org/10.1002/hup.631>
- Wu, J. Y. a. C. I. S. (1997). Tyrosine kinase inhibition reduces i(f) in rabbit sinoatrial node myocytes. *Pflügers Archiv : European journal of physiology*, 434(5), 509--514. doi:10.1007/s004240050430
- Xing, C., Zhuang, Y., Xu, T. H., Feng, Z., Zhou, X. E., Chen, M., . . . Xie, X. Q. (2020). Cryo-EM Structure of the Human Cannabinoid Receptor CB2-G(i) Signaling Complex. *Cell*, 180(4), 645-654.e613. doi:10.1016/j.cell.2020.01.007
- Yanagihara, K., & Irisawa, H. (1980). Inward current activated during hyperpolarization in the rabbit sinoatrial node cell. *Pflügers Archiv*, 385(1), 11-19. doi:10.1007/BF00583909
- Ye, L., Cao, Z., Wang, W., & Zhou, N. (2019). New Insights in Cannabinoid Receptor Structure and Signaling. *Current molecular pharmacology*, 12(3), 239-248. doi:10.2174/1874467212666190215112036

Zar, J. H. (1984). *Biostatistical Analysis - Chapter 18* (2nd Edition ed.). Englewood Cliffs: Prentice-Hall, Inc.

Zhang, D., Gopalakrishnan, S. M., Freiberg, G., & Surowy, C. S. (2010). A Thallium Transport FLIPR-Based Assay for the Identification of KCC2-Positive Modulators. *Journal of Biomolecular Screening*, 15(2), 177-184. doi:10.1177/1087057109355708

Zhao, Q., Kawano, T., Nakata, H., Nakajima, Y., Nakajima, S., & Kozasa, T. (2003). Interaction of G Protein  $\beta$  Subunit with Inward Rectifier K<sup>+</sup> Channel Kir3. *Molecular Pharmacology*, 64(5), 1085. doi:10.1124/mol.64.5.1085

Zipes, D. P., & Fischer, J. C. (1974). Effects of Agents which Inhibit the Slow Channel on Sinus Node Automaticity and Atrioventricular Conduction in the Dog. *Circulation Research*, 34(2), 184-192. doi:10.1161/01.RES.34.2.184

Zolles, G. a. K. N. a. W. D. a. W.-T. J. a. F. B. K. a. R. J. a. F. B. (2006). Pacemaking by HCN Channels Requires Interaction with Phosphoinositides. *Neuron*, 52(6), 1027--1036. doi:<https://doi.org/10.1016/j.neuron.2006.12.005>